

Jørgen Haugum

Modifying a Francis Turbine Model for Mitigating Mechanical Backlash

Master's thesis in Mechanical Engineering

Supervisor: Pål-Tore Storli

Co-supervisor: Truls Edvardsen Aarønes

June 2023

Jørgen Haugum

Modifying a Francis Turbine Model for Mitigating Mechanical Backlash

Master's thesis in Mechanical Engineering
Supervisor: Pål-Tore Storli
Co-supervisor: Truls Edvardsen Aarønes
June 2023

Norwegian University of Science and Technology
Faculty of Engineering
Department of Energy and Process Engineering



Acknowledgements

Writing a master's thesis can be very demanding, especially if you are doing it all by yourself. Luckily, this has not been the case for me, as I have gotten a lot of help through a long semester. For this, I would thank my supervisor Pål-Tore for helping me through the entire project from start to finish, with everything from thesis layout to difficult theoretical hydropower knowledge. Also, I would like to thank my co-supervisor Truls for answering my questions and explaining the theory on turbine governors.

For helping me in the lab, I would like to thank the apprentice Fredrik which provided super accurately manufactured test parts down to one hundredth of a millimeter, enabling high quality experimental tests. I would also like to thank the PhD candidate Johannes for taking time to help me out with measurements on the Francis rig and showing me how to operate it. For giving great advice considering the motion simulations of the CAD-assembly by among others suggesting the choice of software, I would also like to thank my brother Henrik.

In addition to thanking all the contributors for academic assistance, I would also like to thank the master's students and PhD candidates at the Waterpower Laboratory for making the everyday life as a master's student quite nice with lottery Fridays and generally good atmosphere. In the end I will give a special thanks to Nora, for her invaluable support as my girlfriend, study partner and friend throughout my years at NTNU.

Abstract

This master's thesis investigates the mechanical backlash of the guide vane system on the Francis rig at the Waterpower Laboratory, NTNU Trondheim. The work is a continuation of the specialization project by Haugum [1], and both numerical and experimental analyses are conducted to examine the existing guide vane system. Additionally, a new design for the guide vane system is proposed to meet the specified requirement of a total backlash below 1% of maximum actuator stroke length, which should ensure stable governing of the rig. Experimental measurements on the existing system revealed a mechanical backlash of 2.60 ± 0.29 mm, corresponding to an average of 4.15% of maximum stroke length. The suggested new design resulted in an estimated total backlash of about 0.56 mm, equivalent to 0.9% of maximum stroke length, which is deemed satisfactory. However, it is important to acknowledge the presence of several assumptions in the calculations of the estimated backlash, leading to a considerable level of uncertainty regarding the performance of the suggested guide vane system.

Sammendrag

Denne masteroppgaven undersøker mekanisk slark i ledeapparatet på Francis-riggen ved Vannkraftlaboratoriet, NTNU Trondheim. Arbeidet er en videreføring av prosjektoppgaven av Haugum [1], og både numeriske og eksperimentelle analyser er gjennomført for å analysere det eksisterende ledeapparatet. For å oppfylle stabilitetskravet om maksimal slark tilsvarende 1% av maksimalt aktuatorslag, foreslås det også et nytt design av ledeapparatet. Eksperimentelle målinger på det eksisterende systemet avdekket en mekanisk slark på $2,60 \pm 0,29$ mm, som tilsvarer et gjennomsnitt på 4,15% av maksimalt aktuatorslag. For det nye, foreslåtte designet ble det estimert en slark på rundt 0,56 mm, som tilsvarer 0,9% av maksimalt utslag. Dette anses tilfredsstillende i forhold til stabilitetskravene. Likevel er det imidlertid viktig å ta med i betraktningene at det er flere antagelser involvert i beregningene av estimatet, noe som vil føre til en betydelig usikkerhet knyttet til om det foreslåtte ledeapparatet vil ha en slark som er innenfor stabilitetskravene.

Contents

Acknowledgements	i
Abstract	ii
Sammendrag	iii
Contents	iv
List of Symbols and Abbreviations	vi
List of Tables.....	viii
List of Figures	ix
1 Introduction.....	1
1.1 Background	1
1.2 Scope and limitations	1
2 Literature review.....	3
2.1 Stability of hydropower plants	3
2.2 Mechanical slack.....	3
2.3 Slack mitigation measures	4
3 Dynamical motion of guide vane systems.....	6
3.1 Basics of turbine governing	6
3.2 The guide vane system	7
3.3 Mechanical backlash.....	9
3.3.1 Fits and clearances.....	10
4 CAD-models and motion simulations.....	12
4.1 Existing guide vane system	12
4.1.1 Motion simulations	13
4.1.2 Validation of the simulations.....	15
4.2 Changes in system design	16
4.3 Motion simulation results and discussion	17
5 Experimental setup and methods.....	20
5.1 Mock-up	20

5.1.1	Measurement techniques	21
5.1.2	Test procedure	22
5.2	Backlash tests on the rig	23
5.2.1	Cantilever beam connected to the top of the spiral case cover	24
5.2.2	Joints connected to the hydraulic actuator	25
5.2.3	Cantilever beam connected to the governor ring.....	26
5.2.4	Governor ring horizontal displacement	26
5.2.5	Guide vane – governor ring connection.....	27
6	Experimental results and discussion.....	28
6.1	Measurements on mock-up	28
6.2	Measurements on Francis rig guide vane system	30
6.2.1	Measured backlash from separate parts of the guide vane system	31
6.2.2	Uncertainty contributions from sensors	34
6.3	Suggested slack mitigation measures and estimated backlash	35
6.3.1	Estimated backlash from each part of the new system	37
6.3.2	Uncertainty from sensors in the new design.....	41
7	Conclusion	42
8	Further work.....	43
9	References	44
Appendix A	Master’s agreement	47
Appendix B	49
Appendix C	50
Appendix D	60
Appendix E	64
Appendix F	75
Appendix G	76
Appendix H	80
Appendix I	81

List of Symbols and Abbreviations

<i><u>Symbol</u></i>	<i><u>Description</u></i>	<i><u>Unit</u></i>
δ	Deflection	[m]
Δ	Change	[-]
θ	Angular position	[°]
ρ	Density	[kg/m ³]
ω	Rotational speed	[rad/s]
a	Distance	[m]
e	Absolute uncertainty	[m]
E	Young's modulus	[Pa]
f	Relative uncertainty	[%]
f_0	Nominal grid frequency	[Hz]
g	Gravitational acceleration	[m/s ²]
H	Hydraulic head	[m]
I	Second moment of inertia	[m ⁴]
K_i	Integral gain	[-]
K_p	Proportional gain	[-]
L	Length	[m]
M	Torque	[Nm]
n_0	Nominal turbine speed	[min ⁻¹]
p	Number of pole pairs	[-]
P	Load (force)	[N]
P_N	Grid power load	[W]
Q	Volumetric flow	[m ³ /s]
r	Radius	[m]
R	Resolution	[m]
T_a	Acceleration time of the rotating masses	[s]
T_c	Closing time	[s]
T_r	Reflection time	[s]
T_w	Acceleration time of the water masses	[s]
x	Linear position	[m]

<u>Abbreviation</u>	<u>Description</u>
CAD	Computer aided design
GV	Guide vane
GVA	Guide vane angle
IIR	Infinite impulse response
NTNU	Norwegian University of Science and Technology

List of Tables

Table 4.1: Selected slack simulation results.	18
Table 6.1: Mock-up results with moving plate.....	29
Table 6.2: Mock-up results with fixed plate.	29
Table 6.3: Total backlash measured on Francis rig guide vane system.....	30
Table 6.4: Measured displacement of rig parts during guide vane system operation.	31
Table 6.5: Uncertainties from digital sensors.....	35
Table 6.6: Total estimated backlash on the new Francis rig guide vane system.....	36
Table 6.7: Estimated backlash in the new guide vane system.	40
Table 6.8: Uncertainties from digital sensors in the new system.	41
Table 8.1: Priority lists for implementation of backlash-mitigating measures.	43
Table D.1: Motion contact sets.	62
Table D.2: Motion contact properties.....	63
Table D.3: Simulation settings.	63
Table G.1: Dial gauge offset for 4 mm travel.	76
Table G.2: Measured values and absolute uncertainties.	77
Table G.3: Relative uncertainties from measurement variation, calibration, and resolution.....	78
Table G.4: Sensor specifications and relative uncertainty.....	78
Table G.5: Sensor specifications and relative uncertainty on the new system.	79
Table H.1: Calculations and specifications of beam deflections.	80

List of Figures

Figure 3.1: Power balance over the runner-generator system [26].....	6
Figure 3.2: Conventional design for adjustments of the guide vanes. Ref. Kværner Brug AS.	7
Figure 3.3: Guide vane system with slots.	8
Figure 3.4: Mechanical backlash causing a delay in guide vane angle change.....	9
Figure 3.5: Close-running and sliding fit including tolerances [25].....	10
Figure 4.1: The guide vane system at the Waterpower Laboratory, NTNU.	12
Figure 4.2: CAD-assembly of the existing guide vane system.....	13
Figure 4.3: The model used for simulations in Inspire.	14
Figure 4.4: Damper (foreground) and actuator (background). The cylindrical joint in the actuator is shown by the green connection where the cylinder rod is sliding through the cylinder sleeve.	14
Figure 4.5: Experimental actuator stroke and guide vane motion.	15
Figure 4.6: Simulated actuator stroke and guide vane motion. “Pin 19.94” is scaled down to a diameter of 18.25 mm to reach the desired guide vane angle offset.	16
Figure 4.7: Alternative connection between the governor ring and the guide vanes. .	17
Figure 4.8: Comparison of design performance.	19
Figure 5.1: Assembly of the test parts for the new connection.	20
Figure 5.2: Mock-up with the old connection mounted on a welding table.....	21
Figure 5.3: Screenshot from a video of the measurements.	23
Figure 5.4: Dial gauge measurement on the beam fixed to the top of the spiral casing.	24
Figure 5.5: Dial gauge measurement on the backlash experienced in the first actuator joint.....	25
Figure 5.6: Dial gauge measurement on the backlash experienced in the second actuator joint.....	25

Figure 5.7: Dial gauge measurement of deflections on the beam connected to the governor ring.	26
Figure 5.8: Dial gauge measurement on linear, horizontal governor ring displacement.	27
Figure 5.9: Dial gauge measurements on guide vane shaft.....	27
Figure 6.1: Top view of the beam fastened to the spiral casing illustrating the deflection.	32
Figure 6.2: The thinnest part of the beam connected to the governor ring is most exposed to stress.....	33
Figure 6.3: Cross section (left) and CAD-model (right) of an alternative beam design.	37
Figure 6.4: Cross section (left) and CAD-model (right) of an alternative beam design.	38
Figure 6.5: Alternative design of the connection to the guide vane shaft.	39
Figure B.1: Selected fits including tolerances for the hole based system [25].....	49
Figure D.1: Grounded parts.....	60
Figure D.2: Rigid groups.	61
Figure D.3: Joints applied in the model.	61
Figure D.4: Contact sets in the model.....	62
Figure H.1: 2D fixed cantilever beam.	80

1 Introduction

1.1 Background

The Paris Agreement has set ambitious targets for mitigating global warming [2], and one of the strategies adopted to obtain this, is to increase the proportion of renewable production in the energy mix. Solar and wind energy are among the most promising renewable technologies, as they have a huge potential and can produce low-carbon electricity. However, their intermittent nature presents a significant challenge for power grid management, as it requires greater reliance on controllable power sources such as hydropower from reservoirs [3]. Therefore, it is imperative to establish swift governance of hydropower plants to ensure stable energy supply in the future.

To address this challenge and conduct research on modern dynamic operation of hydropower plants, the Waterpower Laboratory at NTNU Trondheim has made significant modifications on the Francis test rig during the academic year of 2021/22. From these modifications the rig aims to be operated with emulated real-world signals from the power grid and the changes included an installation of a proper turbine governor to replace the previously used manually controlled linear actuator. The new turbine governor was designed to automatically adjust the guide vane opening in response to load changes, and thereby improve the power control capabilities. Its characteristics were investigated by two master's theses in 2022 [4], [5], which identified a backlash in the mechanical governor system equal to 4.6% of the full stroke length of the hydraulic actuator controlling the guide vanes, avoiding stable operation of the rig during exterior load variations. Through the specialization project carried out in the fall of 2022, it was also found that the maximum allowable slack, which still enables stable operation is about 1% of the maximum stroke length [1].

1.2 Scope and limitations

The objective of this master's thesis is to design a new mechanical assembly for the turbine governor system of the Francis rig at the Waterpower Laboratory, which mitigates the mechanical backlash experienced on the existing system. The research process will involve a review of relevant literature concerning governing stability of

hydropower plants, mechanical backlash, and backlash mitigation measures. Furthermore, the backlash experienced on the existing guide vane system will be examined through numerical simulations and experimental measurements of the mechanical parts on the rig. The experimental measurements will be done on a mock-up of the guide vane – governor ring connection and on the rig. Moreover, the alternative design of the guide vane system will also be evaluated.

The project will not investigate any aspects of the hydropower system's characteristics regarding runner design or pipe layout, as it will only focus on the mechanical parts of the guide vane system. Also, the project will not present any frequency analysis of the system in the form of APF-diagrams or block diagrams. It will instead rely on the analysis from previous work [1], indicating that mechanical slack under a certain magnitude should enable stable governing.

2 Literature review

2.1 Stability of hydropower plants

Due to the growing electricity demand and production in the start of the 20th century, the technology of turbine governors in electricity production plants was rapidly developed during the 1920's [6]. By 1930, turbine governors were widely used to stabilize the output frequency in steam turbine power plants, and the technology was quickly adopted by the hydropower plants [7], [8]. From the first hydraulic-mechanical regulators the technology has been further developed and investigated through studies done on methods to establish optimum governor settings for stable operation [9], and through mathematical models of the hydropower governing systems [10]. The last decades, numerical models simulating the dynamic operation of the hydropower systems have also been carried out. This includes frequency control models combining both wind and hydropower [11], and simulations of the coupled hydraulic-mechanical-electric system for a hydropower station [12]. In other words, the research on stable operation of hydropower plants is still developing rapidly.

2.2 Mechanical slack

Mechanical slack, also known as mechanical backlash, can be defined as “the play between adjacent movable parts (as in a series of gears)” [13], and is a nonlinearity which will influence the stability of a dynamically operated hydropower plant. Backlash has been investigated in hydropower governors since the 1950s and is a well-known problem in hydropower production. As stated in the introduction of Donaisky et al. [14], one of the pioneering studies to examine the impact of mechanical slack on the speed control system was conducted by Concordia et al. [15], and the paper is notable for identifying the existence of undamped oscillations in the frequency output that result from the nonlinearity. Later, in the 1970s, models for speed-governing systems including their nonlinearities were conducted [16], and in the 1980s the prolonged oscillations documented in prior literature were linked to limit cycles induced by the backlash inherent in the governor model. Approaches on forecasting and examining this were among others outlined by Pantalone and Piezga [17]. The research on the linkage between power plant performance and nonlinearities continued throughout the 2000s, and studies which investigated the linearization of various

features such as dead band, saturation and transport delays were presented [18]. Additionally, studies which investigate the practical considerations for dynamic modelling of hydropower governor systems including nonlinearities were conducted by Villegas Pico and McCalley [19], where the problem of nonlinearities was modelled and compared to measurements from real cases.

Over the last decade, several studies have been done on the measurements of backlash and nonlinearities in real-world powerplants. This includes the study by Saarinen et al. [20], which investigates the rapidity effects on three different Swedish powerplants. The study concludes that a backlash is present somewhere between the actuators and the guide vanes, and the total backlash is measured to be 0.50% (Kaplan turbine), 0.05% (Francis) and 0.25% (Francis) of full actuator stroke length for the three different powerplants. The study states that the oscillations induced by the nonlinearities can be reduced by adjusting the controller parameters. Numerical research on powerplants including backlash has also been conducted the recent years. One of these are carried out by Yang et al. [21], which studies the problem of wear and tear on hydropower systems by adding a backlash of 0.1% to the numerical model. The paper by Liao et al. [22] does also investigate the impact of backlash on the stability of a dynamically operated powerplant through numerical simulations. Here, real-world measurements from a large hydropower plant in China showing backlash in the range from 0.005% to 0.02%, are used as a basis, and simulations are done for a 2.5% load change referred to maximum power output with the backlash varying from 0 to 0.5%. The article concludes that backlash nonlinearity will significantly reduce the range of stable operation with respect to the characteristic parameters K_p , K_i , T_w , T_a , T_c and T_r .

2.3 Slack mitigation measures

As stated by among other [20], the effects of backlash nonlinearities in a hydropower plant can be mitigated by adjusting the characteristic parameters of the system. Nevertheless, if the mechanical slack initially is smaller, the adjustments to stabilize the system will also be easier to handle. Therefore, it will be beneficial to mitigate the mechanical slack. To the best of the author's knowledge, the research field of mechanical slack mitigation measures on hydropower governors is not very prevalent. But, some anti-backlash mechanisms can be taken from other research fields, such as backlash elimination methods from gear transmissions [23]. These measures include minimizing the clearance in joints by applying precise machining methods, adjusting gear center distance, and using conical involute gears. Since the hydropower governor

system does not apply gears in the same manner that is referred to in this article, the measure concerning minimizing clearance would be the most applicable. This will among others mean that it is desirable to apply circular joints instead of pin-to-slot connections because they allow for smaller clearances before the pin seizes the hole or slot [24], [25].

3 Dynamical motion of guide vane systems

To enable stable governing of a hydropower plant, one will have to take various conditions into account. This will among other include the properties of the moving water masses, and the physical design of the plant, which in the end will affect the system characteristics [26]. Another thing which also will affect the characteristics, is the layout of the guide vane system which controls the inflow to the hydraulic turbine, and thus the power output of the system. This chapter will present the basics of turbine governing, and specifically examine the mechanics of the guide vane system, including the theory and effects of backlash nonlinearities.

3.1 Basics of turbine governing

For the electrical grid to maintain a stable frequency, the power plants connected to the grid will have to deliver an electrical power production, P_N , which matches the electricity consume from the customers. In a hydropower plant, it is the turbine governor which solves this problem by adjusting the water flow, Q , through the turbine. In this way the rotational speed, ω , of the turbine system shown by Figure 3.1, will be held constant even if P_N changes.

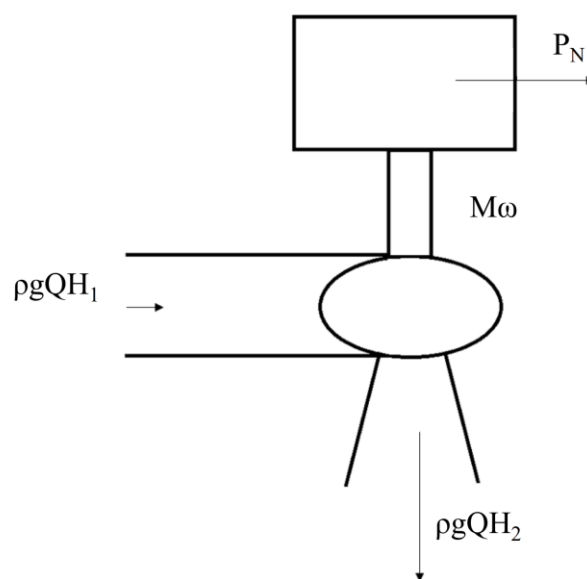


Figure 3.1: Power balance over the runner-generator system [26].

Since the turbine system is synchronous, the rotational speed of the turbine is directly proportional to the electrical frequency from the generator. Thus, the nominal grid frequency, f_0 , is given by Equation 3.1 [26].

$$f_0 = n_0 \frac{p}{60} \quad 3.1$$

Here, n_0 is the nominal turbine speed in revolutions per minute, and p the number of pole pairs in the generator. In other words, to contribute to grid stability the turbine must rotate at a given nominal speed even though the exterior load from the power grid is varying. This is where the importance of a functioning and swift guide vane system becomes clear.

3.2 The guide vane system

For a Francis turbine, the volumetric flow is adjusted by changing the inlet angle of the guide vanes, which as illustrated in Figure 3.2 is airfoil-shaped blades located between the spiral casing and the runner. The top of the guide vane shaft is, via links or slots, connected to a governor ring which again is connected to one or more servo motors or hydraulic actuators. When a change in guide vane opening is desired, the linear motion of the actuators initiates a rotational motion for the governor ring. Due to its linked connection, the rotation of the governor ring will then cause the guide vane shaft to rotate, and the guide vane inlet angle is changed.

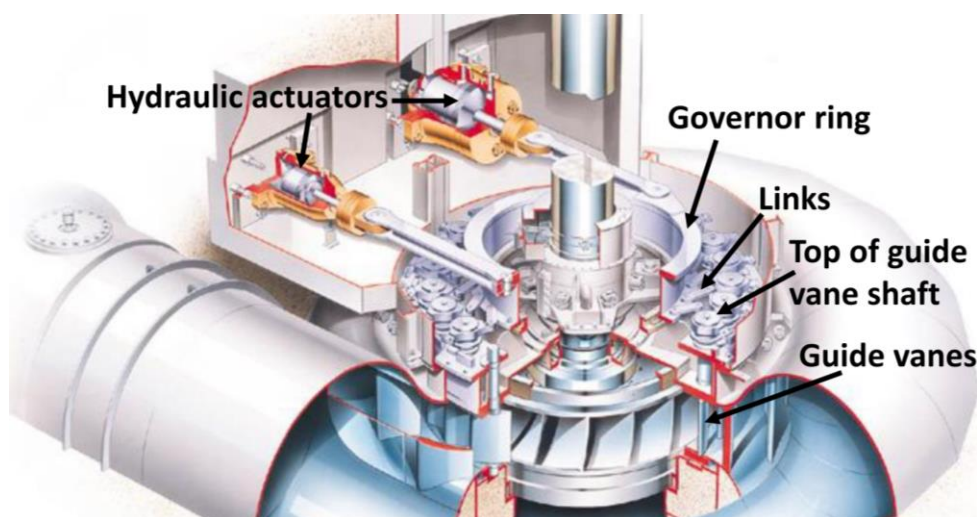


Figure 3.2: Conventional design for adjustments of the guide vanes. Ref. Kvaerner Brug AS.

The layout of the guide vane system will to a large extent be determined by the size of the unit. For medium to large, conventional units it is most common to have two hydraulic actuators to handle the forces involved and rotate the governor ring, one actuator is pushing and one pulling. Additionally, an oblong link is commonly used to connect the ring to the guide vane shaft, and in this way make all the connections circular, as opposed to the configuration which will be presented below.

For smaller units and test rigs, a simpler configuration is often utilized whereby the motion of the guide vanes is activated by a single servo motor or hydraulic actuator. This will make the motion control easier, and it is also containing fewer mechanical parts. Another thing which can be used by the smaller systems, is the application of slots instead of links in the connection between the governor ring and the guide vane shaft. In this configuration, a pin, which is connected to the guide vane shaft via a lever arm, will slide in a slot on the governor ring to enable change of the guide vane angle, as shown in Figure 3.3. By applying this slot-configuration, the layout will contain one less joint as the oblong link will not be needed anymore. This layout can also save some space which might be essential for the smaller configurations. However, as mentioned in Section 2.3, the implementation of a sliding connection can cause an increase of total mechanical backlash. As will be presented in the next subsection, this is not desirable for a dynamical system.

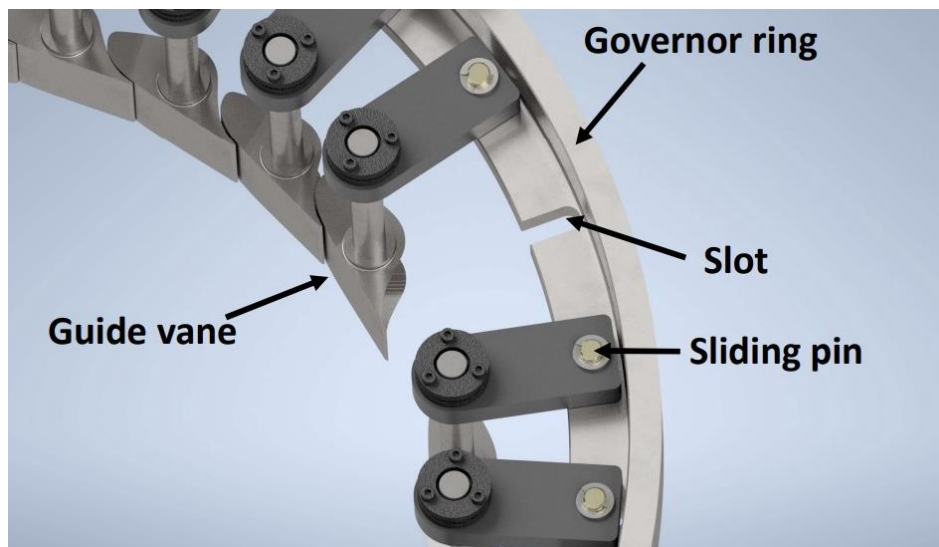


Figure 3.3: Guide vane system with slots.

3.3 Mechanical backlash

As described in Section 2.2, mechanical backlash can affect the stability of the operation of a hydropower plant. This can occur even though the hydropower system is optimized and dimensioned with acceleration time of the water masses, acceleration time of rotating masses, and integration time and gain for the turbine governor, all initially leading to a stable operation during varying exterior load [26]. If a mechanical backlash is present in the guide vane system, the guide vanes might not be able to reach the desired angle calculated by the governor to keep up with the changes in exterior loads. An example of this is given in Figure 3.4, where a mechanical backlash somewhere between the hydraulic actuator and the guide vanes is causing the actuator stroke to move 1.6 mm before the guide vane angle changes. Such a backlash could cause the hydraulic power to not match the load from the grid, causing an uneven power balance over the turbine which again will accelerate the unit and the frequency delivered might not be within the grid requirements, which is 50 ± 0.1 Hz in Norway [27]. The acceleration is causing an offset in turbine speed and frequency, which again will cause the turbine governor to change the guide vane angle to balance the power. However, the backlash is still present, preventing the system to reach the desired value for the guide vane opening, and the unit speed and power production will not manage to settle. In this way the backlash will cause oscillations in frequency output and the system is unstable. It is therefore desirable to mitigate the backlash as much as possible.

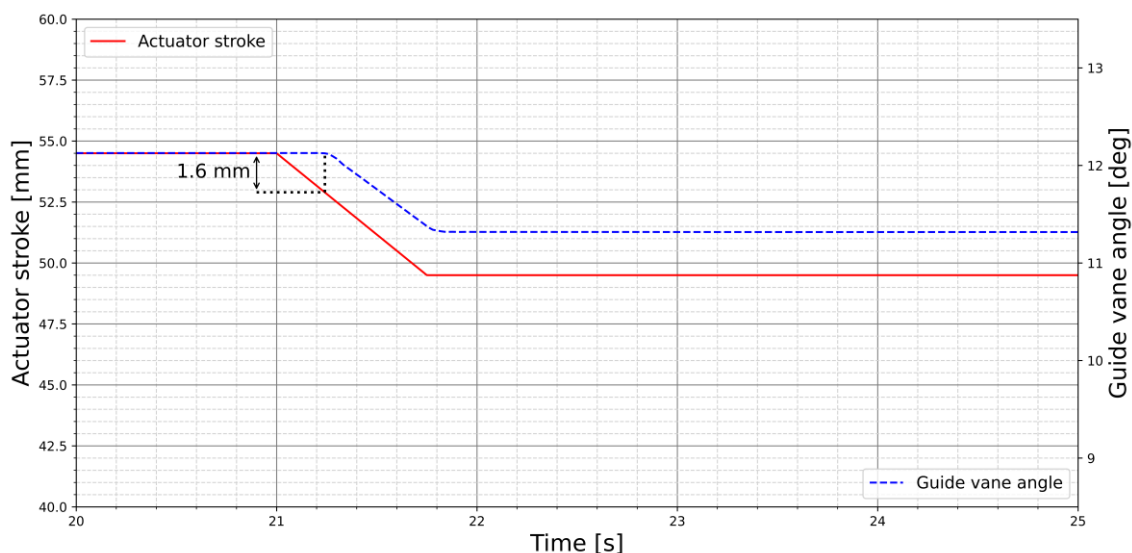


Figure 3.4: Mechanical backlash causing a delay in guide vane angle change.

3.3.1 Fits and clearances

To enable dynamical motions between the parts, every mechanical assembly needs to have a certain engineering fit in the joints. The type of fit and size of clearance between the parts, are mainly decided by the desired characteristics of the joint. For a shaft in a hole, as illustrated in Figure 3.5, the choice of fit depends on how the shaft should be able to move or rotate. E.g., a component designed for small and precise angular motions will demand low clearances, shown by the sliding fit in Figure 3.5, while a component rotating at high speed would need a fit with bigger clearances, as shown by the close-running fit in the same figure [25].

When deciding the fit and thus the nominal clearance, the precision of the manufacturing process must also be considered. This is done through use of tolerances which says something about the uncertainty of the dimensions on the manufactured part. In a hole-shaft connection, tolerances can be used to avoid the shaft to get a diameter greater or equal to the hole, which would restrict dynamical motions by the shaft seizing the hole. For such a case the tolerance is decided by the table shown in Appendix B.

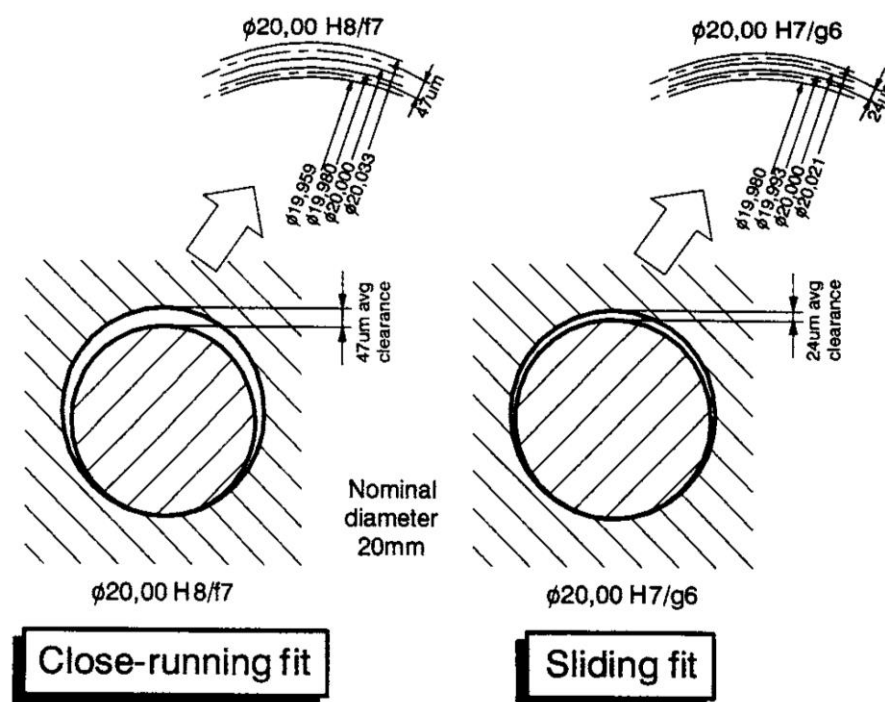


Figure 3.5: Close-running and sliding fit including tolerances [25].

Considering the mechanical backlash of a system, it is also very important to apply the right tolerances and fits to the joints. For a guide vane system which demands

high precision movement, the backlash would need to be as small as possible, meaning that the joints should be manufactured with a sliding fit as precise as possible. Additionally, because a circular connection generally can be made with smaller tolerances than a sliding connection [24], one would prefer shaft-in-hole connections to minimize the total backlash of the system.

4 CAD-models and motion simulations

The guide vane system at the Francis test rig at the Waterpower Laboratory at NTNU is initially designed for steady operation, where functionality and simplicity has been prioritized over precision of the movements. Now, as the test rig will be operated more dynamically, the demand for more precise and backlash-free governing is increasing, and a new design for some of the components should be suggested. This chapter describes the existing system together with a digital analysis done on the dynamical motions. Further, some changes in design to improve the precision of the movements is suggested, and a similar motion analysis is done on this model. To validate the dynamical simulations, the simulation results are compared to lab measurements done on the existing model.

4.1 Existing guide vane system

The existing guide vane system at the rig is utilizing the unconventional layout presented in Figure 3.3, with one hydraulic actuator and pin-slot connections to transfer movement from the governor ring to the guide vanes. The hydraulic actuator is connected to a cantilever beam on both sides; one bolted to the top of the spiral case

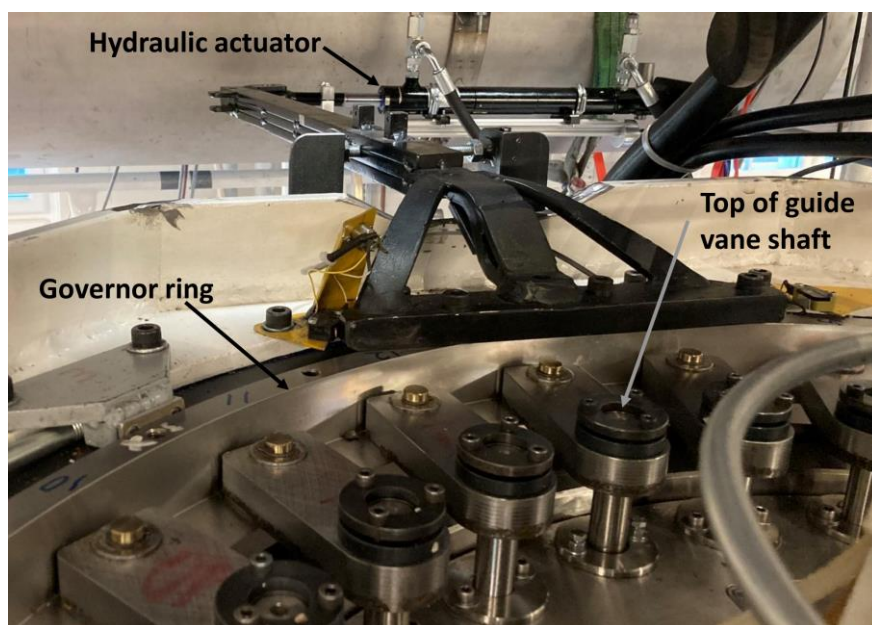


Figure 4.1: The guide vane system at the Waterpower Laboratory, NTNU.

cover, and one to the edge of the governor ring. An image of the layout is presented in Figure 4.1.

To analyze the existing system, a CAD-model with exact dimensions of the involved parts had to be carried out. Since there was no complete CAD-model of the guide vane system (only for the governor ring and the guide vanes) measurements on all involved parts, including clearances in the joints, had to be done. The measurements were done with meterstick and caliper for the bigger dimensions, while the clearances and pin dimensions were measured by micrometer. Based on the measurements and the CAD-files originating from the construction of the Francis rig, an assembly of the parts involved in the system was developed in the CAD-software SolidWorks 2021 [28]. As illustrated by Figure 4.2, this included the arm which is rigidly connected to the top of the spiral casing, two cylinders to model the hydraulic actuator, a long arm from the actuator to the governor ring, and the governor ring with the guide vanes. The technical drawings of the parts are collected in Appendix C.

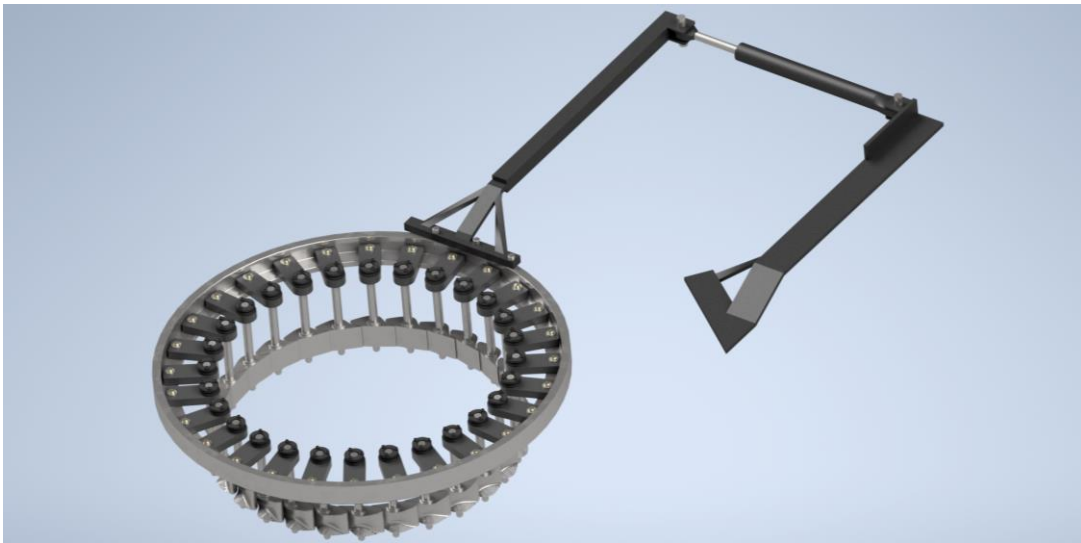


Figure 4.2: CAD-assembly of the existing guide vane system.

4.1.1 Motion simulations

The motion simulations were carried out in the multibody simulation software Altair Inspire 2022 [29]. To do this, a SLDPRT-file of the CAD-assembly was exported from SolidWorks and imported into Inspire to prepare the simulations. The CAD-assembly is shown in Figure 4.3, and as seen by the figure the model is only containing only one guide vane connection to save CPU usage. In this way the software would not need to unnecessarily calculate the motion of the remaining 27 guide vanes.

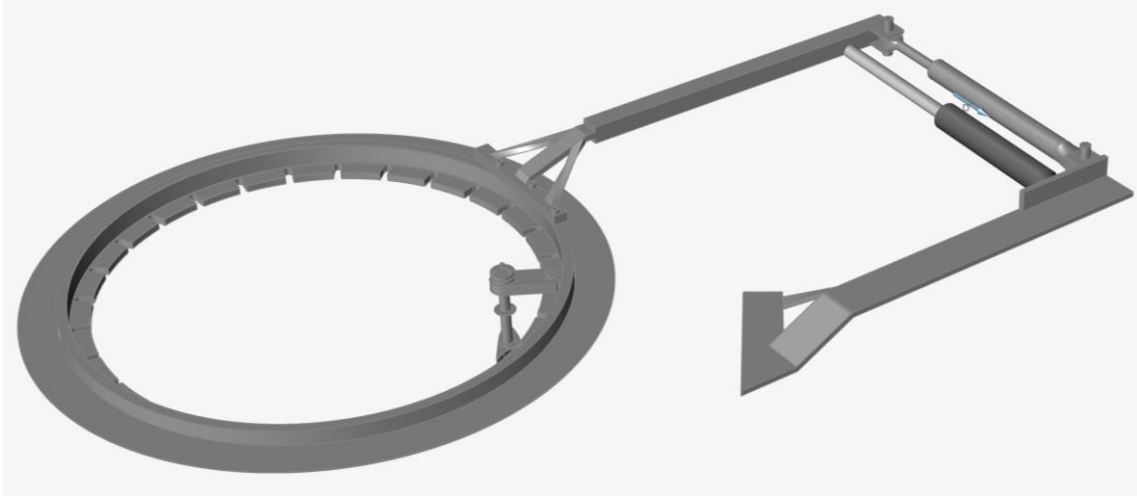


Figure 4.3: The model used for simulations in Inspire.

With the file imported to Inspire, the grounds, rigid groups and joints were defined to enable the desired motions. Additionally, to enable slack in the system, contact groups including their associated stiffness, damping and friction were defined. In this way the motion in the system could be translated by physical contact between the parts, as opposed to perfect joints with no friction and contact which would be the case when the joint function is used instead. To initiate the motion of the model, the aligning cylinder rod and sleeve shown in Figure 4.4, were defined as an actuator, and to add friction and dampen the motion, a linear damper parallel to the actuator was included. The details of the simulation setup can be found in Appendix D.

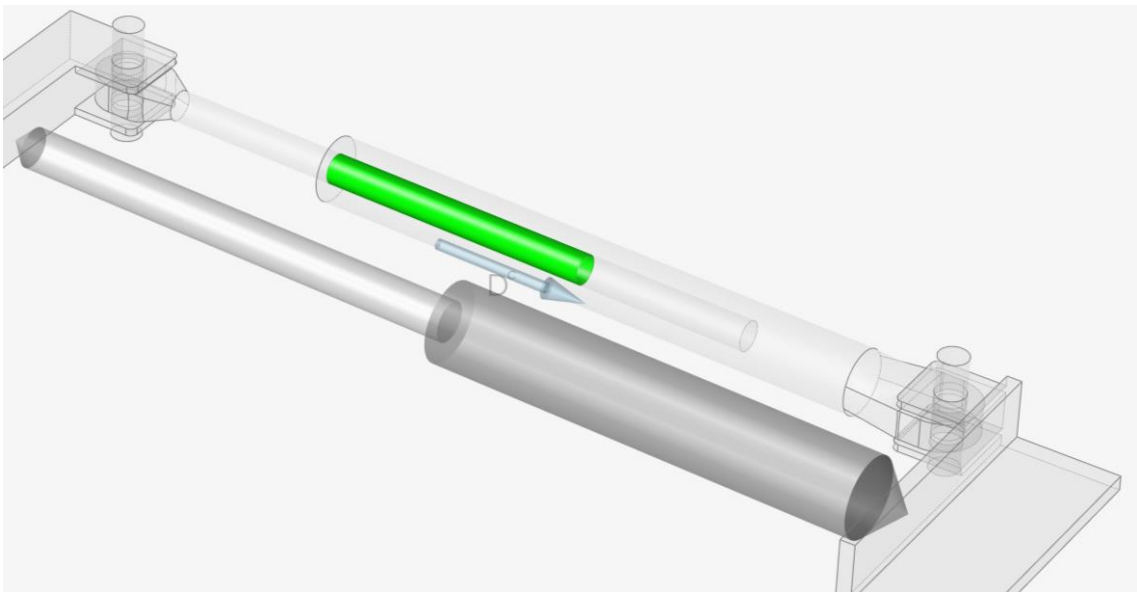


Figure 4.4: Damper (foreground) and actuator (background). The cylindrical joint in the actuator is shown by the green connection where the cylinder rod is sliding through the cylinder sleeve.

4.1.2 Validation of the simulations

To validate the simulations, the motions in the simulated system were compared with data from the real system in the lab. The lab data was sampled in connection with Ingranata’s master’s thesis [5] and was carried out by driving the hydraulic actuator back without any loads from the water. In this way the backlash was provoked.

Because the experimental data had a lot of noise, an infinite impulse response (IIR) filter was applied by utilizing the function `scipy.signal.lfilter` in a Python-code. The data is shown by the red and blue line in Figure 4.5, which respectively illustrates the actuator and guide vane motion. The fact that the guide vane angle was not managing to follow the actuator stroke states that a mechanical backlash was present in the system. As mentioned in Section 1.1, this backlash was found to be about 4.6% of the full actuator stroke length, which over a full opening of the guide vanes of 14° will correspond to an offset of about 0.65° [5]. The value can be found in the plot where even though the actuator position is the same in the time interval 0-4 s as it is for 22-30 s, the guide vane angle deviates by 0.65° due to the backlash.

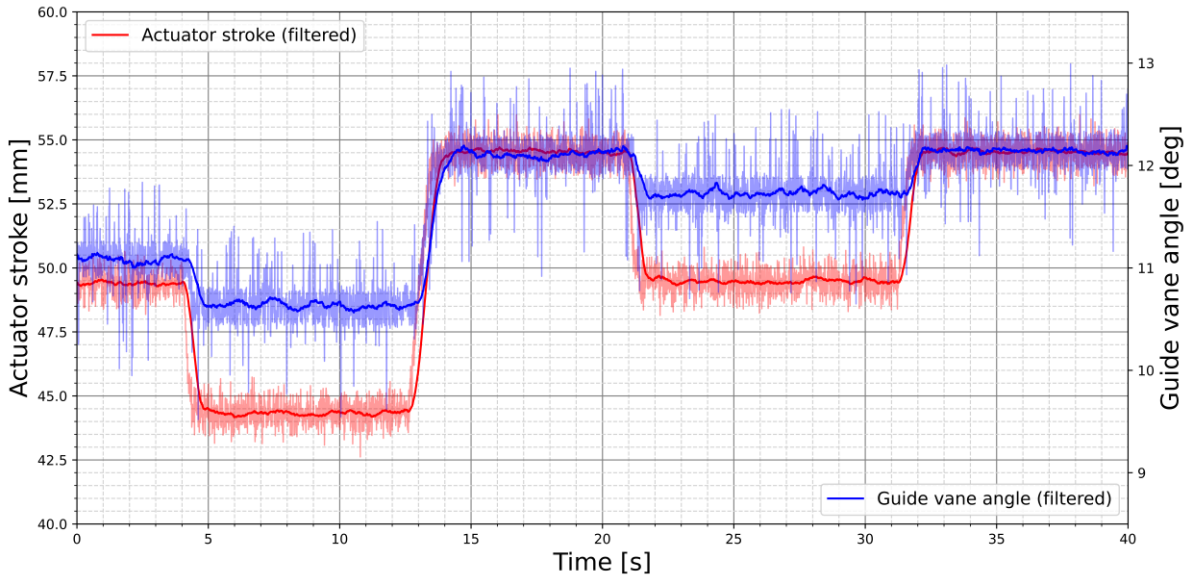


Figure 4.5: Experimental actuator stroke and guide vane motion.

The simulation data was obtained by creating a table with actuator displacement data (displacement vs time) similar to the lab case and importing it into Inspire, enabling the actuator in the simulation to perform the same motions as in the real-world system. Then, the simulation ran with simulation settings like the ones presented in Appendix D. However, because the simulated backlash did not reach the same values as the lab backlash, a scale adjustment on one of the pins connected to the hydraulic actuator

was implemented. The pin called “Pin 19.94” was scaled down to a diameter of 18.25 mm in Inspire. In this way the amount of backlash was found to be the same in the digital model and the real case, and the simulation model was validated to obtain sufficient results for the system. This meant in turn that the model could be used as a basis to compare alternative designs for the governor ring – guide vane connection. The simulated results are shown in Figure 4.6, which also states that the offset in guide vane angle is about 0.65° for the two previously mentioned time intervals.

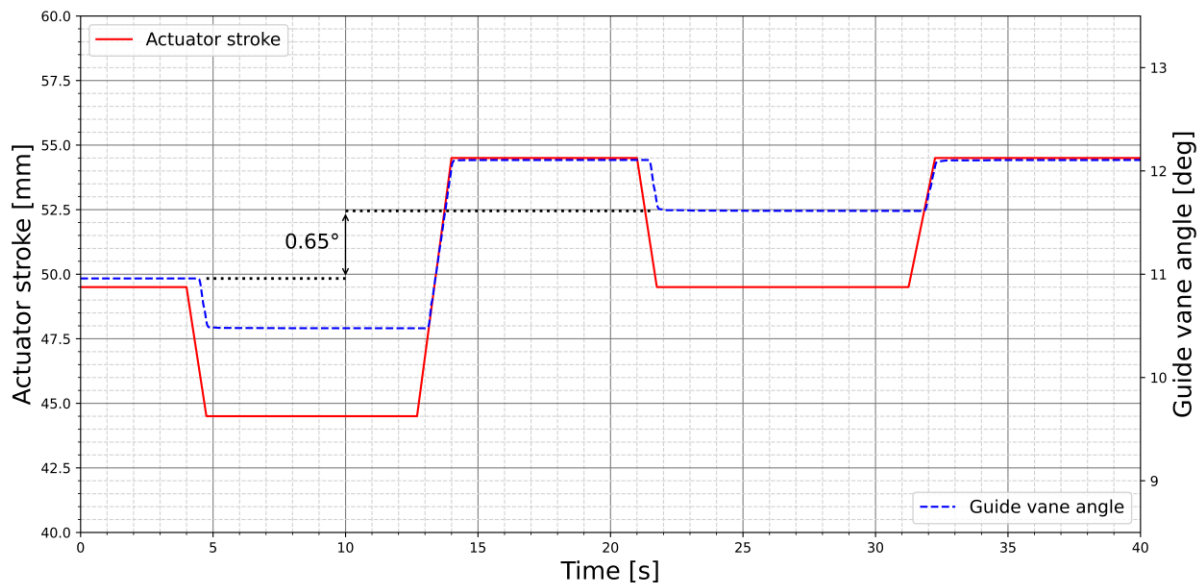


Figure 4.6: Simulated actuator stroke and guide vane motion. “Pin 19.94” is scaled down to a diameter of 18.25 mm to reach the desired guide vane angle offset.

4.2 Changes in system design

To try mitigating the slack experienced in the system, a new design for the governor ring – guide vane connection was developed. The new design takes basis in the conventional guide vane system presented in Section 3.2, utilizing links instead of slots to transfer the motions. Due to the circular fits which allows for smaller clearances without the rod seizing the hole, this layout might mitigate the total backlash of the system.

Like the CAD-model of the original design, the parts were developed in SolidWorks. This included editing the governor ring to contain holes in addition to the slots, as well as making a new rod to fit the hole, a link, and another rod to connect the lever arm to the link. The same guide vane and lever arm as for the previous system was used, and a rendered image of the new assembly, zoomed in on the new connections,

is presented in Figure 4.7. Additionally, the technical drawings of the connections are presented in Appendix E.

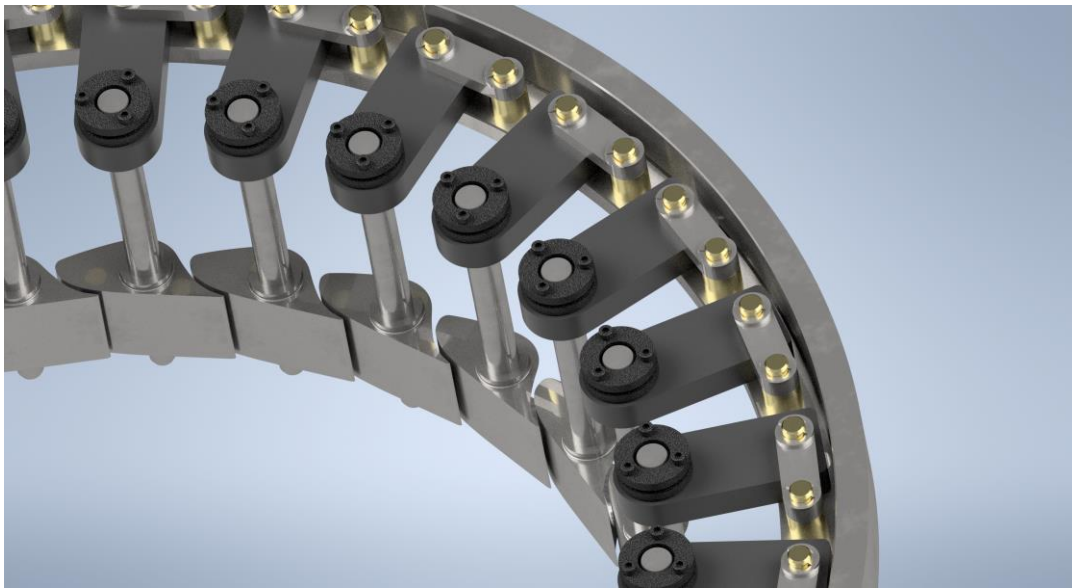


Figure 4.7: Alternative connection between the governor ring and the guide vanes.

After the assembly was finished, a version containing one guide vane group was exported from SolidWorks and imported to Altair Inspire in the same way as described in Section 4.1.1. Simulations with the same settings were then run.

As presented in Section 4.1.2, the simulations done on the original system did not show a satisfactory amount of backlash when compared to measurements done in the lab, and simulations with different scaling of the part “Pin 19.94” were carried out to try match the measured values. The fact that the original model had to be manipulated to get the desired results indicates that there might be some elements in the real system that’s not correctly modelled by the motion simulation. Nevertheless, the numerical simulation setup for both the new and the existing system design are identical, meaning that the results from the simulations of the two systems should be comparable.

4.3 Motion simulation results and discussion

In Table 4.1, the simulation results for some selected pin diameters and a version with perfect joints in the actuator pin joints, are shown in terms of backlash defined by Figure 3.4. From the table it can be seen that the system slack is increasing quite a lot when the clearance in the joint is increased. However, the difference in absolute slack magnitude between the new and the existing design is very small for each pin

case and it is this difference which really says something about the performance of the new design compared to the existing one. On average for all simulations the new design has about 0.05 mm less slack than the existing system, which corresponds to 0.08% of maximum stroke length (62.5 mm).

Table 4.1: Selected slack simulation results.

Pin diameter	Slack Existing design	Slack New design	Slack reduction Existing → New
18.25 mm	2.940 mm	2.902 mm	0.038 mm
19.00 mm	1.627 mm	1.545 mm	0.082 mm
19.94 mm	0.269 mm	0.239 mm	0.030 mm
Perfect joint	0.109 mm	0.080 mm	0.029 mm

As presented in Section 1.1, the total backlash of the existing system is measured to be 4.6% of the maximum stroke length. This means that a reduction of 0.08 percentage points will not do any significant change to the total backlash. It is therefore clear that the numerical simulations in Altair Inspire is either not managing to calculate and illustrate the slack which is coming from the connection between the guide vane shaft and the governor ring, or the main contribution to the total slack is coming from somewhere else in the guide vane system. Also, it can indicate that the model does not manage to correctly account for stiffness and deflections of the involved parts.

Figure 4.8 displays a more illustrative version of the data shown in Table 4.1. The figure is showing the correlation between pin diameter and slack magnitude on both the new and the existing system with eight different diameters applied to “Pin 19.94”. This version confirms the tendencies from Table 4.1, as the slack is increasing for increasing pin diameter for both designs. Also, it is showing that for all eight cases the slack of the new design is smaller than for the existing design with corresponding clearance in the pin joint, and that the difference in slack magnitude between the existing and the new guide vane connection looks quite independent of the pin diameter. From the data it can be shown that the average slack is 1.38 mm for the existing design, while the new design performs an average of 1.43 mm. This will mean that the simulations show an average slack reduction of 3.34% for the new design compared to the existing one.

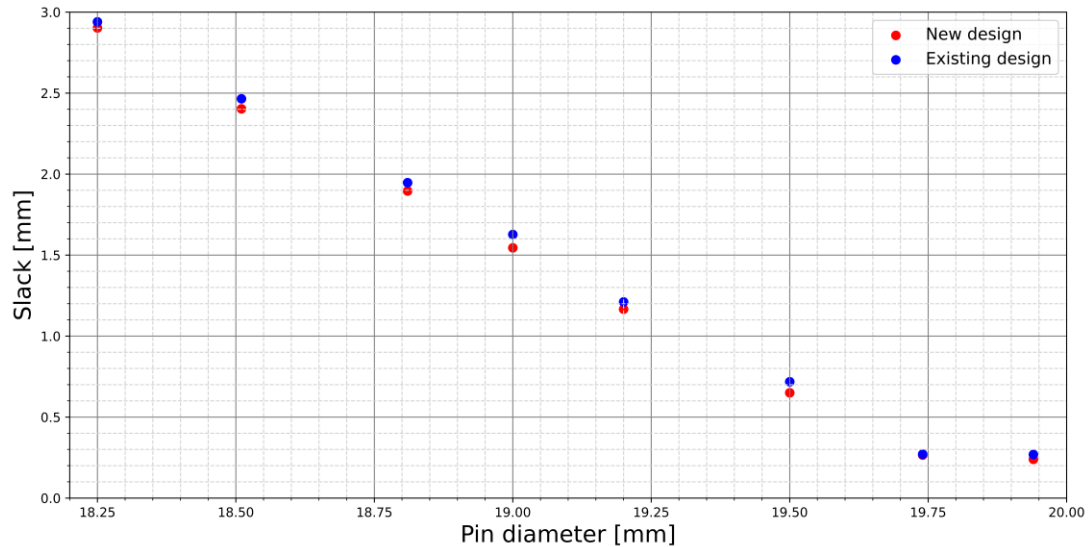


Figure 4.8: Comparison of design performance.

By once again investigating Table 4.1, it can be observed that the slack is reduced by 0.16 mm just by excluding the slack coming from the two joints which the actuator is connected to. This means that according to the simulations, the slack contribution from these two joints is about twice the magnitude of the contribution from the guide vane shaft – governor ring connection. Additionally, the slack in the real system can come from other physical elements such as elasticity in the beams, or clearance inside the actuator which both are neglected in the motion simulations.

Summarizing, it can be stated that it seems like the motion simulation do not manage to pick up all the physical aspects present in the system. This can be seen from the total backlash of the system which is much smaller for the numerical results of the unmanipulated system than it is for the lab measurements. Regardless of that, the simulations are anyway showing that the new design suggestion is performing just a little better than the existing one, with a slack reduction of 0.05 mm. In the end it should also be made clear that the simulations indicates that a majority of the backlash is originating from other joints or components in the model.

To check the characteristics of the new design more thoroughly, the components should also be produced and tested physically. The experimental setup and testing of both the new and the old assembly will be presented in the following section.

5 Experimental setup and methods

In this section the experimental setup and testing of the new connection will be presented. The description will include how the mock-up used to test the connection was set up, which measurement techniques that was used, and how the test was executed. Furthermore, a description of the execution of the additional tests conducted on the Francis rig guide vane system will be provided.

5.1 Mock-up

The parts used in the mock-up were manufactured in the workshop at the Waterpower Laboratory and the details about them are presented in Appendix E. Additionally, a simplified sketch of the test assembly including the dial gauges used to measure displacement of the parts is presented in Figure 5.1.

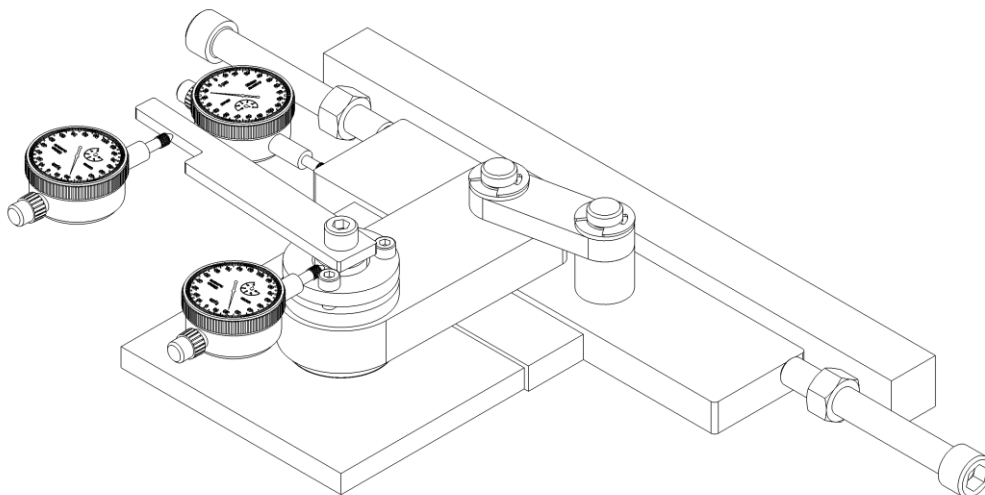


Figure 5.1: Assembly of the test parts for the new connection.

The mock-up shown in Figure 5.1 was mounted on a welding table with screw clamps and mounting brackets from a milling machine. In this way, the characteristics of the new versus the old connection could easily be tested with a minimum of new parts being manufactured. A picture of the mock-up with the old connection is presented in Figure 5.2.

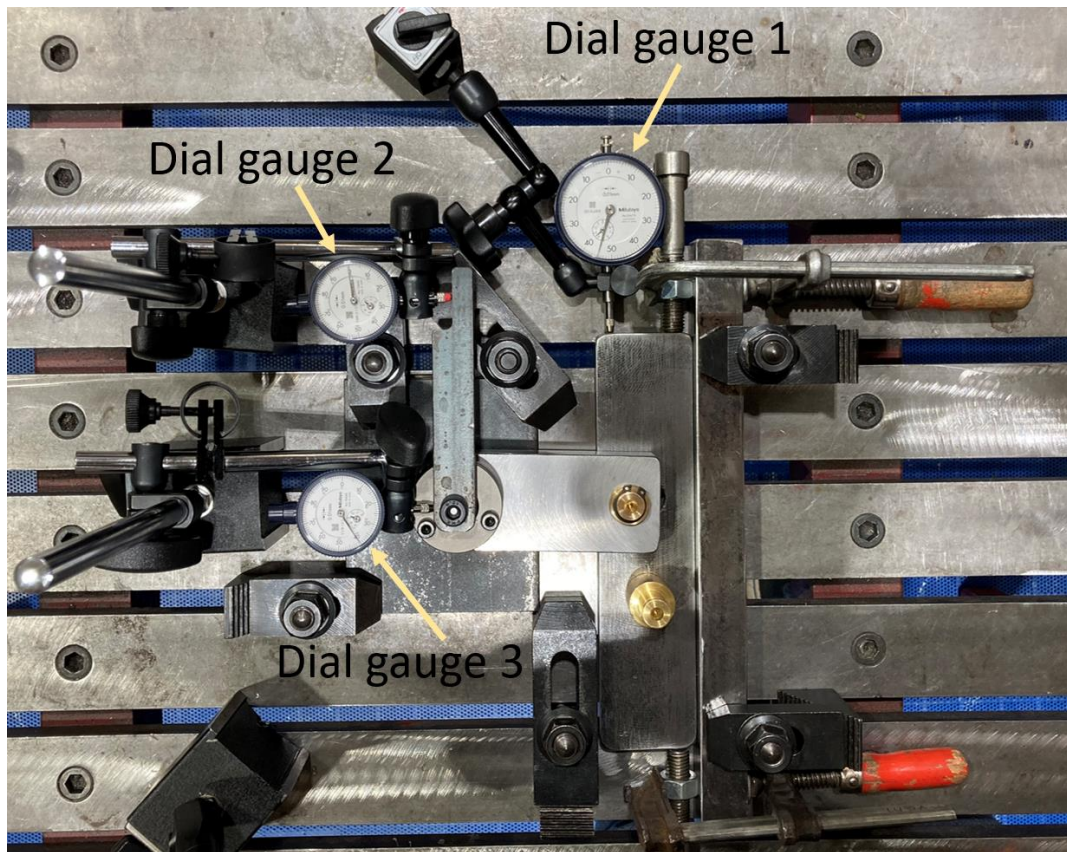


Figure 5.2: Mock-up with the old connection mounted on a welding table.

To simulate the movement of the governor ring, the mounting plate for the rod connected to the lever arm was placed between a slide rail and a space bar which both were fastened to the welding table. In this way the mounting plate could, by rotating the bolts fastened to the sliding rail, slide controlled over the table in a linear motion. The guide vane shaft, which was connected to a fixed plate through a ball bearing, would then rotate and simulate the motion of the guide vanes.

5.1.1 Measurement techniques

To measure the movements of the components in the mock-up, three dial gauges fastened to the table with magnetic stands, were used. In this way the motion of selected parts could easily and precisely be evaluated without having to extensively postprocess the data as would be the case for a digital distance and angle sensor.

As seen in the top of Figure 5.2, the first dial gauge was sat parallel to the sliding plate, to measure its linear motion. The dial gauge is therefore measuring a simplification of the case from the real Francis rig where the governor ring is doing a

radial motion. Nevertheless, because the task of the mock-up was to test the differences in slack between the old and the new connection, it was found that converting the motion from radial to linear would be sufficient. Dial gauge 1 was of the type Mitutoyo 2047S.

Further, a second dial gauge of type Mitutoyo 1044S was applied to the left of the first one in Figure 5.2, to measure the radial displacement of the guide vane shaft. This was done by mounting a rod on top of the guide vane shaft and measuring the linear displacement of the rod 100 mm from the guide vane shaft center. By utilizing Equation 5.1, with x being the linear displacement measured by the dial gauge, the angular displacement or change in guide vane angle, θ , could be calculated. It should be noted that the displacement x is a fraction of the circumference of the circle with a radius of 100 mm and it should therefore be considered as a curved displacement. But, as for the measurements with the first dial gauge, measuring the linear displacement was found to be satisfactory.

$$\theta = 360^\circ \frac{x}{2\pi 100mm} \quad 5.1$$

In addition to the first two, a third dial gauge of type Mitutoyo 1044S was also implemented to the mock-up. This was mounted normal to the guide vane shaft to measure whether the results on dial gauge number 2 was due to bending of the shaft or just pure radial motions. In this way the uncertainties of the measurements presented in Appendix G would be a little more restricted.

5.1.2 Test procedure

To capture the test results, a camera with a framerate of 30 fps was mounted to a magnetic stand, recording dial gauge 1 and 2, as presented in Figure 5.3. Then, to initiate the motion, the bolt in the top right corner of Figure 5.3 was slowly turned with the use of an Allen wrench. After the plate was displaced 3-4 mm, the bolt was turned back to its initial position, and the bolt on the other side of the plate was turned to push the plate back again. This procedure was then repeated a couple of times. In this way the motion which provokes mechanical backlash in the real guide vane system on the Francis rig, was simulated. After recording the entire sequence, the connection between the lever arm and the sliding plate was changed from the old to the new version, and the same test was conducted and recorded once again.



Figure 5.3: Screenshot from a video of the measurements.

In addition to conducting tests with moving the moving plate, tests with fixed slot-hole plate were conducted for both the new and the old connection. In this test, the side of the lever arm connected to the plate was manually pulled back and forth, while the readings on dial gauge 2 was recorded. By doing this, one might uncover some effects which the first test failed to cover due to the lack of loads applied on the system.

5.2 Backlash tests on the rig

Initially, it was assumed that the main contributor to the backlash experienced in the rig came from the guide vane – governor ring connection, and that the testing on other parts of the rig would be redundant. But, due to indications from the executions of the experiments on the mock-up, it was found that extensive tests on the other parts of the guide vane system would be necessary to mechanically measure the backlash experienced during operation of the rig. The tests are done without water running in the system.

5.2.1 Cantilever beam connected to the top of the spiral case cover

The first element tested on the rig, was the horizontal movement of the cantilever beam fastened to the top of the spiral case cover. This was done by mounting the magnetic stand of a Mitutoyo 2047S dial gauge on a pillar independent on the movement of the beam and putting the measuring pin against the beam edge. The pin was put 70 mm from the tip of the beam and the setup is illustrated in Figure 5.4.

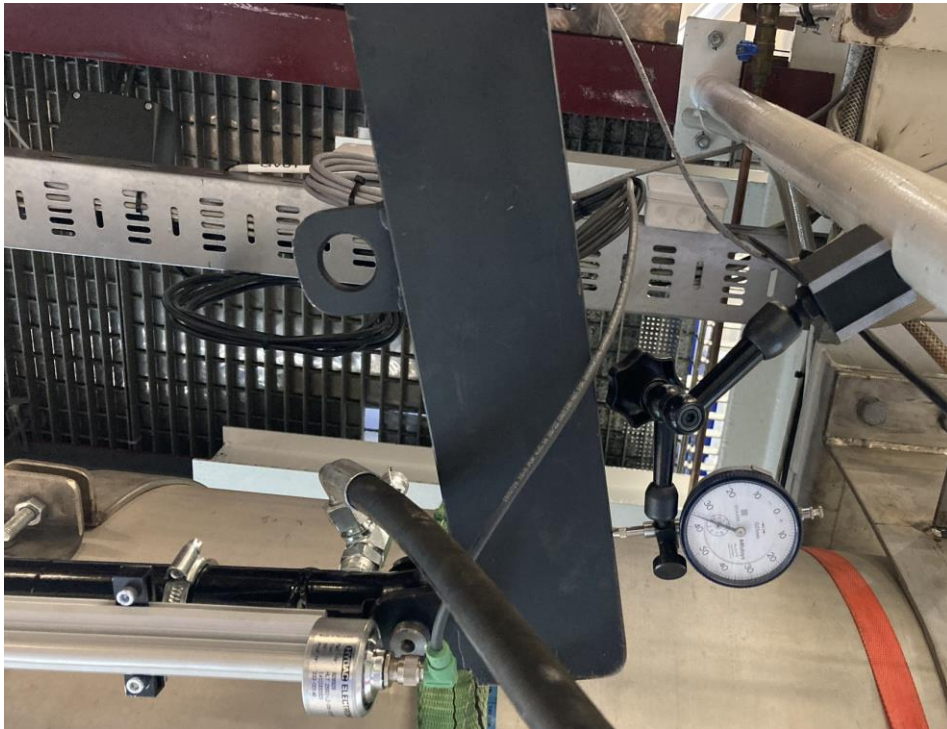


Figure 5.4: Dial gauge measurement on the beam fixed to the top of the spiral casing.

After the dial gauge was mounted, the guide vane system was initiated by driving the actuator with the set-point value based on actuator stroke position. To see how much the beam would move in the actuator stroke direction when the load from the actuator was applied, the actuator stroke set-point value was adjusted 1 mm at the time for about 5 mm before the stroke was adjusted back again. In this way the experienced backlash was provoked. During the operation of the guide vane system, the dial gauge was recorded with the same camera used in Section 5.1. For the following tests, the same guide vane system operation and recording were used.

5.2.2 Joints connected to the hydraulic actuator

To measure the mechanical backlash in the joint between the beam connected to the spiral casing and the hydraulic actuator, the magnetic stand was fastened to the beam as presented in Figure 5.5. The measurement pin of a Mitutoyo 1044S dial gauge was then put towards a rigid part of the actuator as shown in the same figure before the test was conducted.

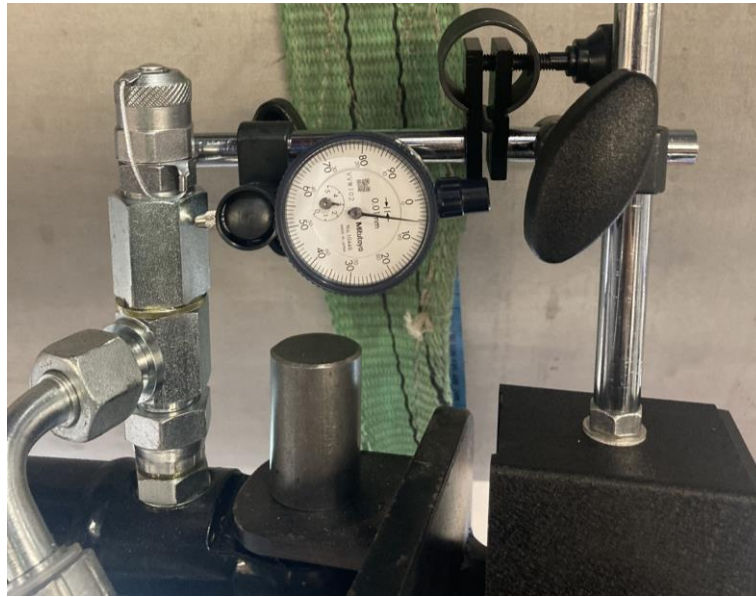


Figure 5.5: Dial gauge measurement on the backlash experienced in the first actuator joint.

The same dial gauge used to measure the backlash in the first joint, was then mounted on the beam connected to the governor ring, to measure backlash in the second joint. Figure 5.6 is showing how the measurement pin was sat towards a rigid part of the moving rod on the actuator to detect movement.



Figure 5.6: Dial gauge measurement on the backlash experienced in the second actuator joint.

5.2.3 Cantilever beam connected to the governor ring

To be able to measure the deformation of the beam bolted to the governor ring, a long and narrow steel plate was first fastened to the beam by the use of a screw clamp as shown in Figure 5.7 a). Then, the magnetic stand was fastened to the top of the beam, and the measurement pin on the dial gauge was placed on the edge of the narrow steel plate, on the line of attack from the actuator force. In this way the dial gauge would show the deflection difference between the beam which is subjected to loads from the hydraulic actuator, and the steel plate which is not exposed to any significant loads.

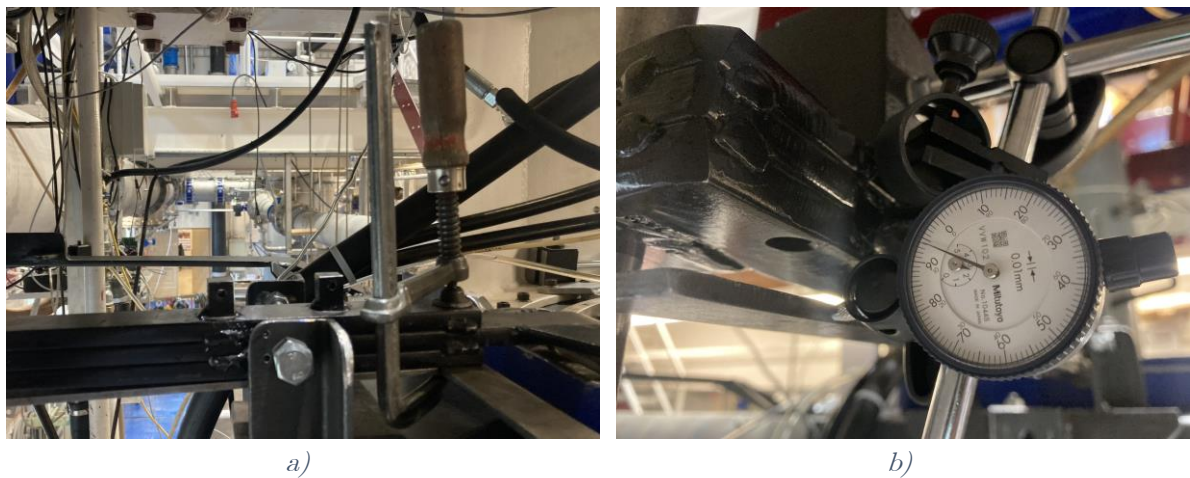


Figure 5.7: Dial gauge measurement of deflections on the beam connected to the governor ring.

5.2.4 Governor ring horizontal displacement

The linear horizontal displacement of the governor ring in the actuator stroke direction was determined by setting the pin of the dial gauge against the outer edge of the governor ring, while the magnetic stand was fastened to the top of the spiral casing, as illustrated in Figure 5.8. The figure shows a CAD-representation of the setup a), and a picture from the test b). By executing this test, the measurement of any horizontal movement of the ring prior to the initiation of rotation was facilitated.

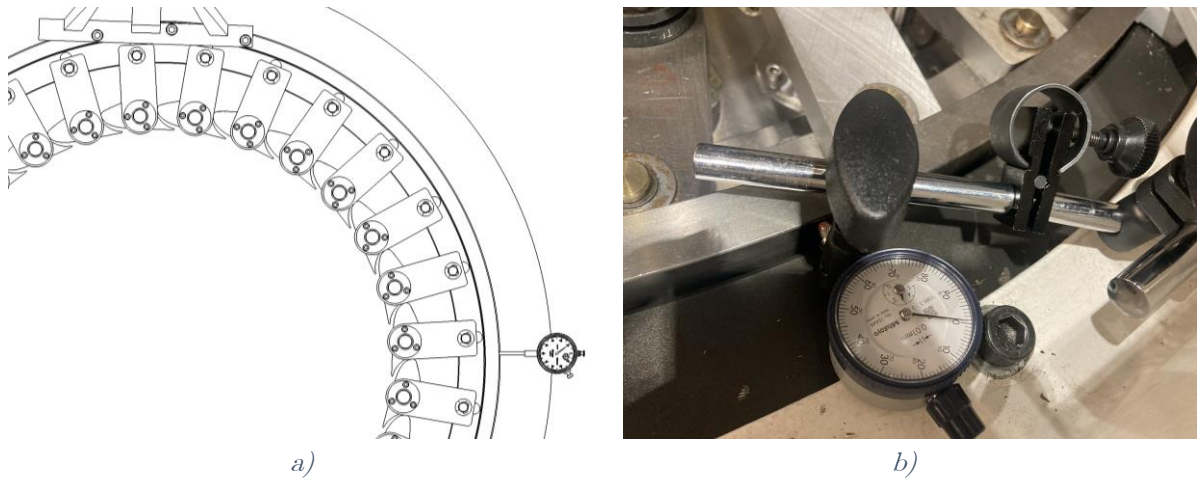


Figure 5.8: Dial gauge measurement on linear, horizontal governor ring displacement.

5.2.5 Guide vane – governor ring connection

Unlike the previously presented measurements on the rig, the backlash test of the guide vane – governor ring connection was conducted without any movement from the hydraulic actuator. In fact, the test was conducted similarly to the mock-up tests with fixed plate described in the end of Section 5.1.2. Even though this test was already done on the mock-up it was important to execute it on the rig as well, because small differences in geometry and clearances could result in deviations in the measurements. As seen from Figure 5.9, a plastic cup made to fit perfectly on top of the guide vane shaft was tightened by a hose clamp to enable the shaft rod described in Section 5.1.1 to be mounted on top of it. In this way the radial displacement of the guide vane shaft was measured when the lever arm was manually pushed and pulled back and forth. As for all the other test executed, the readings on the dial gauge were recorded.



Figure 5.9: Dial gauge measurements on guide vane shaft.

6 Experimental results and discussion

In the following subsections the results from the experimental analysis will be presented, and the performance of the new connection between the guide vane shaft and the governor ring will be compared to the characteristics of the existing design. Additionally, the test results from the measurements done on the Francis rig will be presented and discussed.

As for all other experiments which includes measured values, errors and uncertainties will apply for the measurements. This will include uncertainties from random errors originating from instrument resolution, and systematic errors from instrument calibration, not aligning the instruments perfectly, variation in measurements, or other factors which has been failed to account for. The uncertainties presented in the results are based on the calculations presented in Appendix G.

6.1 Measurements on mock-up

To analyze the slack measurements, the recordings of the different tests described in Section 5.1.2, were watched frame by frame to see how much the plate simulating the guide vane ring had to be displaced before the angle of the guide vane shaft was changed. The correlation between plate displacement and change in shaft angle was especially investigated during the change in plate movement direction, because this is where the mechanical slack would be visual. To give as reliable results as possible, several takes of each case were analyzed before the tendency was written down.

As presented by the results in Table 6.1, the backlash measured in the mock-up with moving plate was observed to be smaller than the resolution of the instruments. Nevertheless, when the recordings were played frame by frame there was a visible change in the readings on dial gauge 1 of a bit below 0.005 mm before the indicator on dial gauge 2 started to move. This was the case for both the old and the new connection. According to these results, the backlash in the guide vane shaft – governor ring connection is equivalent to <0.015 mm of actuator stroke length, using the conversion ratio described in Appendix F.

Table 6.1: Mock-up results with moving plate.

Test case	Linear plate displacement	Angular shaft movement	Actuator stroke equivalent
Moving plate old connection	< 0.005 mm	< 0.003°	< 0.015 mm
Moving plate new connection	< 0.005 mm	< 0.003°	< 0.015 mm

These results states that the backlash coming from the guide vane – governor ring connection is very small. In fact, the backlash originating from this connection would only be about 0.5% of the measured backlash of 0.65° which is a suspiciously low value. Due to this, it was assumed that the test fails to take some significant phenomena into account. These phenomena can be friction or torque in the joints, which might be present on the rig. Therefore, to try provoking the backlash in the guide vane – governor ring connection, the tests with the fixed plate described in the end of Section 5.1.2, was performed. The results from this test, originating from the readings on dial gauge 2, are shown in Table 6.2.

Table 6.2: Mock-up results with fixed plate.

Test case	Linear shaft-rod displacement	Angular shaft movement	Actuator stroke equivalent
Fastened plate old connection	0.120 ± 0.021 mm	0.069 ± 0.012°	0.31 ± 0.05 mm
Fastened plate new connection	0.020 ± 0.008 mm	0.011 ± 0.004°	0.05 ± 0.02 mm

For the results to be comparable to the first test, the linear shaft-rod displacement was transformed to angular shaft movement and then to a corresponding actuator stroke using Equation 5.1 and F.3 respectively. As seen from the actuator stroke equivalents, the tests with the plate fastened resulted in significantly greater magnitudes of slack than the measurements initially recorded. Additionally, the difference between the old and the new connection becomes clearer for this test, as the new connection gives a slack corresponding to 0.05 ± 0.01 mm actuator stroke, while the old connection results in a slack of 0.31 ± 0.03 mm. This means that the new connection will give a significant slack reduction of about 5/6, compared to the old one. It should also be noted that the readings on dial 3, shown in Figure 5.2, was negligible in all tests, meaning that the motion of the guide vane shaft was strictly radial without any deflection, and the risk of conducting misleading results is reduced.

However, these results are still far away from the slack values experienced during the operation of the Francis rig guide vane system. In fact, the measurements indicates

that the slack from the existing connection between guide vane shaft and the governor ring is only about 10% of the total slack which corresponds to a guide vane angle of 0.65° . Therefore, it was assumed that the main contribution to the total backlash was coming from somewhere else in the guide vane system, and the movement of the remaining parts in the assembly had to be investigated.

6.2 Measurements on Francis rig guide vane system

The results from the measurements of the total backlash on the Francis rig guide vane system, are presented in Table 6.3 as actuator stroke equivalents. From the table, it can be seen that the mechanical backlash experienced is a lot higher when the entire system is evaluated, than if only the guide vane – governor ring connection is concerned. This is due to the displacements and deflections which will be presented in detail in Section 6.2.1. Also, it should be noted that uncertainty from the measurements by the digital sensors will be a significant part of the total experienced backlash, as it would be the biggest contribution to the total uncertainty of ± 0.29 mm. In the end this will cause the total backlash measured on the Francis rig to be 2.60 ± 0.29 mm, which corresponds to a maximum value of 2.87 mm and a minimum of 2.33 mm, or 4.6% and 3.7% of maximum stroke length. As previous measurements done in the laboratory, presented among others in Figure 4.5, has shown a backlash of about 0.65° of guide vane angle, or 4.6% of maximum actuator stroke, the backlash measurements presented in this section may be defined as satisfactory. However, it is important to acknowledge that certain factors may have been overlooked, as the upper limit of the results presented only barely covers the backlash value experienced during rig operation.

Table 6.3: Total backlash measured on Francis rig guide vane system.

Backlash source	Actuator stroke eq.
Displacement and deformation of parts	2.60 ± 0.09 mm
Sensor uncertainty	± 0.27 mm
Total backlash	2.60 ± 0.29 mm

As presented by Haugum [1], the maximum allowable backlash to obtain stable governing is about 1% of maximum actuator stroke of the Francis rig at the Waterpower Laboratory. For a maximum opening angle of 14° , it is found that the actuator stroke is about 62.5 mm. Thus, the measured backlash of 2.60 mm is

corresponding to 4.15% which is well above the stability limit. To reduce the backlash below this limit, certain measures will be presented in Section 6.3.

6.2.1 Measured backlash from separate parts of the guide vane system

In Table 6.4, the results from the measurements described in Section 5.2 are presented. The results are given in actuator stroke equivalents which means that the values written in Table 6.4 are the component of the movement or deformation which goes in the hydraulic actuator stroke direction. For the guide vane connection, the measured values have been converted to actuator stroke equivalent slack using the same method as for the connections in Section 6.1. Additionally, it should be mentioned that the uncertainties are based on the calculations in Appendix G.

Table 6.4: Measured displacement of rig parts during guide vane system operation.

Backlash origin	Actuator stroke equivalent
Cantilever beam on spiral casing	1.08 ± 0.06 mm
1 st joint on hydraulic actuator	0.26 ± 0.04 mm
2 nd joint on hydraulic actuator	0.16 ± 0.04 mm
Cantilever beam on governor ring	0.71 ± 0.04 mm
Governor ring, horizontal movement	0.03 ± 0.01 mm
Guide vane shaft connection	0.36 ± 0.03 mm
Total mechanical backlash	2.60 ± 0.09 mm

According to the measurements on the rig, the first and biggest contributor to the backlash is the deformation of the cantilever beam fastened to the top of the spiral casing cover, which occurs because of the force from the hydraulic actuator working on the beam. The dial gauge measurements of the beam displacement showed that a point about 70 mm from the tip of the beam is moving 1.00 ± 0.05 mm. Because the hydraulic actuator is connected 25 mm from the tip of the beam, the dial gauge measurement must be transformed to actuator stroke equivalent slack. This is done by using similar triangles, assuming that the deflection is linear and that it is starting where the support brace is connected as illustrated in Figure 6.1. From this we can obtain a backlash originating from the cantilever beam connected to the spiral case cover of 1.08 ± 0.06 mm in actuator stroke direction, which corresponds to about 42% of the total measured backlash.

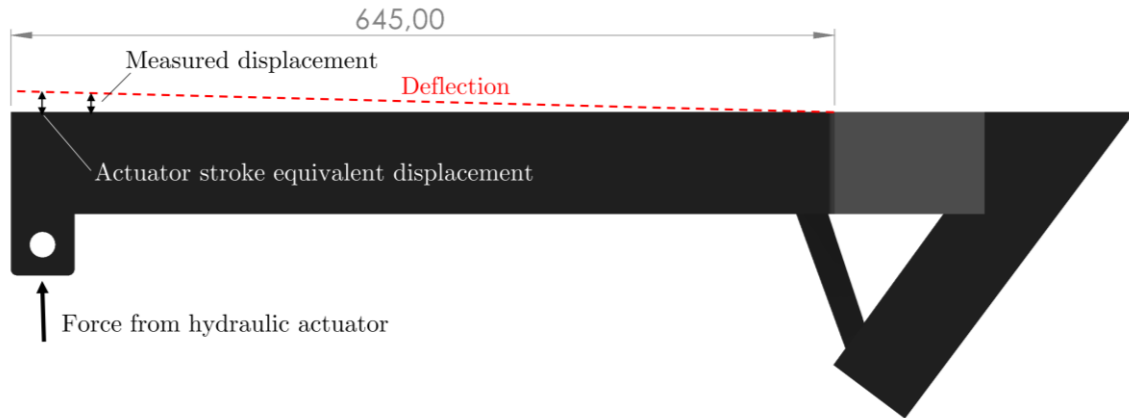


Figure 6.1: Top view of the beam fastened to the spiral casing illustrating the deflection.

The magnitude of the deflection can at first glance be perceived as surprisingly large, especially if the structural design of the beam, presented by the technical drawing “Fast bjelke” in Appendix C, is superficially investigated. The beam is in fact 80 mm wide in the direction of the applied force, and one would therefore believe that the beam should be stiff enough to withstand load in the horizontal direction better. However, by applying beam theory [30] to a simplified version of the cantilever beam (without the L-shape at the end), and a cantilever span of 650 mm with a load of 500 N applied 25 mm from the tip, one would see that the deformation of the beam would lead to a deflection of about 0.5 mm in horizontal direction for the point where the load is applied. A deflection of 0.5 mm in each direction (the actuator can both push and pull the beam) which leads to a total deflection of 1.0 mm, would therefore from a theoretical point of view be expected. The calculations are presented in Appendix H.

The cantilever beam connected to the governor ring is also experiencing deflection due to load from the hydraulic actuator. As presented in the fourth row of Table 6.4, the deflection which contributes to the backlash is measured to be 0.71 ± 0.04 mm and occurs because of friction in the governor ring joint. This means that the beam bolted to the ring must be pushed by a certain force before the ring turns, and the force applied to the beam will then cause stress and strain along its arm, which again will cause a deflection on the tip of the beam. To theoretically calculate this deflection, one could not directly use the same formulas as was used for the last example, because the beam is not bolted to a rigid part, but a part which eventually will rotate for a certain load. Therefore, it is hard to tell if a deflection of 0.71 mm on the point where the actuator force is working, is an expected value or not. Either way, because of the long and narrow arm of the beam, 40x36x750mm from the place where the support braces

are connected, a significant deflection is expected. It should also be noted that a highly exposed part of the beam is the part right after the support braces are connected to the arm, as presented in Figure 6.2. Here, the cross section is only 40x12 mm, and is vulnerable for bending moment which can contribute to large deflections further down the arm. When later improving the beam performance to reduce the backlash, reinforcement of this section of the beam would therefore be important.

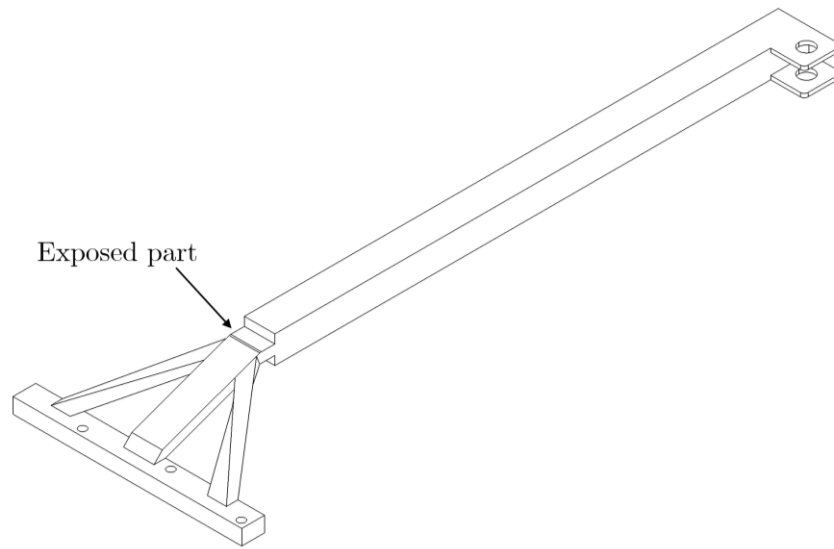


Figure 6.2: The thinnest part of the beam connected to the governor ring is most exposed to stress.

In the start of Section 6.2 it was mentioned that some factors may have been failed to take into account when doing the measurements. One such factor could be the deflection originating from the first part of the beam bolted to the governor ring. In fact, as described in Section 5.2.3, the plate used to measure deflection is fastened after the stress-exposed area illustrated in Figure 6.2, meaning that deformation happening between this point and the governor ring is not measured. Therefore, the backlash originating from this beam might be greater than the measurements show.

In addition to the backlash contribution from the beam deflections, a significant part of the total mechanical backlash, is coming from the joints connected to the hydraulic actuator. The magnitude of this backlash is measured to 0.26 ± 0.04 mm and 0.16 ± 0.04 mm for the joint connected to the spial casing beam and the governor ring beam respectively. According to the clearances found when doing the measurement of the parts described in Section 4.1, these backlash magnitudes were expected. In fact, the measurements of the joints uncovered a clearance of 0.12 mm and 0.06 mm for the first

and second joint, which due to bending of the pin and oblique movements can cause the measured slack experienced to be over the double the measured clearance.

For the linear, horizontal measurement on the governor ring, a displacement of 0.03 ± 0.01 mm was found. This indicates that the ring is shifted by 0.03 mm in the direction of the actuator stroke before it can initiate rotational motion. This displacement might be caused by imperfections in the joint between the governor ring and the surrounding casing. From previous projects on the rig, similar problems have been identified, and certain measures have already been implemented. This includes reinforcement of the ring joint by adding more supportive bearings and taps to reduce the clearance and travel of the ring, which again will increase the precision in the joint.

Reducing the clearance further would likely increase the friction in the joint, resulting in greater deflection on the beams due to the increased force required for rotating the governor ring. Consequently, it is presumed that the governor ring has already been optimized, and a backlash contribution of 0.03 mm would be deemed acceptable.

The link between the guide vane shaft and the governor ring, was initially thought to be the main contributor to the experienced backlash. Nevertheless, as the mock-up tests in Section 6.1 indicated, the contribution from the guide vane connection is a bit lower than expected. Similar to the mock-up results, the test described in Section 5.2.5 showed a shaft-rod displacement of 0.14 ± 0.01 mm. This corresponds to an actuator stroke equivalent backlash of 0.36 ± 0.03 mm, which is about 14% of the total measured slack. Even though this is a lower value than expected, it is still a significant amount of the total mechanical backlash experienced, and it might therefore be desirable to mitigate this slack contribution as well.

6.2.2 Uncertainty contributions from sensors

The uncertainties in the backlash measurements presented in Table 6.4, are only arising from the manual, mechanical measurement techniques and as stated in the last row of the table, the total mechanical uncertainty is not significantly large ($\pm 3.7\%$ of the backlash). However, as already stated in Table 6.3, the backlash experienced during operation of the rig, will also rely on the uncertainty and resolution of the digital sensors applied on the actuator stroke and the guide vane shaft. If the sensor is not able to give the exact position of the measured value, the error of the measurement

can in fact cause the backlash to look bigger or smaller than it is, depending on the error to be positive or negative.

In Table 6.5, the relative and absolute uncertainty from the guide vane and actuator stroke positioning sensors are presented. These values are derived from the specifications listed in Table G.4 and by utilizing Equation G.4 in Appendix G. The uncertainties presented are originating from the resolution and hysteresis error listed by the manufacturer, which combined will give an uncertainty relative to the measured mechanical backlash.

Table 6.5: Uncertainties from digital sensors.

Sensor	Relative uncertainty	Absolute uncertainty
GV angle: Stegmann AG 612 13-bit	$\pm 10.3\%$	± 0.27 mm
Actuator stroke: HYDAC HLT 2550-L2	$\pm 1.97\%$	± 0.05 mm

As seen from the table, the uncertainty originating from the guide vane angle sensor is much larger than that from the actuator stroke. This is because of the angle sensor has a much lower resolution and a greater hysteresis error than the actuator stroke. Additionally, due to the conversion from guide vane angle, the uncertainty originating from the angle sensor will be amplified when it is converted to actuator stroke equivalent backlash. In the end this will mean that the absolute uncertainty coming from the angle sensor will have a significant value of ± 0.27 mm, while the uncertainty originating from the actuator stroke sensor is only contributing with ± 0.05 mm.

6.3 Suggested slack mitigation measures and estimated backlash

To fulfill the stability requirements by Haugum [1], the total slack must be reduced about 75% of the existing measured value to reach below the limit of 0.63 mm. Due to the risk of not including all the backlash contributors in the calculations, an additional safety factor should also be considered to be applied.

As presented in Figure 3.2, a conventional governor system often has the hydraulic actuator mounted directly to the governor ring instead of applying beams as done in the Waterpower Laboratory. This would be a possible solution for mitigation of backlash in the system as it would eliminate several parts which contributes to mechanical slack and deflection. However, this solution would require extensive

modifications to the Francis rig as there is limited space around the governor ring, and the hydraulic actuator would not fit in there without conducting major changes in the layout. Therefore, to keep the design adjustments within manageable amounts, it is decided to base the alternative guide vane system design on the existing one and apply improvements for each individual part. The technical drawings of the modified parts and the assembly of the new system is presented in Appendix I.

In Table 6.6 the total estimated backlash of the new, suggested guide vane system design is presented. The estimation is including the combined absolute uncertainty from digital sensors and is showing a total estimated backlash of 0.56 ± 0.07 mm, which is a slack reduction by 78% compared to the existing system. The estimated slack including uncertainty gives an upper limit of 0.63 mm or 1.0% of maximum stroke length, and a lower limit of 0.49 mm or 0.78%. This would again mean that the maximum estimated value of the experienced slack in the new system is just within the requirements.

The detailed calculations of the estimation will be presented in Section 6.3.1, and as stated there the estimated backlash value for the new system involves many assumptions. Therefore, there remains a risk that the new system does not manage to fix the problem of unstable governing of the rig even though the value listed in Table 6.6 is within the stability limits. In fact, without a real-world test of the new system it would be challenging to ascertain its performance with certainty. However, all calculations indicates that the experienced slack will be reduced by a great amount if the measures suggested in Section 6.3.1 and 6.3.2 are applied, and it is also likely to reach the overall goal of a total experienced backlash below 1% of maximum actuator stroke length.

Table 6.6: Total estimated backlash on the new Francis rig guide vane system.

Backlash source	Actuator stroke eq.
Displacement and deformation of parts	0.56 mm
Sensor uncertainty	± 0.07 mm
Total backlash	0.56 ± 0.07 mm

6.3.1 Estimated backlash from each part of the new system

To mitigate the backlash originating from the cantilever beam fastened to the spiral casing cover, the beam must be reinforced. This can among others be done by applying support braces to shorten the cantilever arm, or to change the cross section of the beam to increase the second moment of inertia in the bending direction [30]. The easiest solution would be a reinforcement by support bracings, but because there are few rigid objects near the beam to fasten the braces, this solution might be a bit inconvenient. Therefore, changing the beam cross section could be a more effective and practical solution. In fact, if the cross section is changed in the way presented in Figure 6.3, by applying an H-beam construction, and the same simplified beam deflection calculations as presented in the Section 6.2 is applied, the deflection in the point where the load takes place, is reduced to about 0.1 mm, which corresponds to a backlash contribution of 0.2 mm, This would reduce the backlash originating from the beam connected to the spiral case cover by over 80%, which would be a great contribution to reach the overall goal of 1% or 0.63 mm backlash. The calculations of the deflections are presented in Appendix H.

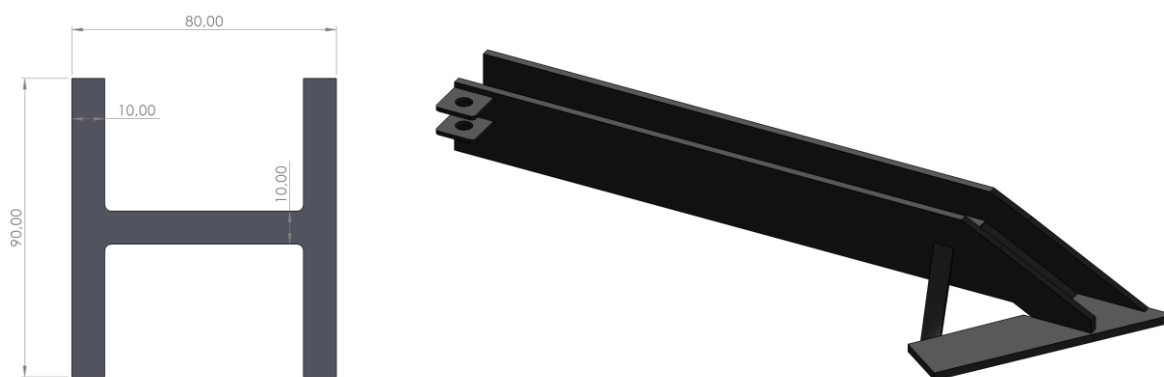


Figure 6.3: Cross section (left) and CAD-model (right) of an alternative beam design.

The implementation of the vertical plates on each side of the existing beam, could quite easily be done by welding the plates onto the edge of the horizontal plate on the existing design. This would of course make the beam heavier, and the loads on the bolts connected to the top of the spiral casing would increase. Nevertheless, the bolts should with a significant margin withstand the increase in weight from about 7 kg to 15 kg, because it already handles the loads from the hydraulic actuator which applies a much larger load on the bolts than the weight of the beam does.

Even though the beam connected to the governor ring is not fastened by the same mechanism as used in the first cantilever beam, it is assumed that the same equations can be used to compare the stiffness of the existing beam with an alternative design. A simplification of the existing version of the beam presented in Appendix C as “Stag og trekant”, can be considered as a cantilever beam with an arm of 725 mm and a rectangular cross section of 40x36 mm. If a force of 500 N is applied 25 mm from the tip of the beam, the deflection of the point where the force is applied would be about 1.5 mm, as calculated in Appendix H . This magnitude is a lot greater than the measured value, but it is assumed to give an approximate estimation of the performance relative to an alternative design.

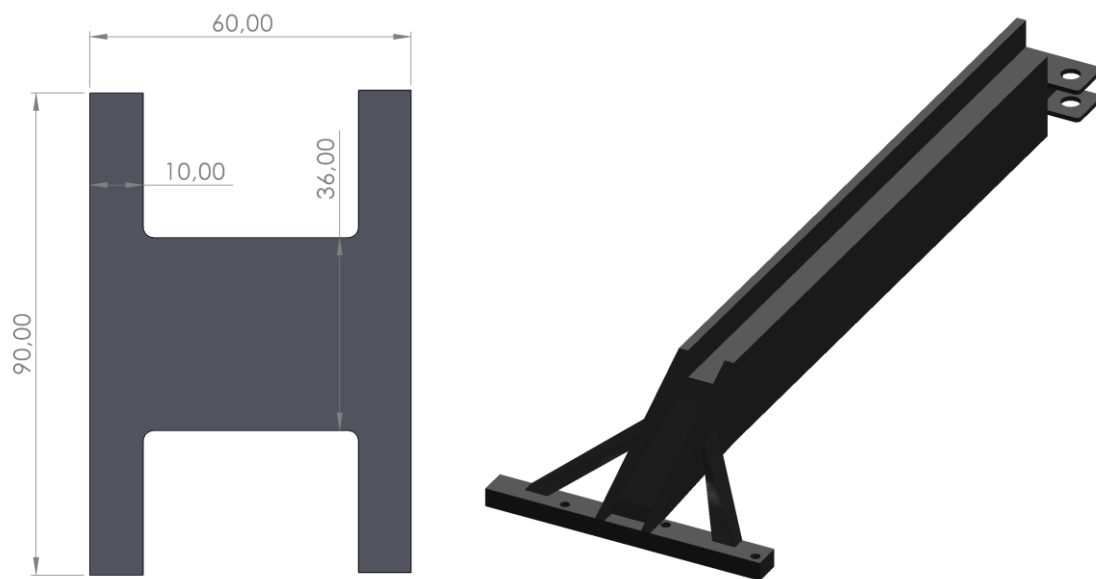


Figure 6.4: Cross section (left) and CAD-model (right) of an alternative beam design.

If the deflection equation used for the existing cross section is used for the alternative design presented to the left in Figure 6.4, the deflection would only be about 0.2 mm, which is a reduction of about 86% from the 1.5 mm deflection calculated from applying the existing cross section. As the calculation does not take the thin part between the straight beam and the governor ring into account, the approximation might show a bit optimistic result in favor of the new design. However, we can assume that the deflection reduction would still be above 80% for a design which in addition to reinforce the straight arm, also has reinforced the bridge between the governor ring bolts and the arm, as was suggested in Section 6.2. This would mean that the new version of the beam connected to the governor ring would contribute to a backlash of about 0.14 mm.

The suggestion for the new design is presented in the right part of Figure 6.4, and like the design changes for the first beam it is suggested to weld the support plates on each side to the existing beam. It should also be noted that the new design will double the beam weight from about 10 to 20 kg, which might be a challenge when mounting the new part.

For the joints which the hydraulic actuator is connected to, the clearance should be minimized. This can be done by increasing the pin diameter to 19.98 mm which according to tolerance theory will be the narrowest fit applicable before the risk of seizing becomes too high [25]. A pin diameter of this size would reduce the clearance to 0.02 mm, which again will mean that the backlash should be reduced thereafter, with a reduction of 83% and 67% for the first and second joint respectively. If the backlash would follow this reduction rate, the new measured backlash originating from the joints would then be about 0.04 mm and 0.05 mm.

As presented in the end of Section 6.2, the implementation of new guide vane connections might be a bit more extensive than the other backlash reducing measures, as it would require changing all the 28 connections, and include modifications to the governor ring. But, to achieve a total backlash below the stated maximum value, the backlash originating from these links might also be reduced. To do this, it is suggested to implement the link design presented in Section 4.2, and reproduced in Figure 6.5.

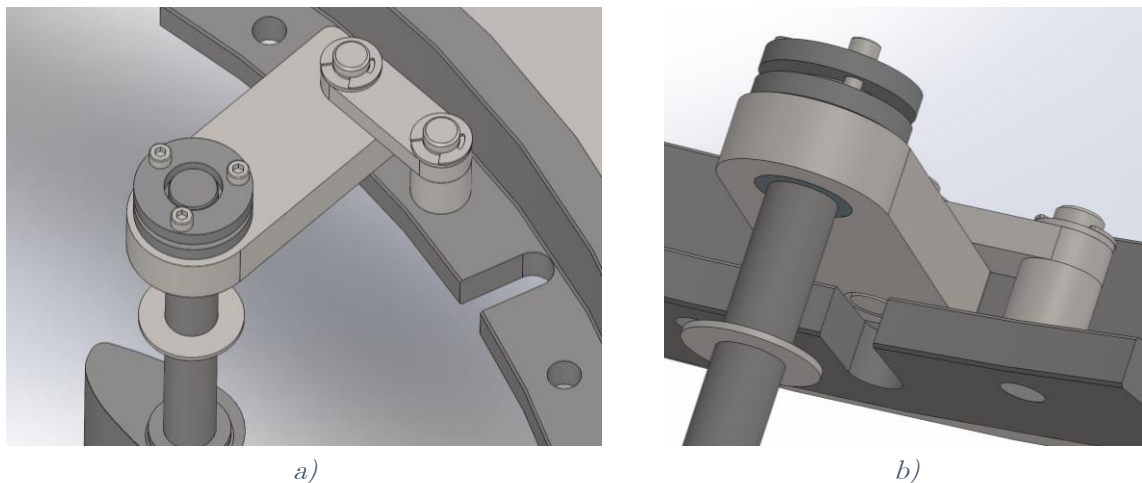


Figure 6.5: Alternative design of the connection to the guide vane shaft.

Since the rig measurements on the existing guide vane connection showed an increase of about 17% compared to the measurement on the mock-up version of the existing

connection, it is assumed that the deviation in measurements for an alternative, new design would follow the same pattern. Therefore, the actuator stroke equivalent backlash contribution from the new guide vane connection is approximated to be about 0.10 mm, which is a reduction of 71% compared to the existing design.

In Table 6.7, all estimated backlash contributions for the alternative design described in this section are listed and summed. As seen in the end of the table, the estimated sum of all backlash contributions from mechanical parts will be 0.56 mm, which corresponds to a slack reduction of 78% compared to the existing design. According to these results, the performance of the new design is indicating that it will manage to obtain a slack magnitude within the requirements of 0.63 mm.

Table 6.7: Estimated backlash in the new guide vane system.

Backlash origin	Actuator stroke equivalent
Cantilever beam on spiral casing	0.20 mm
1 st joint on hydraulic actuator	0.06 mm
2 nd joint on hydraulic actuator	0.04 mm
Cantilever beam on governor ring	0.14 mm
Governor ring, horizontal movement	0.03 mm
Guide vane shaft connection	0.10 mm
Total mechanical backlash	0.56 mm

The estimated backlash sum thus indicates that the new design will perform sufficiently. But, as it was for the existing design, the uncertainty of the results should also be considered. To define a sufficient uncertainty of the estimation might be difficult, as it is many unknown factors and assumptions involved. Therefore, to avoid presenting a misleading uncertainty for the mechanical backlash estimation, it has been decided to leave this out and instead emphasize that the given backlash value is an estimation based on several assumptions.

However, the uncertainties from the digital sensor can still be calculated quite straight forward, as it was done for the existing design. In the following subsection, this uncertainty is presented.

6.3.2 Uncertainty from sensors in the new design

In Section 6.2.2, it was concluded that the guide vane angle sensor plays a significant role of the backlash experienced in the system. Therefore, reducing this contribution will also be an important part of reducing the overall experienced backlash. To do this, it will be necessary to implement a new angle sensor with higher resolution and lower hysteresis error. A good suggestion for this, might be a 15-bit Stegmann AG 615, which will reduce both the resolution uncertainty and the hysteresis error compared to the 13-bit Stegmann AG 612 which is used today. In fact, the AG 615 comes with a maximum resolution of $360^\circ/2^{15} = 0.011^\circ$, which is about four times the resolution on the existing device. Additionally, the hysteresis error is only 0.005° which also is a lot lower than the 0.04° stated in the specifications of AG 612.

Calculations of the sensor uncertainties on the new system are done in the end of Appendix G, and the results, which are shown in Table 6.8, are stating that applying the suggested guide vane sensor will cause a significant change in absolute uncertainty originating from the digital sensors. In fact, the combined absolute uncertainty from the sensors, will be ± 0.07 mm as presented in Table 6.6. This corresponds to a reduction of about 73% compared to the absolute digital uncertainty in the existing system. These values are obtained without changing the specifications of the actuator stroke sensor. Thus, it is found that the actuator stroke sensor's performance is sufficient.

Table 6.8: Uncertainties from digital sensors in the new system.

Sensor	Relative uncertainty	Absolute uncertainty
GV angle: Stegmann AG 615 15-bit	$\pm 9.64\%$	± 0.05 mm
Servo stroke: HYDAC HLT 2550-L2	$\pm 9.11\%$	± 0.05 mm

7 Conclusion

In this project, the mechanical backlash in the Francis turbine rig at the Waterpower Laboratory at NTNU has been investigated through numerical and experimental analysis. Additionally, an alternative mechanical design of the guide vane system has been developed. The experimental measurements conducted on the rig, showed a total backlash of 2.60 ± 0.29 mm. This corresponds to a backlash equal to 4.15% of maximum actuator stroke length, with an upper limit of 4.6% and a lower limit 3.7%. As the experienced backlash from previous rig operations was 4.6% of maximum actuator stroke, the measurements on the existing guide vane system were found satisfactory, but it also indicated that some backlash factors most likely have been failed to account for. The suggestion for a new design included reinforcement of both beams in the guide vane system, reduction of clearance in the joints connected to the hydraulic actuator, implementation of new links between the governor ring and the guide vane shafts, and an enhancement of the guide vane angle sensor. If all these measures are implemented, the total experienced backlash for the new system was estimated to be 0.56 ± 0.07 mm stroke length, meaning that the overall goal of a total backlash below 1% of maximum stroke length corresponding to 0.63 mm, could be achieved. However, it should be noted that the calculations of the total backlash of the new design includes a considerable number of assumptions, and it is therefore not certain that the new design exclusively would lead to stable governing of the Francis rig.

8 Further work

A natural continuation of this work would be to implement the suggested modifications on the Francis rig. This could be done by conducting the least comprehensive and most significant adjustments first, and then continuing with less slack-contributing adjustments, as shown in the right-hand side column of Table 8.1. After implementing each measure, the effects of the adjustment can be tested to see whether the next measure is needed. In Table 8.1, the backlash measures are presented in prioritized order based on estimated backlash-reduction contribution, installation complexity and both combined $\left(\frac{\textit{slack reduction}}{\textit{complexity}}\right)$.

Table 8.1: Priority lists for implementation of backlash-mitigating measures.

	Slack-reduction contribution	Installation complexity	$\left(\frac{\textit{Slack reduction}}{\textit{Complexity}}\right)$
1.	Beam, spiral casing	Pin diameters	Beam, spiral casing
2.	Beam, governor ring	Beam, spiral casing	Beam, governor ring
3.	GV connections	Beam, governor ring	Pin diameters
4.	Pin diameters	GVA sensor	GVA sensor
5.	GVA sensor	GV connections	GV connections

9 References

- [1] J. Haugum, “Governing of a Francis turbine Model Subjected to Load Variations,” Specialization project, NTNU, Trondheim, Norway, 2022.
- [2] United Nations Environment Programme, “Paris Agreement,” Dec. 2015, Accessed: Dec. 17, 2022. [Online]. Available: <https://wedocs.unep.org/xmlui/handle/20.500.11822/20830>
- [3] G. Notton *et al.*, “Intermittent and stochastic character of renewable energy sources: Consequences, cost of intermittence and benefit of forecasting,” *Renew. Sustain. Energy Rev.*, vol. 87, pp. 96–105, May 2018, doi: 10.1016/j.rser.2018.02.007.
- [4] L. Rostad, “Implementation of a turbine governor on the Francis test rig at The Waterpower Laboratory,” NTNU, Trondheim, Norway, 2022.
- [5] A. Ingranata, “Development, implementation and validation of a hydropower plant model with Francis turbine,” Master’s thesis, NTNU, Trondheim, Norway, 2022.
- [6] S. Bennett, *A history of control engineering, 1930-1955*, vol. 47. IET, 1993.
- [7] R. C. Buell, R. J. Caughey, E. M. Hunter, and V. M. Marquis, “Governor performance during system disturbances,” *Electr. Eng.*, vol. 50, no. 1, pp. 37–41, Jan. 1931, doi: 10.1109/EE.1931.6430149.
- [8] Bany, Wallau, Butcher, Wyatt, Wensley, and Place, “Discussion at annual convention: Papers on automatic stations,” *J. AIEE*, vol. 44, no. 3, pp. 263–270, Mar. 1925, doi: 10.1109/JAIEE.1925.6537126.
- [9] L. M. Hovey, “Optimum Adjustment of Hydro Governors on Manitoba Hydro System,” *Trans. Am. Inst. Electr. Eng. Part III Power Appar. Syst.*, vol. 81, no. 3, pp. 581–586, Apr. 1962, doi: 10.1109/AIEEPAS.1962.4501366.
- [10] H. Brekke and L. Xin-Xin, “A new approach to the mathematic modelling of hydropower governing systems,” in *1988 International Conference on Control - CONTROL 88.*, Apr. 1988, pp. 371–376.
- [11] G. Martínez-Lucas, J. I. Sarasúa, J. Á. Sánchez-Fernández, and J. R. Wilhelmi, “Power-frequency control of hydropower plants with long penstocks in isolated systems with wind

- generation,” *Renew. Energy*, vol. 83, pp. 245–255, Nov. 2015, doi: 10.1016/j.renene.2015.04.032.
- [12] Q. Wu, L. Zhang, and Z. Ma, “A model establishment and numerical simulation of dynamic coupled hydraulic–mechanical–electric–structural system for hydropower station,” *Nonlinear Dyn.*, vol. 87, no. 1, pp. 459–474, Jan. 2017, doi: 10.1007/s11071-016-3053-1.
- [13] M. Nordin and P.-O. Gutman, “Controlling mechanical systems with backlash—a survey,” *Automatica*, vol. 38, no. 10, pp. 1633–1649, Oct. 2002, doi: 10.1016/S0005-1098(02)00047-X.
- [14] E. Donaisky, G. H. C. Oliveira, E. A. P. Santos, G. V. Leandro, A. M. Pena, and J. A. Souza, “Semi-physical piecewise affine representation for governors in hydropower system generation,” *Electr. Power Syst. Res.*, vol. 136, pp. 181–188, Jul. 2016, doi: 10.1016/j.epsr.2016.02.022.
- [15] C. Concordia, L. K. Kirchmayer, and E. A. Szymanski, “Effect of Speed-Governor Dead Band on Tie-Line Power and Frequency Control Performance,” *Trans. Am. Inst. Electr. Eng. Part III Power Appar. Syst.*, vol. 76, no. 3, pp. 429–434, 1957, doi: 10.1109/AIEEPAS.1957.4499581.
- [16] I. C. Report, “Dynamic Models for Steam and Hydro Turbines in Power System Studies,” *IEEE Trans. Power Appar. Syst.*, vol. PAS-92, no. 6, pp. 1904–1915, Nov. 1973, doi: 10.1109/TPAS.1973.293570.
- [17] D. K. Pantalone and D. M. Piegza, “Limit Cycle Analysis of Hydroelectric Systems,” *IEEE Trans. Power Appar. Syst.*, vol. PAS-100, no. 2, pp. 629–638, Feb. 1981, doi: 10.1109/TPAS.1981.316919.
- [18] B. Strah, O. Kuljaca, and Z. Vukic, “Speed and active power control of hydro turbine unit,” *IEEE Trans. Energy Convers.*, vol. 20, no. 2, pp. 424–434, Jun. 2005, doi: 10.1109/TEC.2004.837278.
- [19] H. Villegas Pico and J. McCalley, “Modeling and analysis of speed controls in hydro-turbines for frequency performance,” in *2011 North American Power Symposium*, Aug. 2011, pp. 1–7. doi: 10.1109/NAPS.2011.6024847.
- [20] L. Saarinen, P. Norrlund, and U. Lundin, “Field Measurements and System Identification of Three Frequency Controlling Hydropower Plants,” *IEEE Trans. Energy Convers.*, vol. 30, no. 3, pp. 1061–1068, Sep. 2015, doi: 10.1109/TEC.2015.2425915.
- [21] W. Yang, P. Norrlund, L. Saarinen, J. Yang, W. Guo, and W. Zeng, “Wear and tear on hydro power turbines – Influence from primary frequency control,” *Renew. Energy*, vol. 87, pp. 88–95, Mar. 2016, doi: 10.1016/j.renene.2015.10.009.

- [22] Y. Liao *et al.*, “Influence mechanism of backlash nonlinearity on dynamic regulation stability of hydropower units,” *Sustain. Energy Technol. Assess.*, vol. 51, p. 101917, Jun. 2022, doi: 10.1016/j.seta.2021.101917.
- [23] W. Luo, G. Liu, and H. Wang, “Study on Anti-backlash Mechanism Used in Precise Transmission: A Review,” in *Advances in Mechanical Design*, J. Tan, Ed., in Mechanisms and Machine Science. Singapore: Springer Nature, 2022, pp. 1449–1470. doi: 10.1007/978-981-16-7381-8_89.
- [24] P. J. Drake, Ed., *Dimensioning and Tolerancing Handbook*. New York: McGraw Hill, 1999.
- [25] B. Griffiths, “5 - Limits, Fits and Geometrical Tolerancing,” in *Engineering Drawing for Manufacture*, B. Griffiths, Ed., London: Butterworth-Heinemann, 2003, pp. 88–110. doi: 10.1016/B978-185718033-6/50019-7.
- [26] T. Nielsen, “Dynamisk dimensjonering av vannkraftverk.” Vannkraftlaboratoriet, NTNU, Dec. 1990.
- [27] “Nasjonal veileder for funksjonskrav i kraftsystemet.” Statnett, Jul. 01, 2022.
- [28] “SolidWorks 2021.” Dassault Systèmes. Accessed: Apr. 25, 2023. [Online]. Available: <https://www.3ds.com/products/solidworks>
- [29] “Altair Inspire 2022.” Altair Engineering Inc. Accessed: Apr. 25, 2023. [Online]. Available: <https://altair.com/inspire>
- [30] K. Bell, *Konstruksjonsmekanikk (Del II: fasthetslære)*, 1st ed. Bergen, Norway: Fagbokforlaget, 2015.
- [31] R. Hogan, “How to Calculate Resolution Uncertainty,” *ISOBudgets*, Apr. 28, 2016. <https://www.isobudgets.com/calculate-resolution-uncertainty/> (accessed May 18, 2023).
- [32] “Measurements and Error Analysis.” Advanced Instructional Systems, Inc. and the University of North Carolina, 2011. Accessed: May 21, 2023. [Online]. Available: https://www.webassign.net/question_assets/unccolphysmechl1/measurements/manual.pdf
- [33] *Hydraulic turbines, storage pumps and pump-turbines — Model acceptance tests*, Second edition. IEC 60193, 1999.
- [34] “Moment of Inertia and Centroid Calculator.” SkyCiv Engineering. Accessed: May 24, 2023. [Online]. Available: <https://skyciv.com/free-moment-of-inertia-calculator/>

Appendix A Master's agreement

Norwegian University of
Science and Technology

Faculty of Engineering
Department of Energy and Process Engineering

EPT-M-2023



MASTER WORK

for
student Jørgen Haugum

Spring 2023

"Modifying a Francis Turbine Model Governor for obtaining stable governing"
Modifisering av regulator for en Francis modellturbin for å oppnå stabil regulering

Background

During the spring of 2022, Master's theses given by L. Rostad and A. Ingranata investigated the implementation of a proper turbine governor on the Francis rig in the Waterpower Laboratory at NTNU Trondheim. These theses concluded that a mechanical backlash present in the governor system avoids stable governing of the test rig when it is subjected to load variations from a simulated grid. The problem with mechanical backlash was further investigated in the project work by J. Haugum in the autumn of 2022, and a certain maximum value for the mechanical backlash to obtain stable governing of the rig was found. It is likely that the existing experimental setup is unable to meet the criteria regarding mechanical slack in order to obtain stable governing.

Objective

The student is to perform a desktop and experimental study with the aim of finding a new solution to the mechanical assembly of the governor and guide vane enabling stable governing.

The following tasks are to be considered:

1. Literature review of governing stability of hydropower plants, mechanical slack and slack mitigation measures
2. Establish a CAD model of the existing governing system and execute a tolerance analysis of this
3. Propose a new solution for the mechanical assembly connecting the governor ring to the guide vane taps and execute a tolerance analysis of this new solution
4. Have a model of one connection of the new setup made and test this in a mock-up to measure the characteristics of the new setup

-- " --

Address
N-7034 Trondheim
Norway

Location
K. Hejes vei 1b

Tel. +47 73 59 38 60
Fax +47 73 59 35 80
Org. no. NO 974 767 880

Page 1 of 2

The master work comprises 30 ECTS credits.

The work shall be edited as a scientific report, including a table of contents, a summary in Norwegian, conclusion, an index of literature etc. When writing the report, the candidate must emphasise a clearly arranged and well-written text. To facilitate the reading of the report, it is important that references for corresponding text, tables and figures are clearly stated both places.

By the evaluation of the work the following will be greatly emphasised: The results should be thoroughly treated, presented in clearly arranged tables and/or graphics and discussed in detail.

The candidate is responsible for keeping contact with the subject teacher and teaching supervisors.

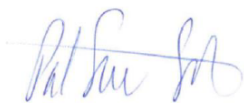
Risk assessment of the candidate's work shall be carried out according to the department's procedures. The risk assessment must be documented and included as part of the final report. Events related to the candidate's work adversely affecting the health, safety or security, must be documented and included as part of the final report. If the documentation on risk assessment represents a large number of pages, the full version is to be submitted electronically to the supervisor and an excerpt is included in the report.

According to "Utfyllende regler til studieforskriften for teknologistudiet/sivilingeniørstudiet ved NTNU" § 20, the Department of Energy and Process Engineering reserves all rights to use the results and data for lectures, research and future publications.

Submission deadline: To be found in Inspira.

- Work to be done in Waterpower laboratory
 Field work

Department for Energy and Process Engineering 11/1 2023



Pål-Tore Storli
Supervisor

Co-Supervisor(s): Truls Edvardsen Aarones, Hymatec/NTNU

Appendix B

Fits and Clearances

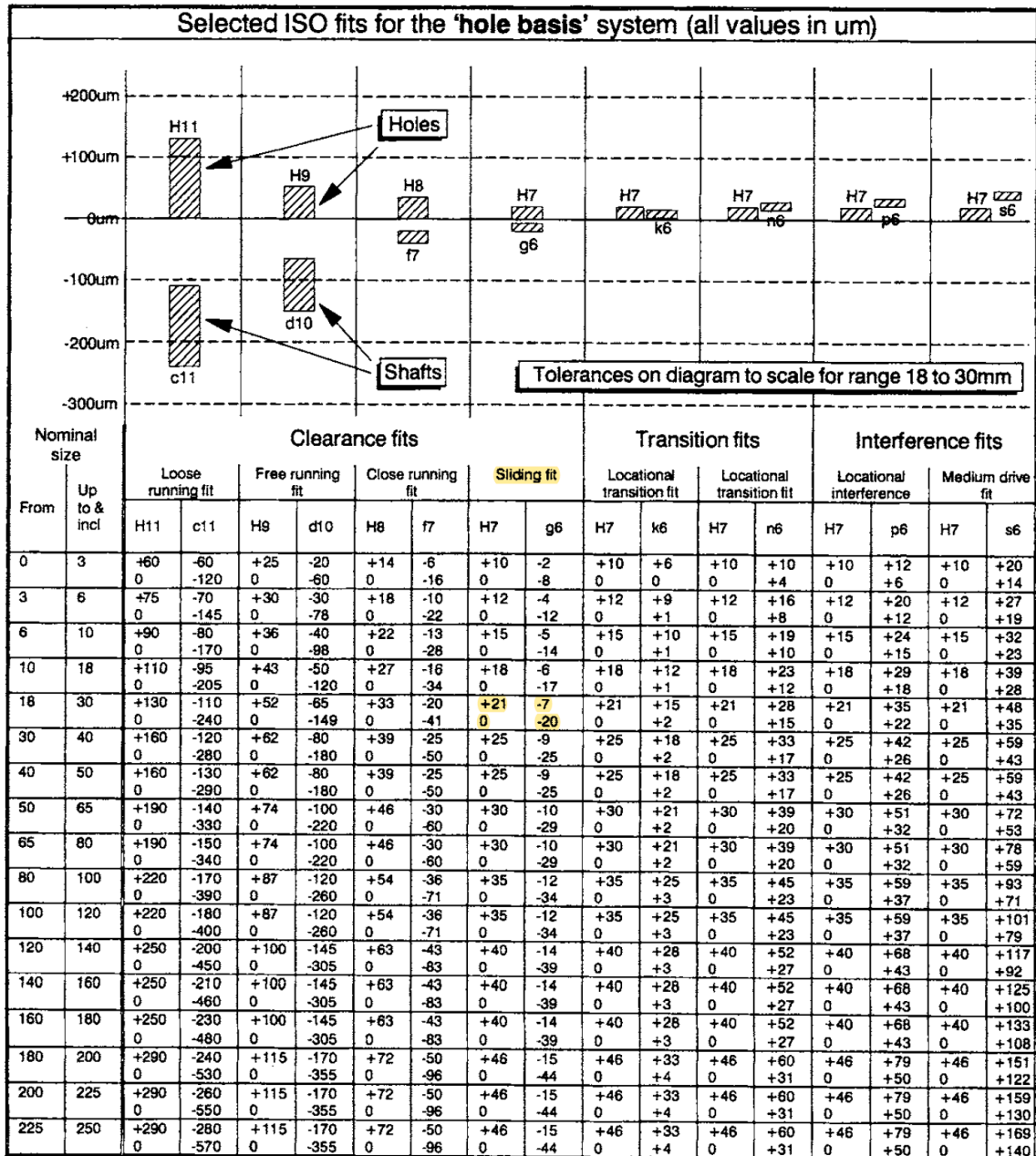


Figure B.1: Selected fits including tolerances for the hole based system [25].

Appendix C

Technical drawings original system

In this section the technical drawings for the original system is presented. All drawings are made in SolidWorks and if not specified the dimensions are given in mm. Some of the details for “Guide vane Asm” are given in Appendix E.

4

3

2

1

F

F

E

E

D

D

C

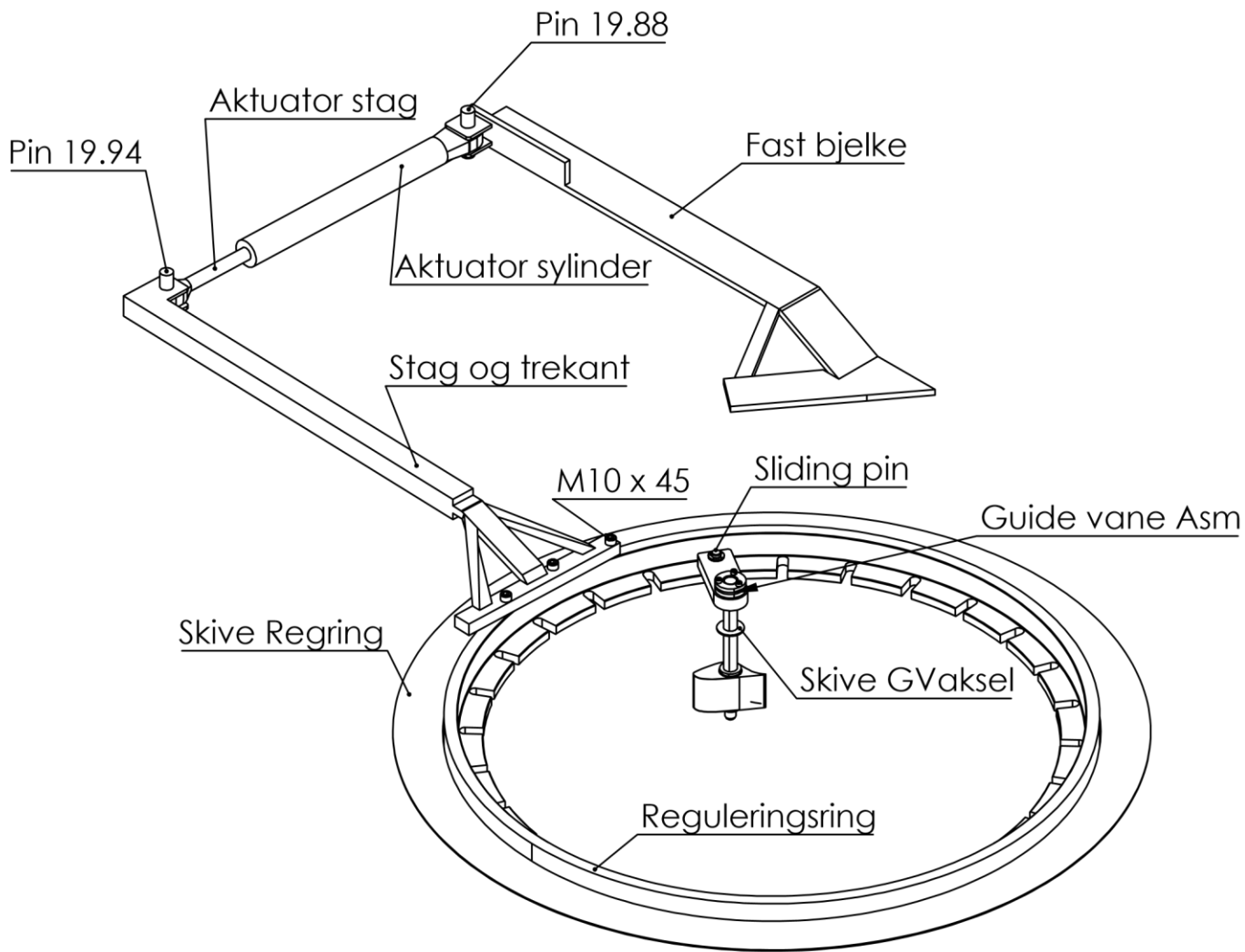
C

B

B

A

A



ISOMETRIC VIEW
SCALE 1:10



Drawn: JH	Date: 05.05.2023
Material:	
SCALE: 1:10 SHEET 1 OF 1	

Description: Assembly of original system	Sheet size: A4
Part name: Slotlinked system Asm	

4

3

2

1

4

3

2

1

F

F

E

E

D

D

C

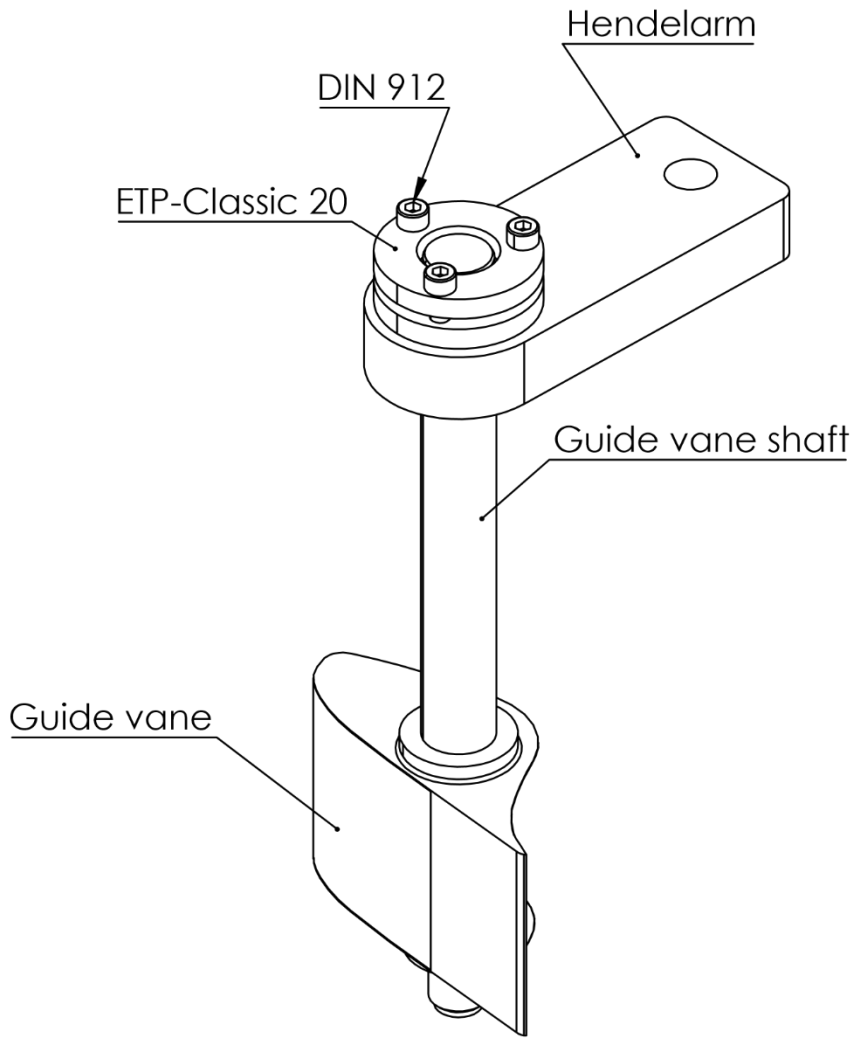
C

B

B

A

A



ISOMETRIC VIEW
SCALE 1:2



Drawn: JH	Date: 05.05.2023
Material:	
SCALE: 1:2	SHEET 1 OF 1

Description: Assembly of guide vane connection	
Part name: Guide vane Asm	Sheet size: A4

4

3

2

1

4

3

2

1

F

F

E

E

D

D

C

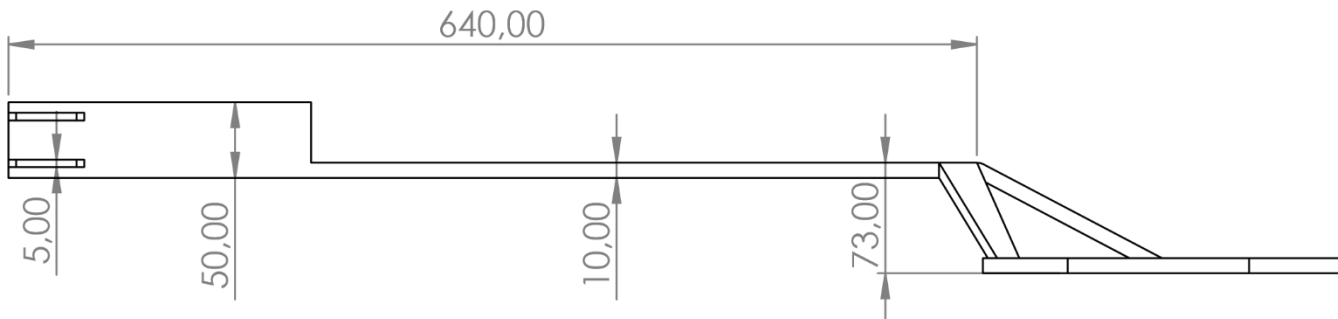
C

B

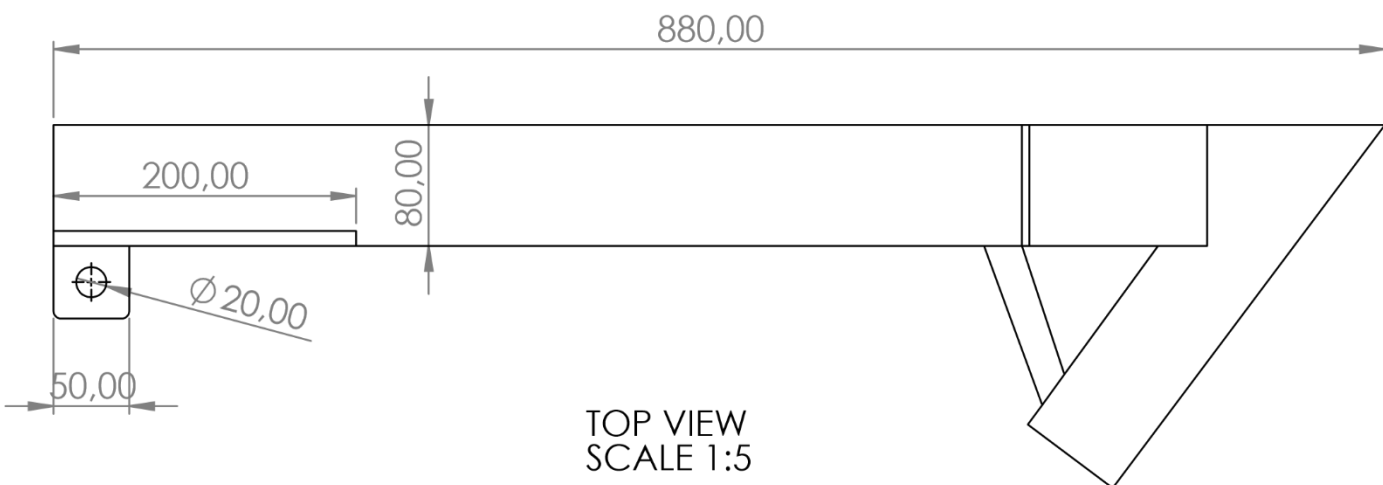
B

A

A



SIDE VIEW
SCALE 1:5



TOP VIEW
SCALE 1:5



Drawn: JH	Date: 08.05.2023
Material: Steel	
SCALE: 1:5	SHEET 1 OF 1

Description:	
Part name: Fast bjelke	Sheet size: A4

4

3

2

1

4

3

2

1

F

F

E

E

D

D

C

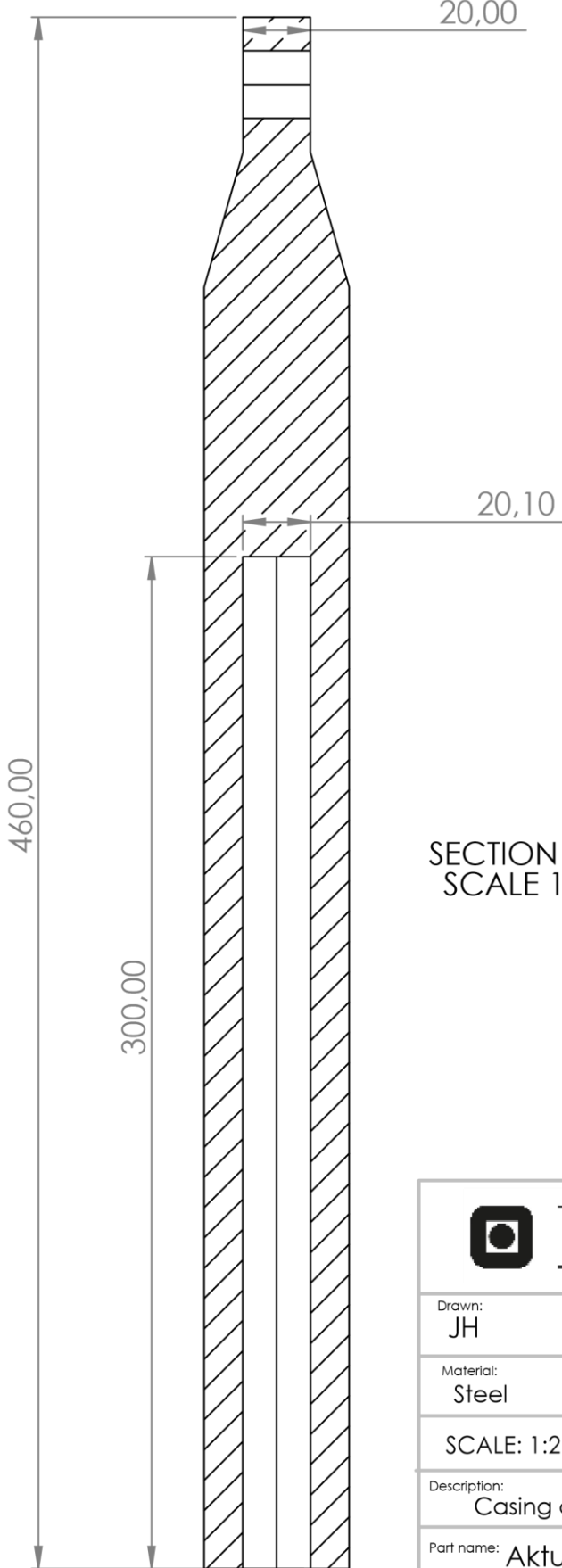
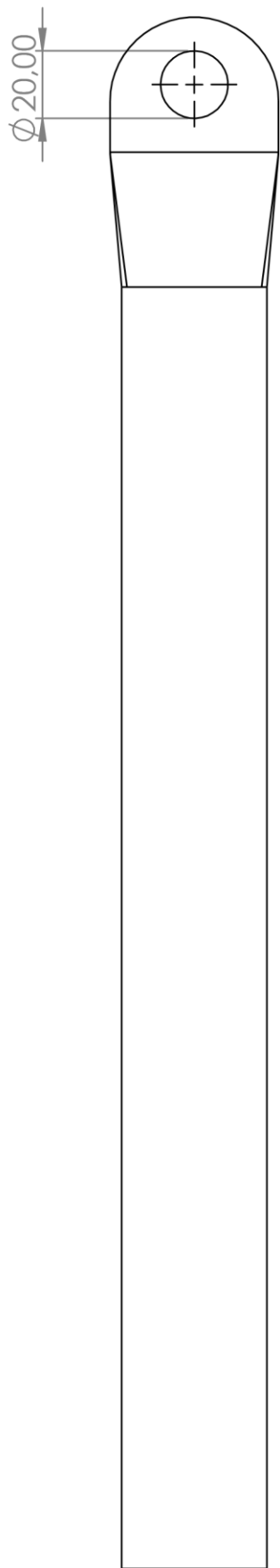
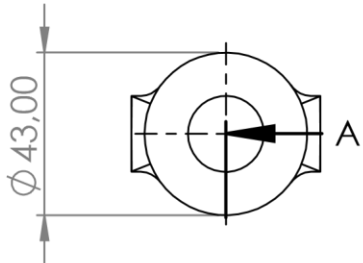
C

B

B

A

A



SECTION A-A
SCALE 1 : 2



Drawn:
JH

Date:
05.05.2023

Material:
Steel

SCALE: 1:2

SHEET 1 OF 1

Description:
Casing of the actuator

Part name: Aktuator sylinder Sheet size: A4

4

3

2

1

4

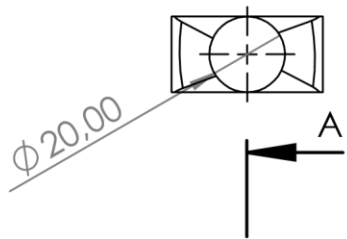
3

2

1

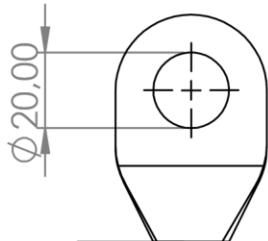
F

F



E

E



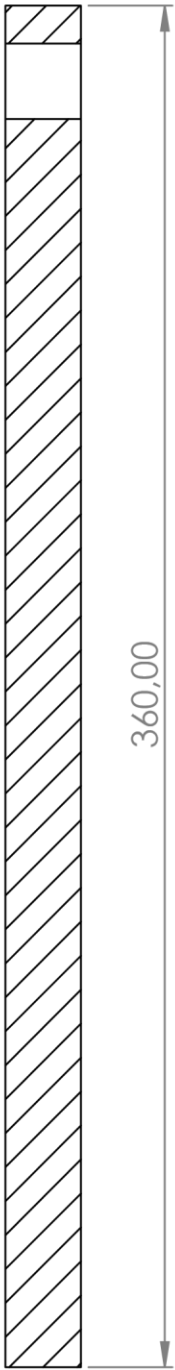
D

D



C

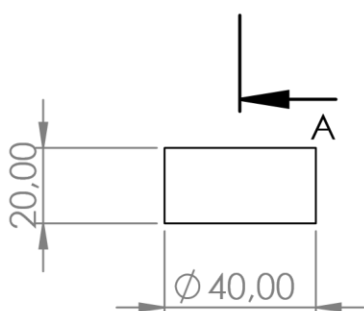
C



SECTION A-A
SCALE 1 : 2

B

B



A

A

Drawn: JH	Date: 05.05.2023
Material: Steel	
SCALE: 1:2	SHEET 1 OF 1

 **NTNU**

Description:
Rod inside actuator

Part name: Aktuator stag

Sheet size: A4

4

3

2

1

4

3

2

1

F

F

E

E

D

D

C

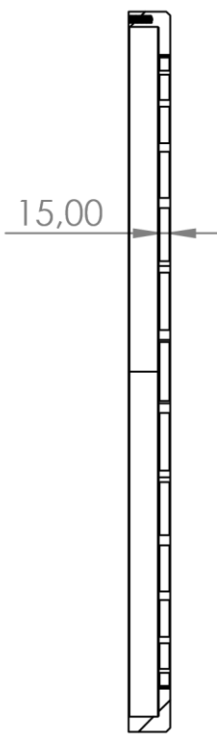
C

B

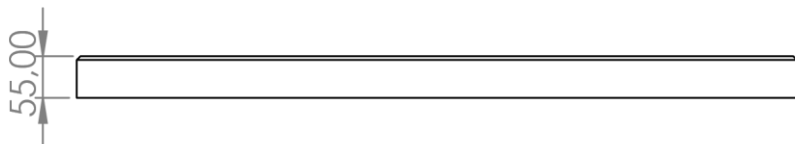
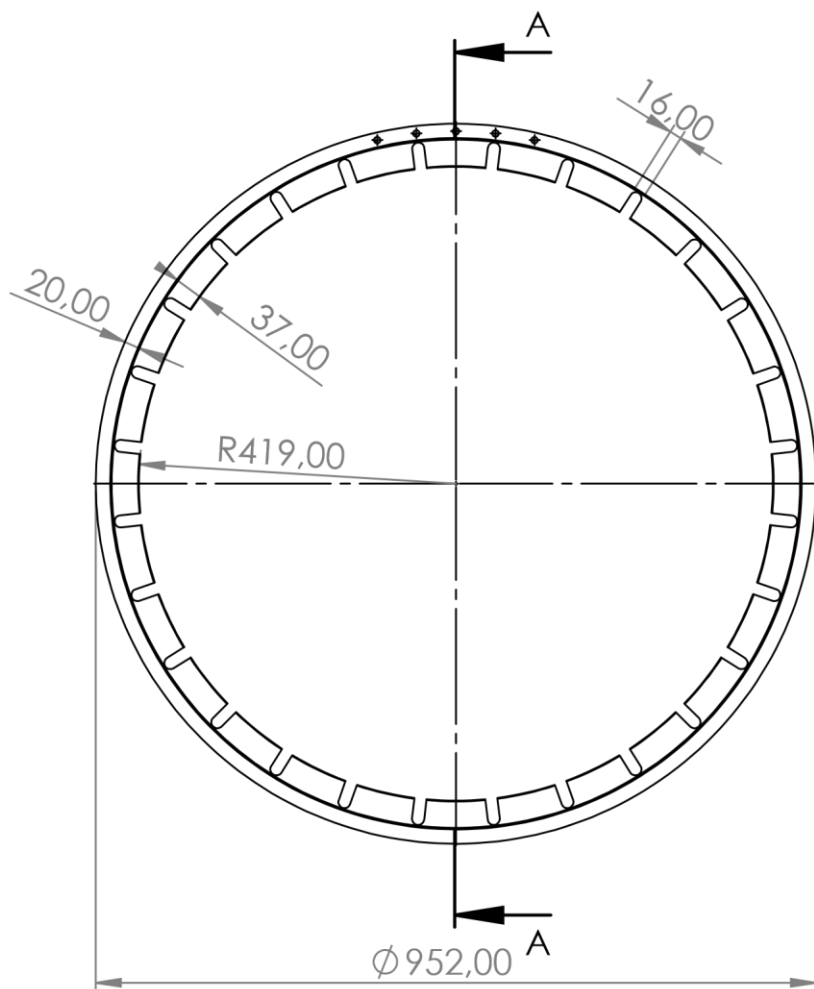
B

A

A



SECTION A-A
SCALE 1 : 10



Drawn: JH	Date: 08.05.2023
Material: Steel	Description:
SCALE: 1:10	SHEET 1 OF 1



Part name: Reguleringsring	Sheet size: A4
-------------------------------	-------------------

4

3

2

1

4

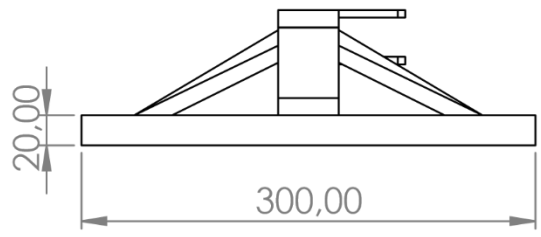
3

2

1

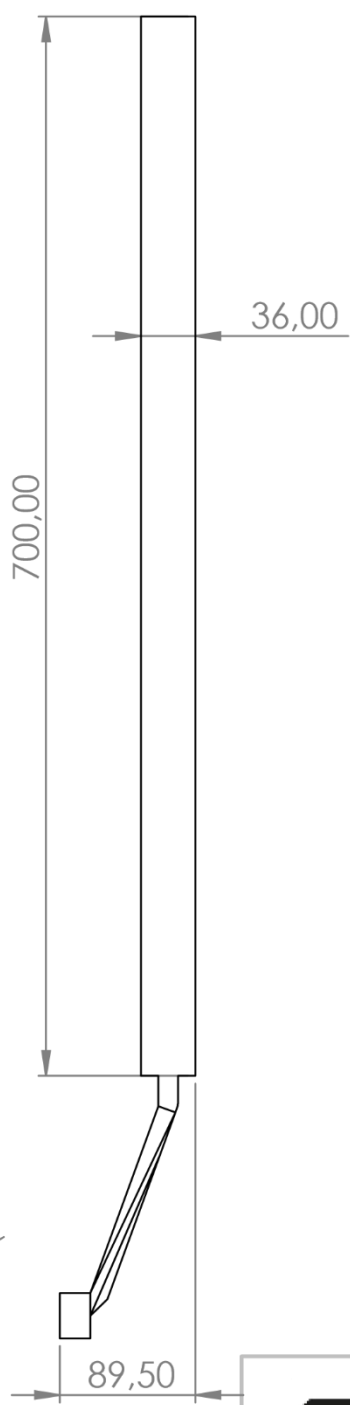
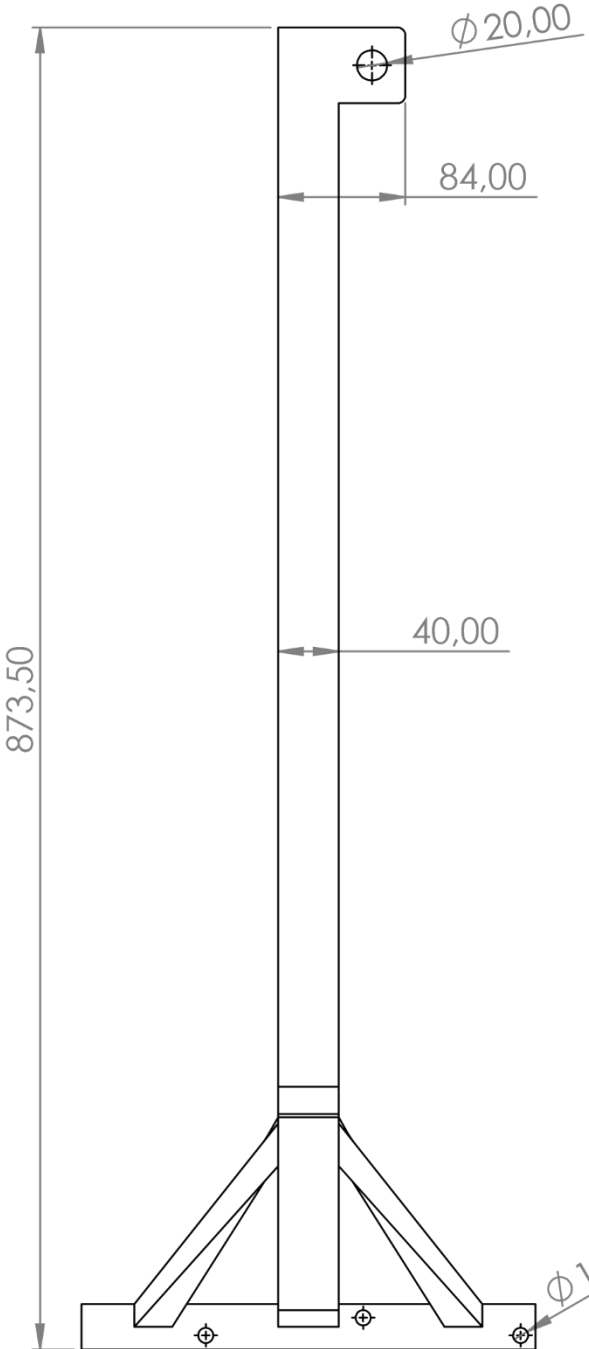
F

F



E

E



D

D

C

C

B

B

A

A

Drawn: JH	Date: 08.05.2023
Material: Steel	Description:
SCALE: 1:5	SHEET 1 OF 1



Part name: Stag og trekant Sheet size: A4

4

3

2

1

4

3

2

1

F

F

E

E

D

D

C

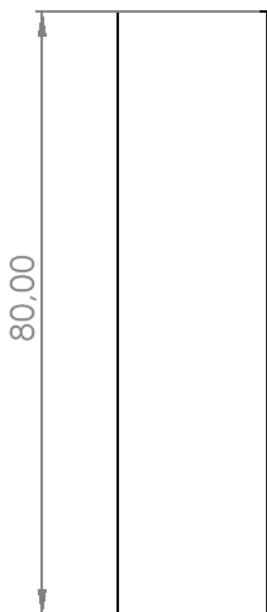
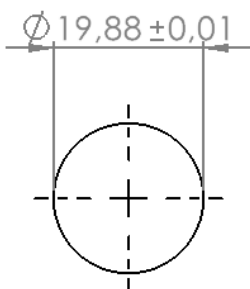
C

B

B

A

A



Drawn: JH	Date: 08.05.2023
Material: Steel	
SCALE: 1:1	SHEET 1 OF 1

 NTNU	
Description:	
Part name: Pin 19.88	Sheet size: A4

4

3

2

1

4

3

2

1

F

F

E

E

D

D

C

C

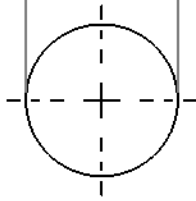
B

B

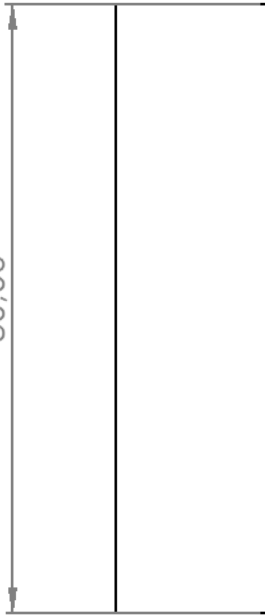
A

A

Ø 19,94 ±0,01



80,00



Drawn: JH	Date: 08.05.2023
--------------	---------------------

Material: Steel	Description:
--------------------	--------------

SCALE: 1:1	SHEET 1 OF 1
------------	--------------



Part name: Pin 19.94	Sheet size: A4
-------------------------	-------------------

4

3

2

1

Appendix D

Simulation settings in Altair Inspire

To carry out results as good as possible, the component properties and simulation settings in Altair Inspire had to be adjusted. In the following section, the details of each joint, rigid group, and contact set are presented in addition to the characteristics of simulation settings. All figures are screenshots from Altair Inspire.

The basis of the model was set from defining the ground as the parts “Fast bjelke”, “Skive GVaksel” and “Skive Rengring”, with names referring to the assembly drawing in Appendix C. The ground is presented by the red-marked parts in Figure D.1. The two parts “Skive GVaksel” and “Skive Rengring” was added to the model to easier define the circular motion of the governor ring and the guide vane shaft.

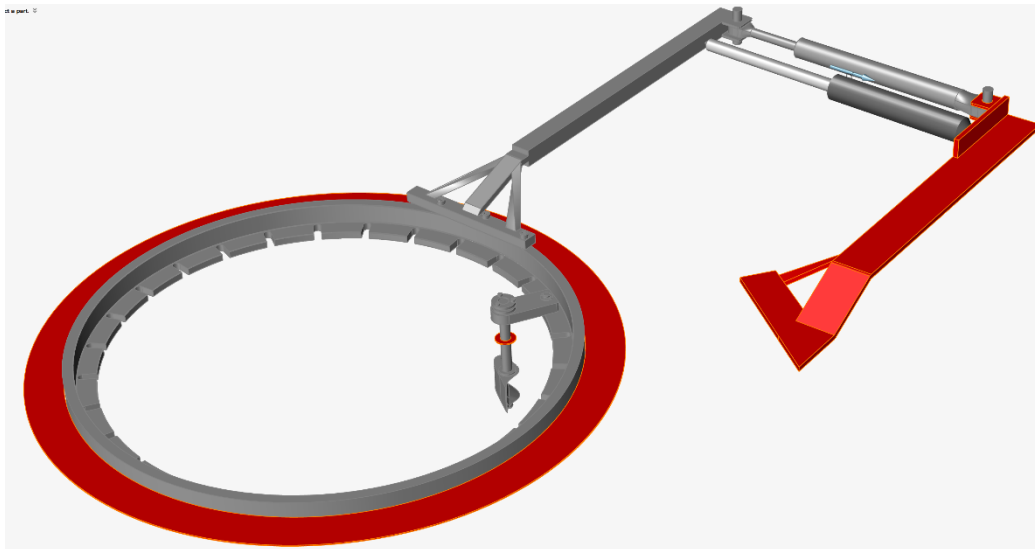


Figure D.1: Grounded parts.

After defining the ground, rigid groups were added. This included the guide vane group and the governor ring group presented by the orange-outlined parts in Figure D.2 a) and b) respectively.

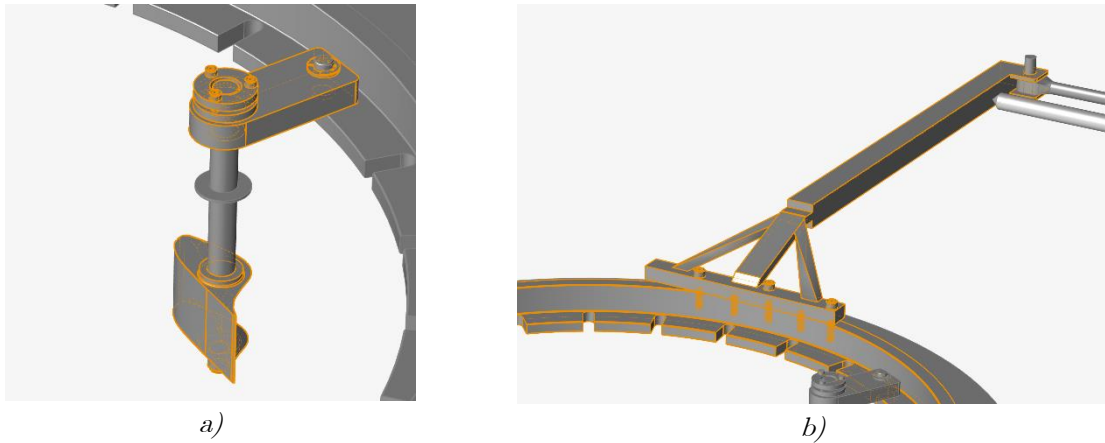


Figure D.2: Rigid groups.

The joints were then implemented to the model. When a CAD-file is uploaded to Altair Inspire, the program will automatically locate possible joints, and the user will have to choose which to use. In this model, three joints were accepted. This included a circular joint for the guide vane shaft through “Skive GVaksel”, a circular joint for the two cylinders which together makes the origin of the actuator, and a pin connection for the governor ring inside the “Skive Regring”. The joints are presented in Figure D.3 a), b) and c) respectively.

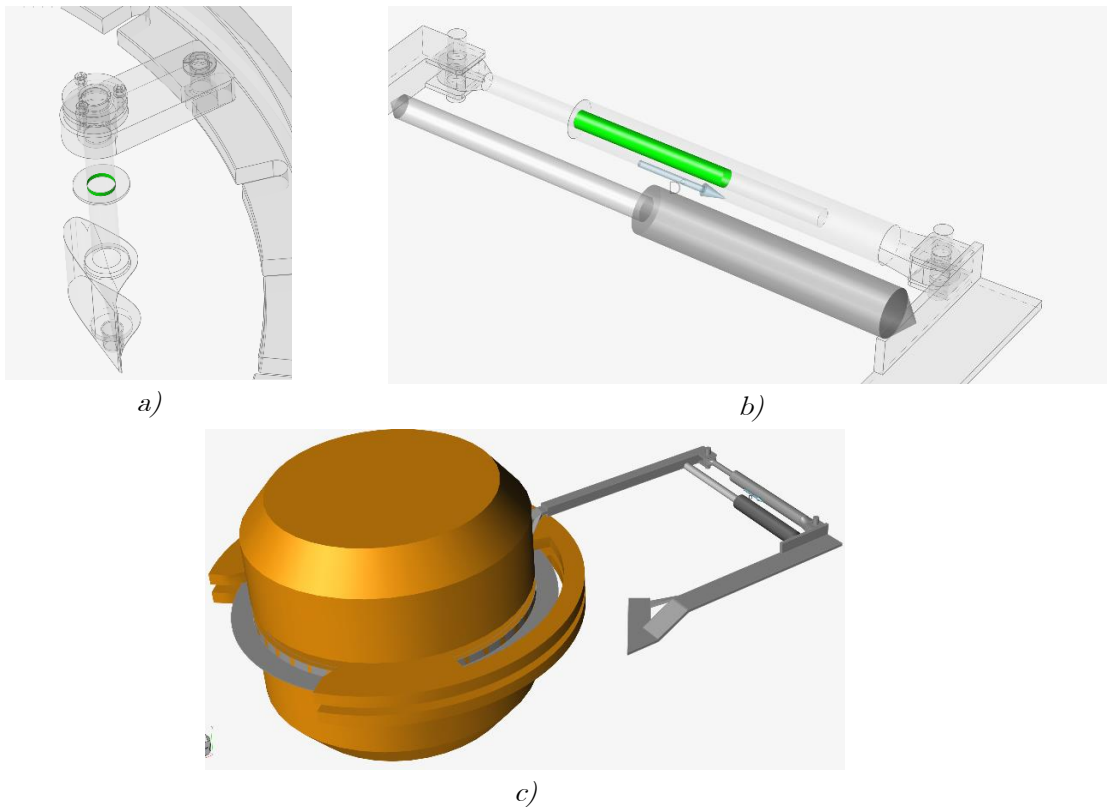


Figure D.3: Joints applied in the model.

To enable physical contact in the model, four motion contact sets presented by the red markings of Figure D.4, were included. The contact sets and their belonging parts are listed in Table D.1, and the parameter settings, which were sat equally for all sets are presented in Table D.2.

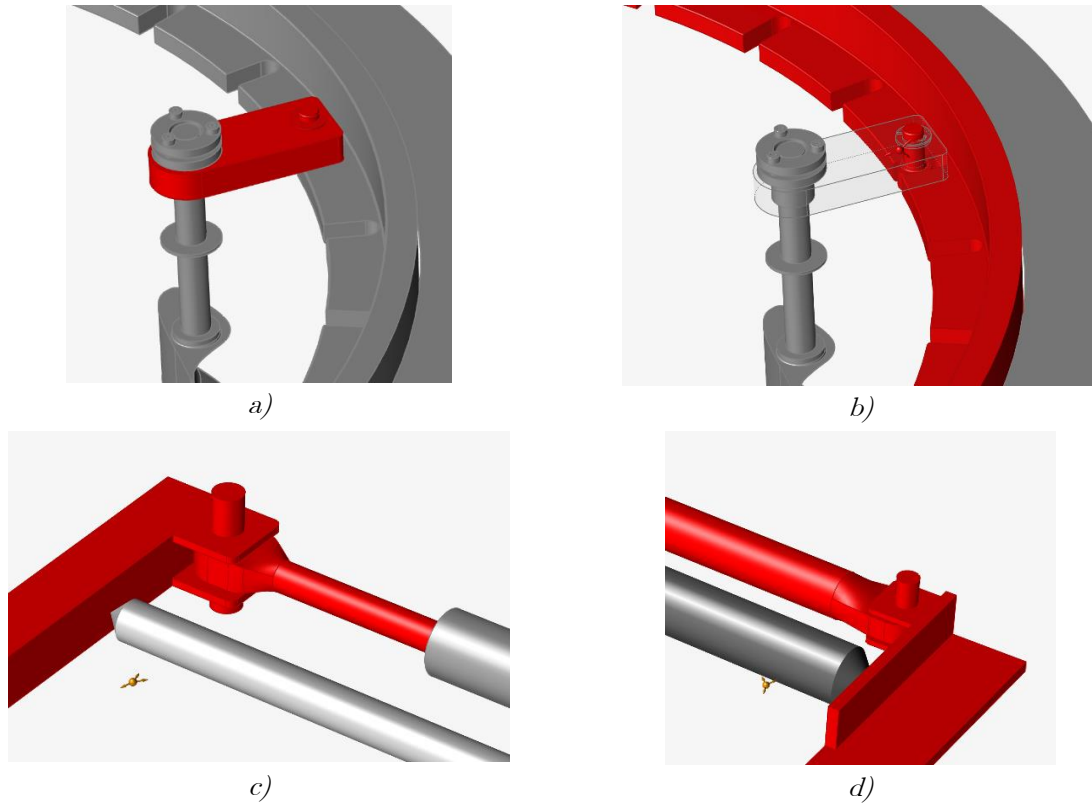


Figure D.4: Contact sets in the model.

Table D.1: Motion contact sets.

Motion contact no.	Parts included
1	Hendelarm, Washer, Mattssons, Sliding pin
2	Sliding pin, Reguleringsring
3	Stag og trekant, Pin 19.94, Aktuator stag
4	Fast bjelke, Pin 19.88, Aktuator sylinder

Table D.2: Motion contact properties.

Parameter	Value
Stiffness	1.995*10 ⁹ N/m
Damping	100.0 Ns/m
Exponent	2.10
Penetration depth	0.10 mm
Static friction coefficient	0.2
Dynamic friction coefficient	0.1
Stiction transition velocity	0.001 m/s
Friction transition velocity	0.002 m/s

As described in Section 4.1.1, an actuator was added to the cylindrical joint in Figure D.3 b) to initiate the motions in the model with the desired displacements. Here, default settings were used. The linear damper placed parallel to the actuator did also utilize default settings, and a damping coefficient of 500.0 Ns/m.

When the parameters were set for the parts and connections, the simulation settings were adjusted. The adjustments done in the simulation tab is listed in Table D.3. If the setting is not listed, the default option was used.

Table D.3: Simulation settings.

Parameter	Value
Simulation end time	50 s
Output ratio	50 Hz
Analysis type	Transient
Gravity	No
FlexContact ⁺	Yes
Active contact iteration	Yes
Deformation allowed	1.0 ± 0.01 mm

NB: All parts (except the scaled pin specified in Section 4.1.2) have the same dimensions as presented in Appendix C, and the material Steel AISI 304 is used.

Appendix E

Technical drawings of mock-up parts

In this section the technical drawings for the new design suggestion for the guide vane shaft – governor ring connection will be presented. The first drawing is an assembly of the mock-up, while the remaining drawings are used to manufacture the parts and are made by lab apprentice F. Fløttum based on CAD models and specifications given by J. Haugum. Unless otherwise stated the dimensions are given in mm.

For the connection between “Rod_RR” and “Slot hole rig” Loctite has been used to minimize the clearance. The same method was used to fasten “Rod_GV” to “Hendelarm”. If the new guide vane – governor ring connection is to be used on the Francis rig, it should also be considered to use Loctite in these connections to prevent backlash. The connections between the rods and “Symmetrisk Link” are ordinary sliding fits.

4

3

2

1

F

F

E

E

D

D

C

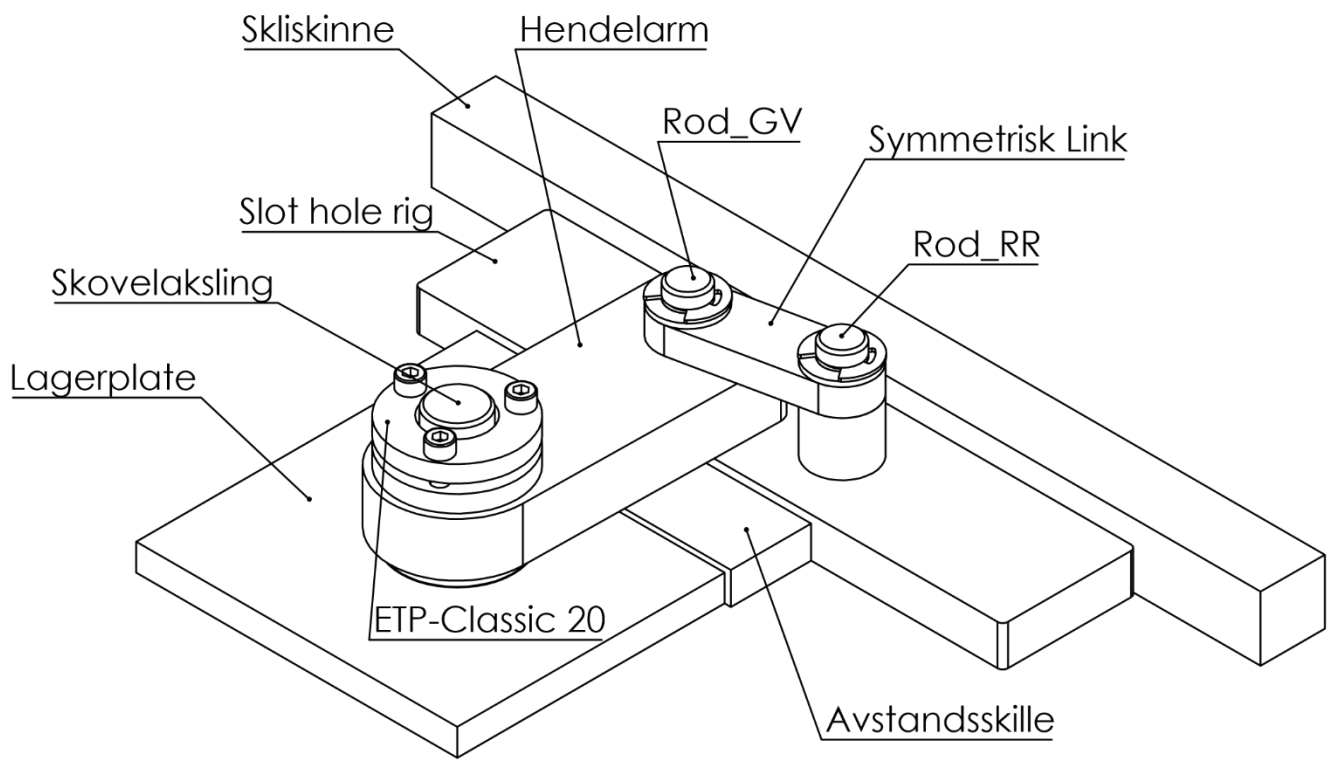
C

B

B

A

A



ISOMETRIC VIEW
SCALE 1:2



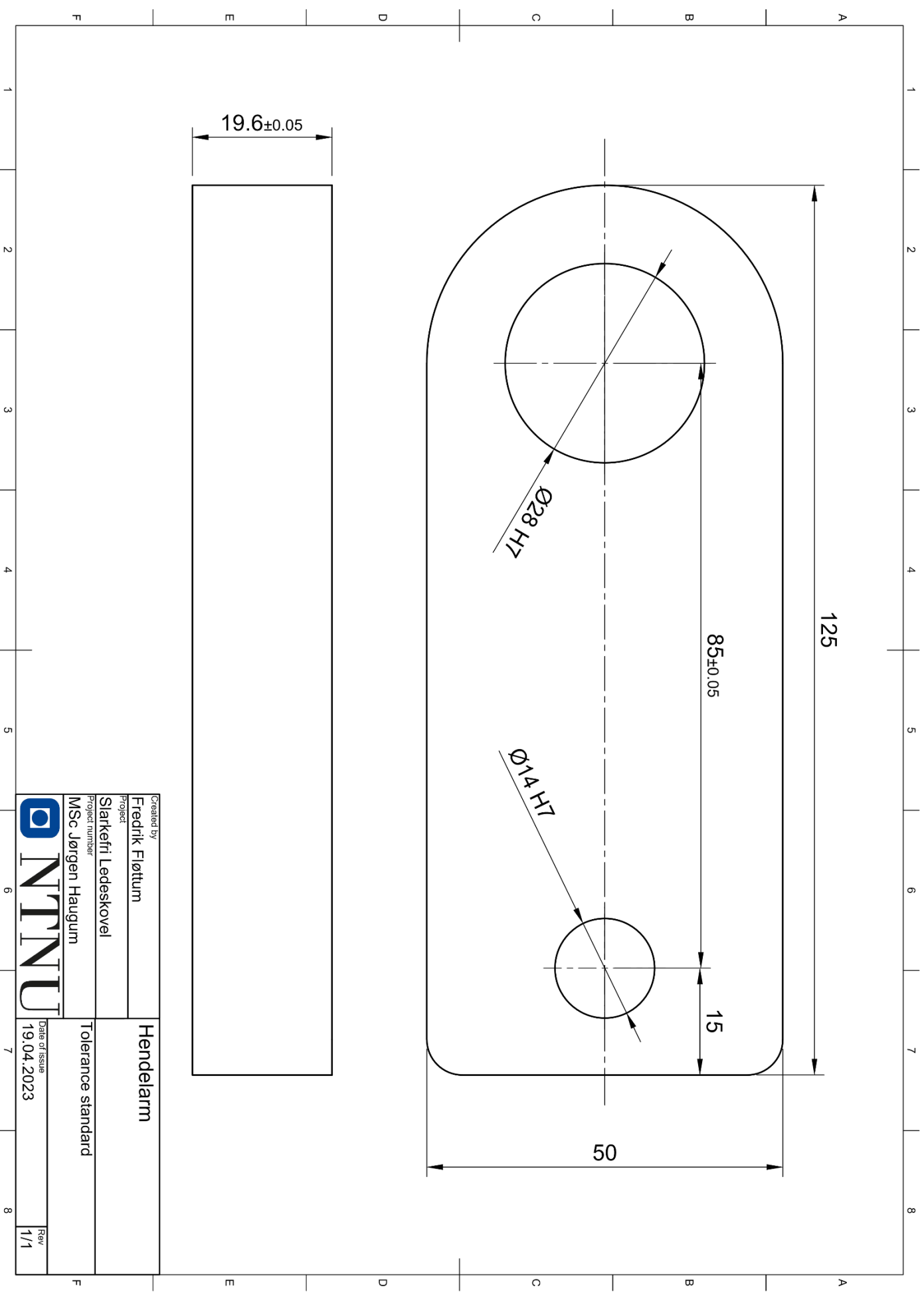
Drawn: JH	Date: 09.05.2023	Description: Mock-up assembly new connection
Material:		
SCALE: 1:2	SHEET 1 OF 1	Part name: Top-linked mockup
		Sheet size: A4

4

3

2

1



19.6±0.05

125

85±0.05

15

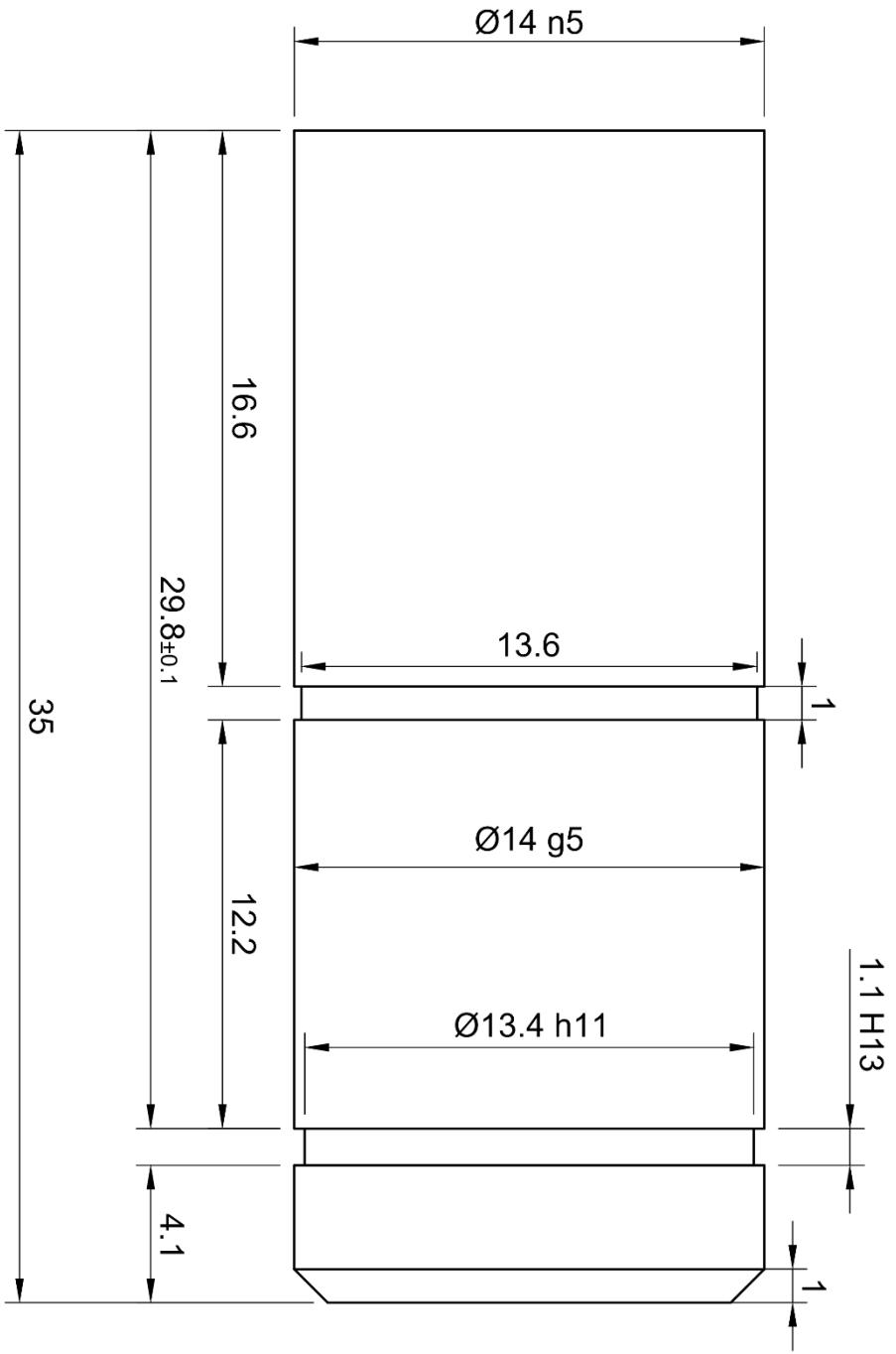
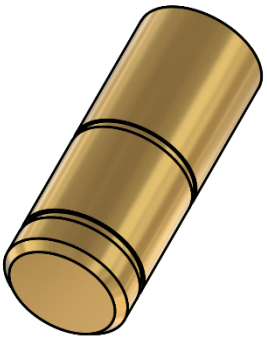
50

Ø28 H7

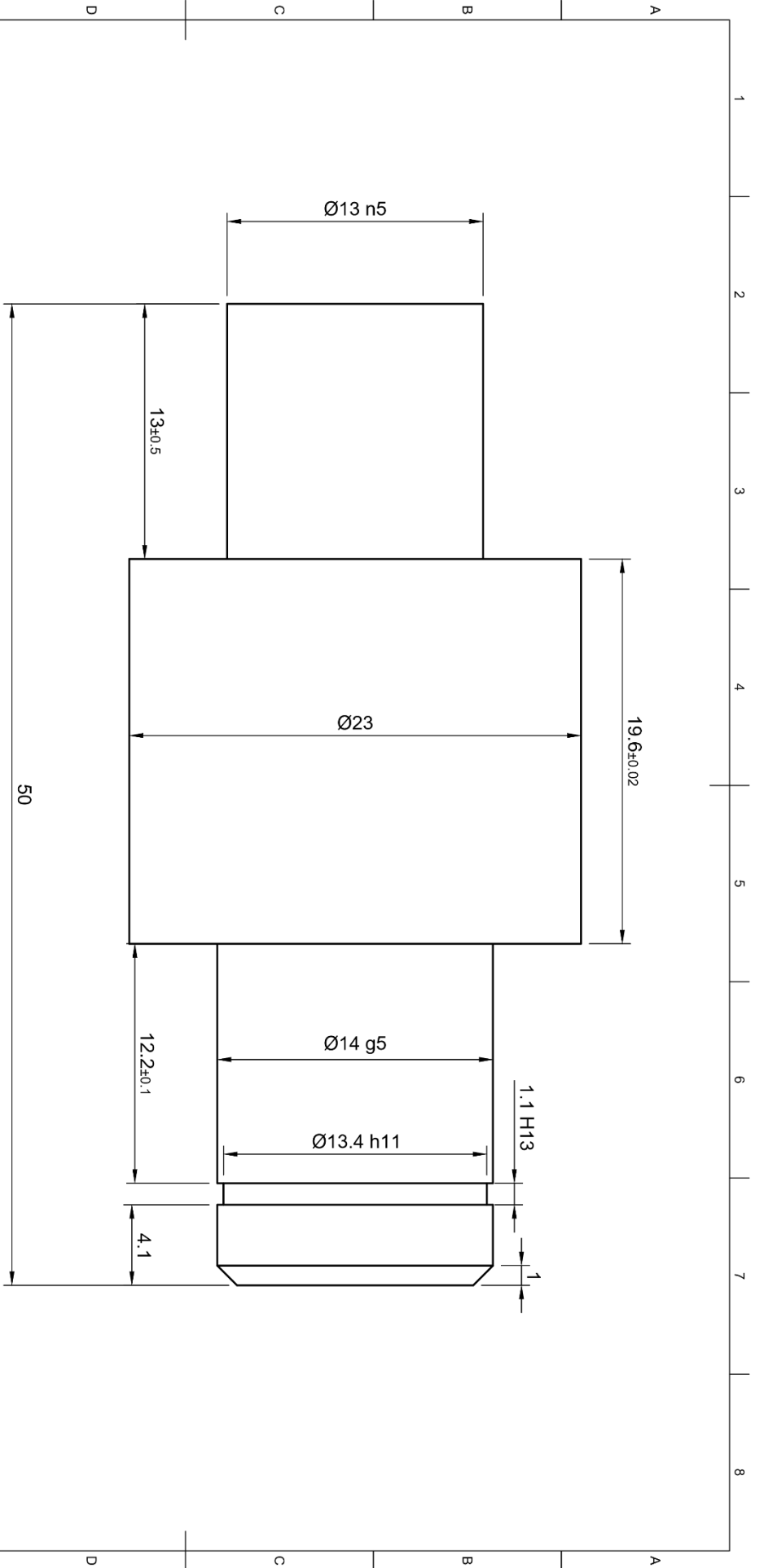
Ø14 H7


Created by	Fredrik Fløttum	
Project	Slårkefri Ledeskovel	
Project number	MSc Jørgen Haugum	
	Handelarm	
	Tolerance standard	
Date of issue	19.04.2023	
Rev	1/1	

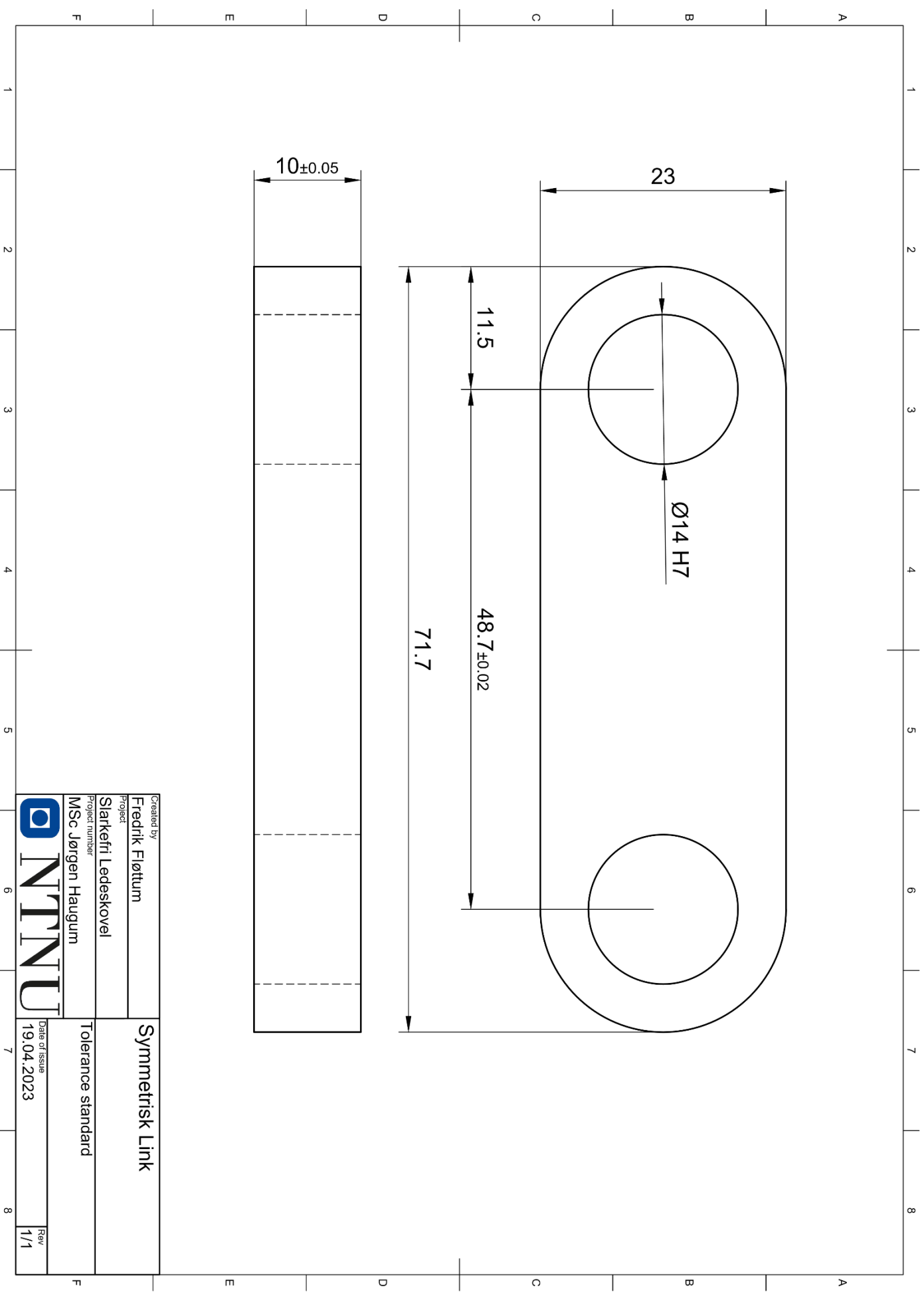




Created by	Frederik Fløttum	Rod_GV
Project	Slarkefri Ledeskovel	
Project number	MSc Jørgen Haugum	Tolerance standard
NTNU		Date of issue
		26.04.2023
		Rev
		1/1

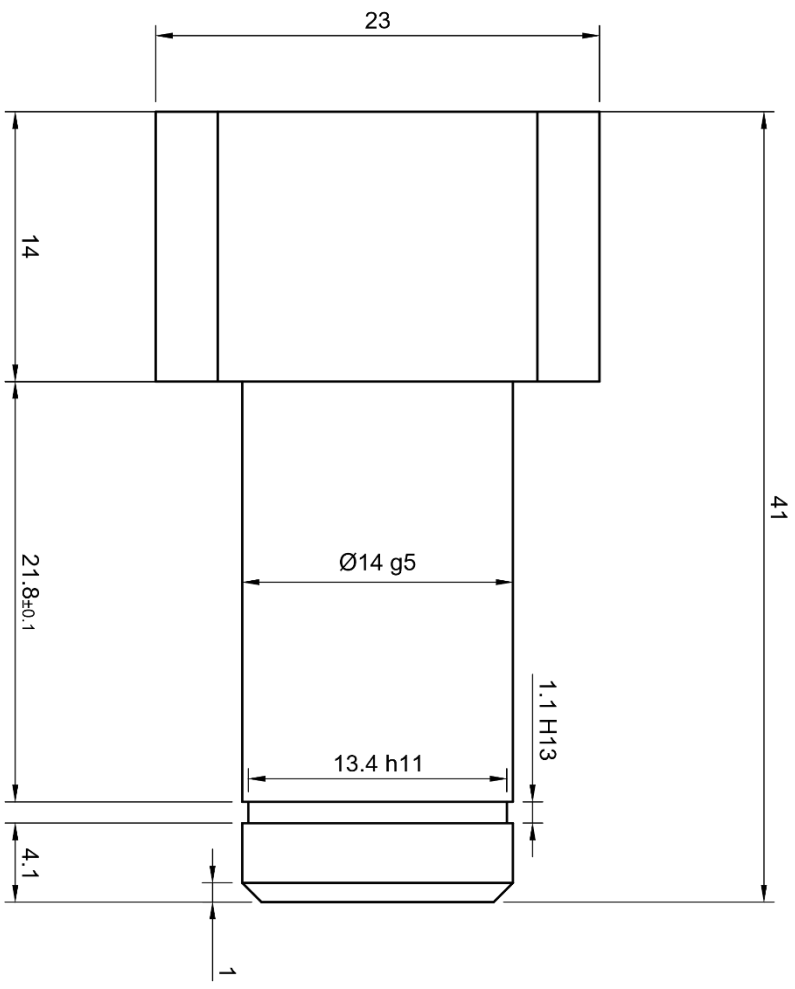
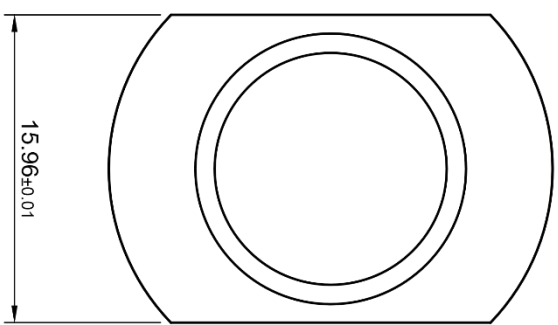
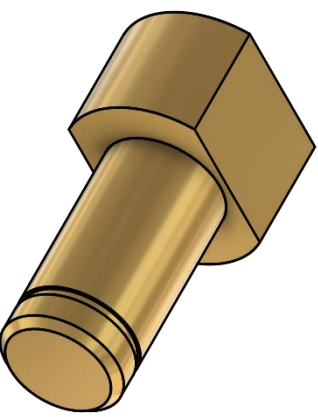
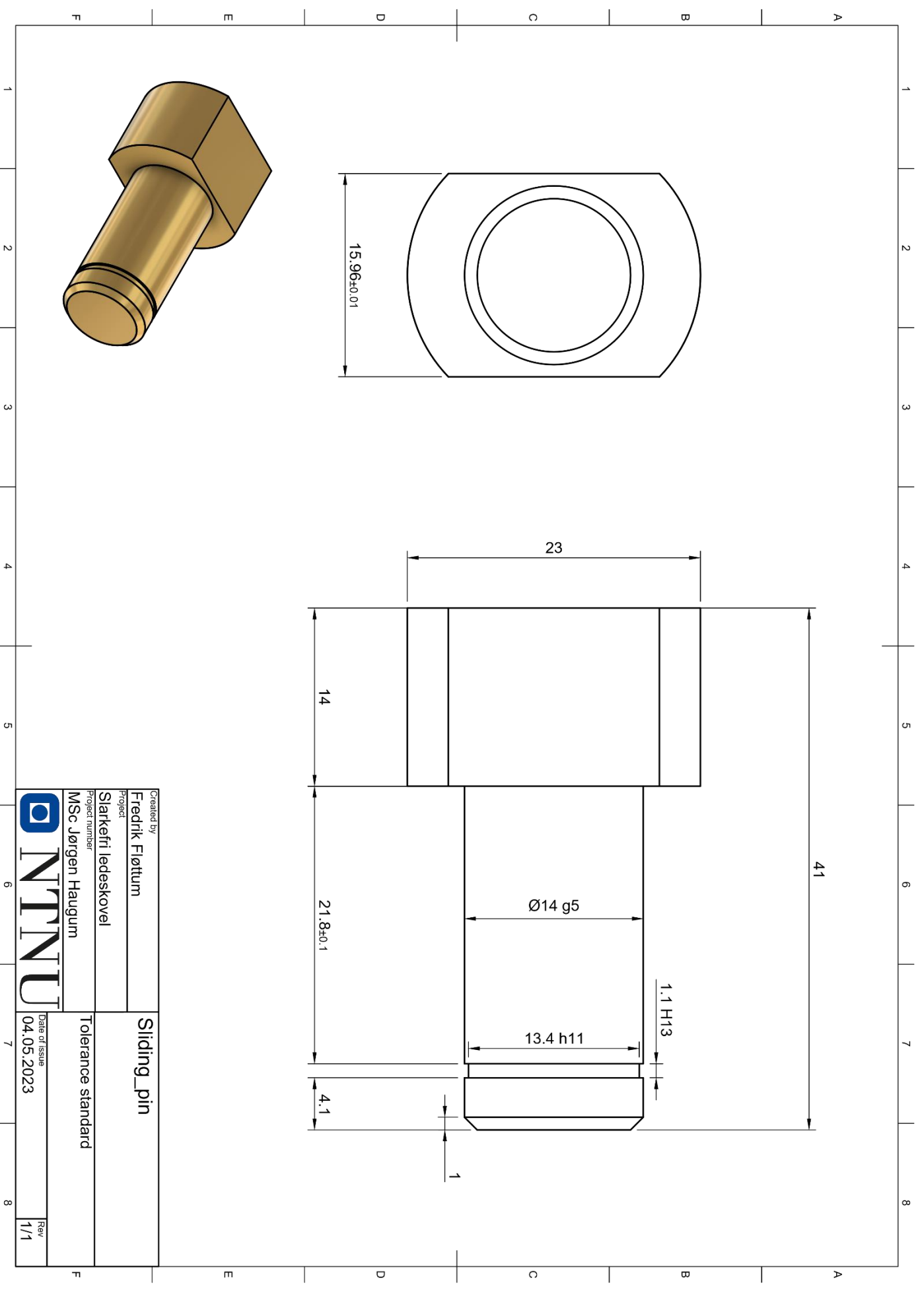



Created by Fredrik Fløttum	Rod_RR
Project Slarkefri Ledeskovel	Tolerance standard
Project number MSc Jørgen Haugum	Date of issue 27.04.2023
	Rev 1/1

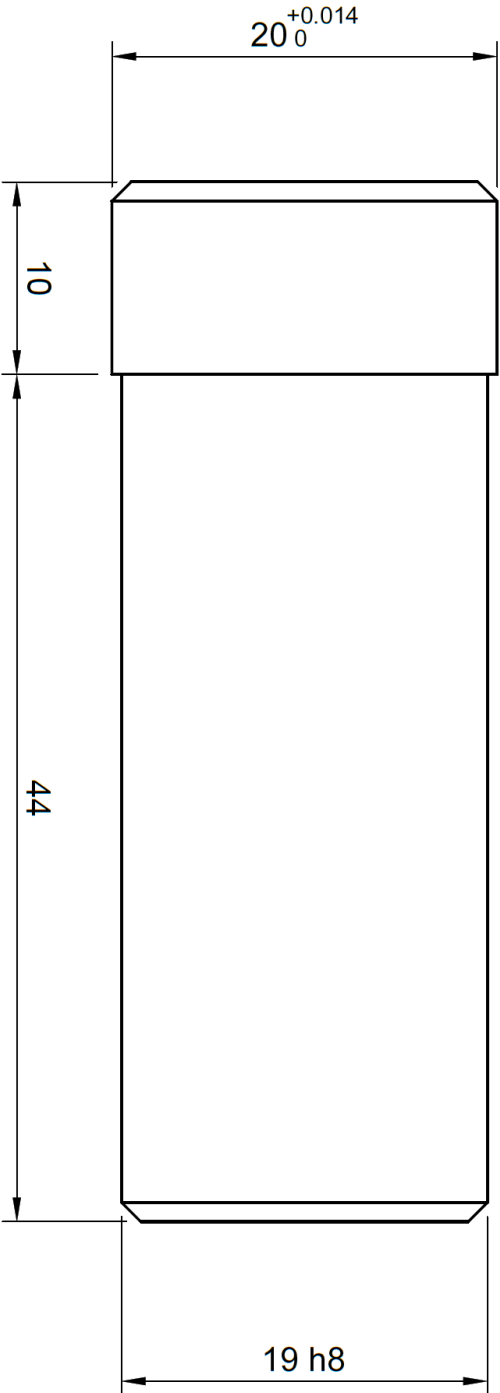



Created by Fredrik Fløttum	Symmetrisk Link
Project Slarkefri Ledeskovel	
Project number MSc Jørgen Haugum	
Tolerance standard	
Date of issue 19.04.2023	Rev 1/1

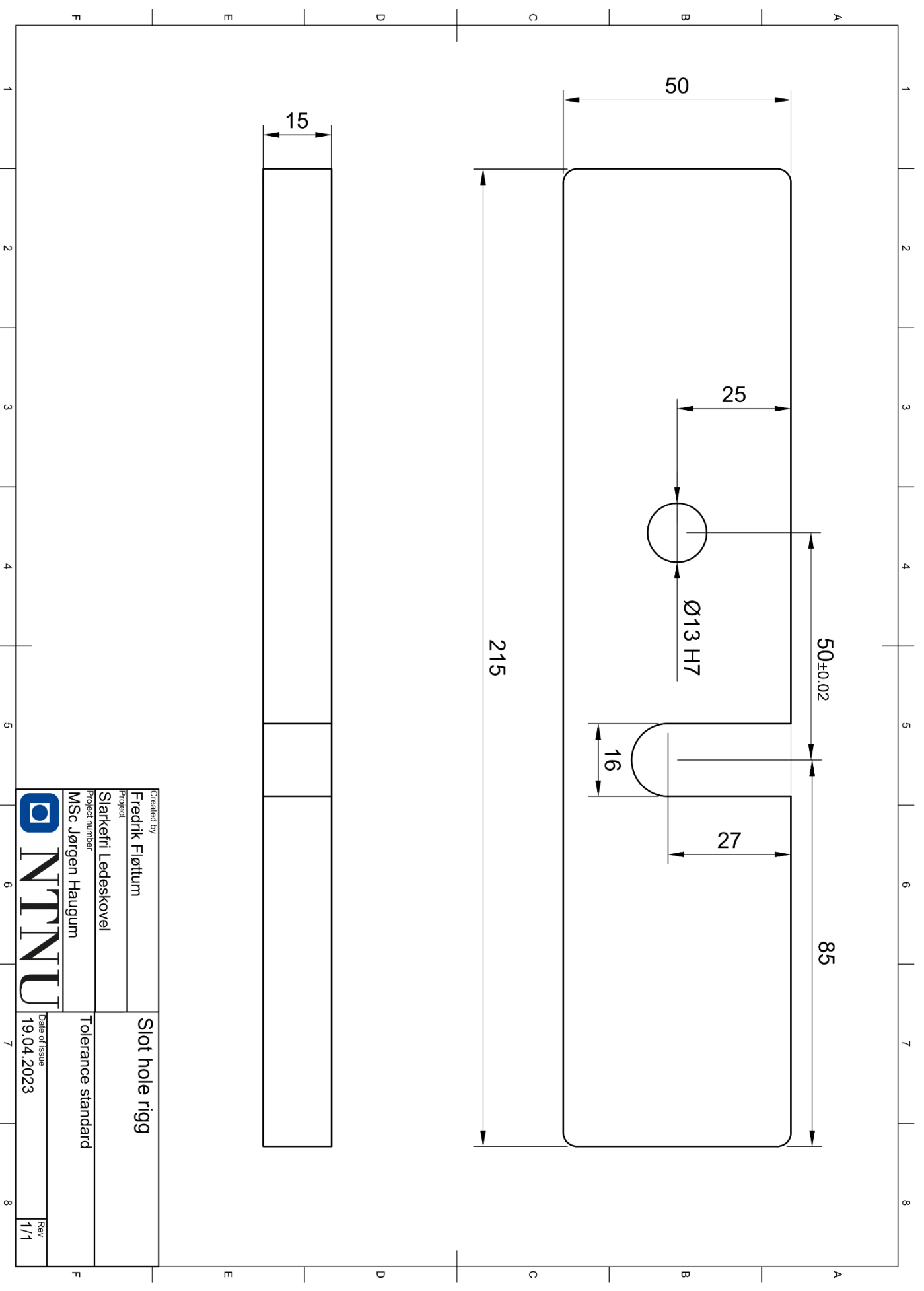




Created by	Frederik Fløttum	Sliding_pin
Project	Slarkerfi ledeskovel	
Project number	MSc Jørgen Haugum	Tolerance standard
 NTNU		Date of issue
		04.05.2023
		Rev
		1/1

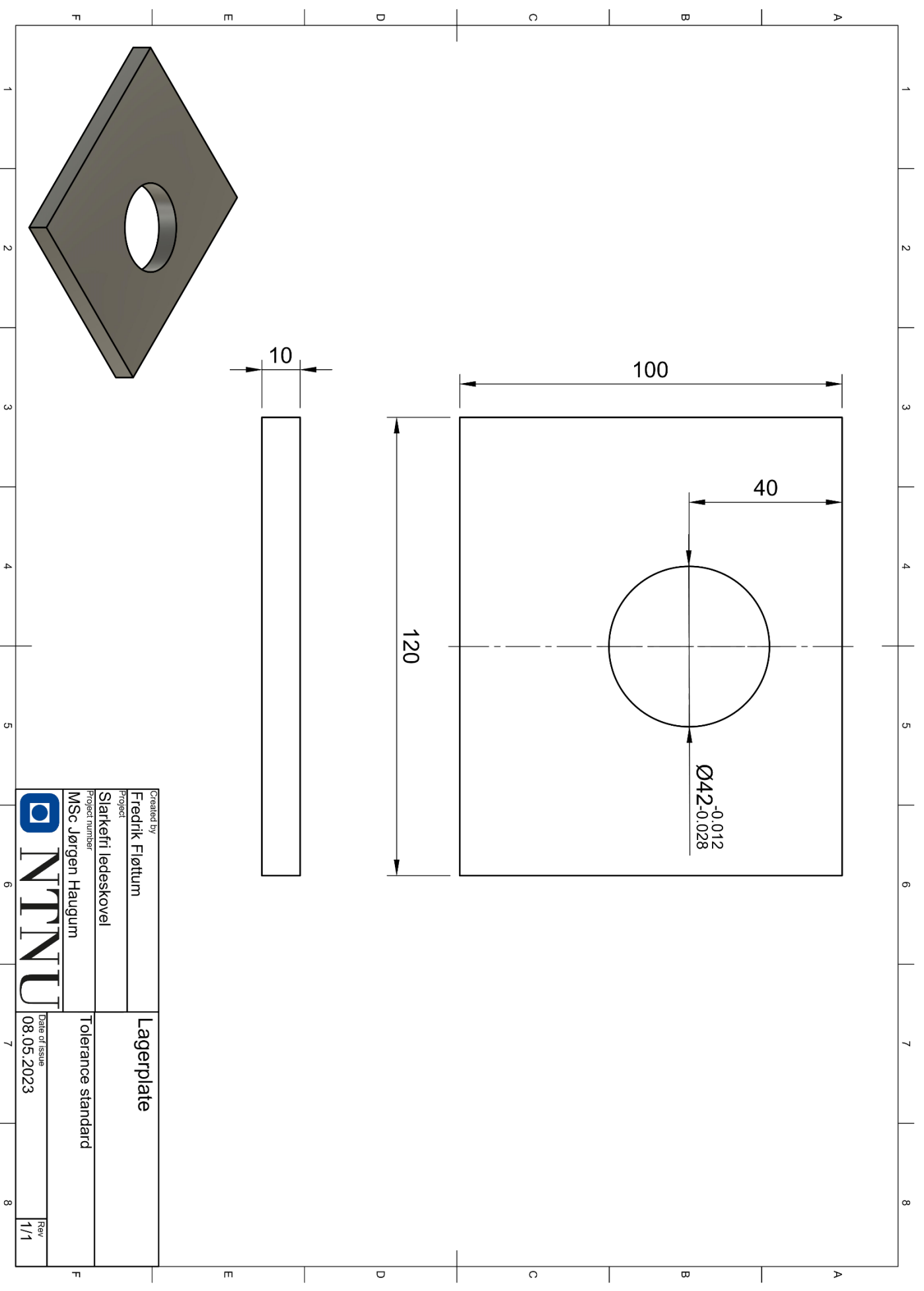


Created by		Skovrelaksling	
Fredrik Fløttum			
Project			
Slarkefri ledeskovel			
Project number		Tolerance standard	
MSc Jørgen Haugum			
		Date of issue	
		09.05.2023	
		Rev	
		1/1	



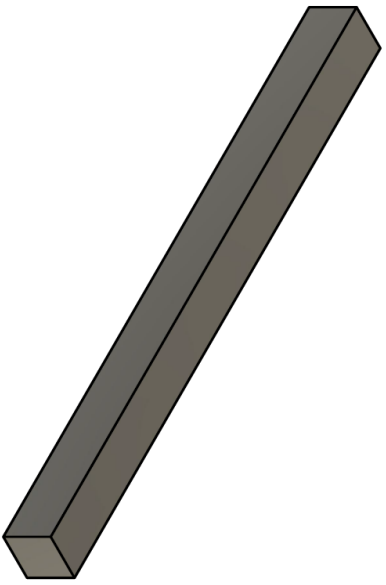
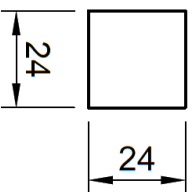
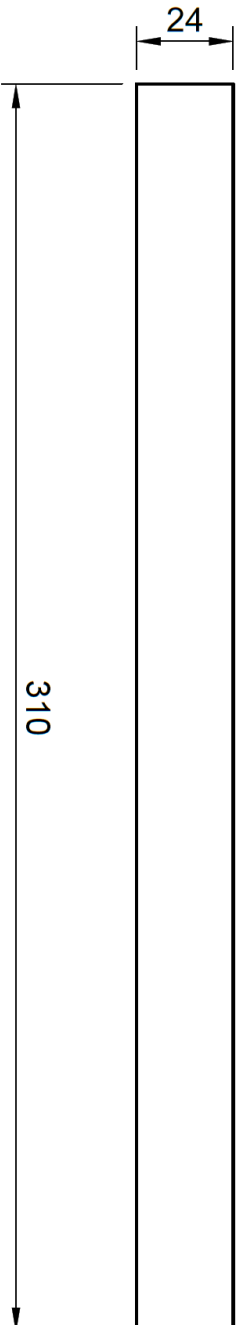
Created by	Fredrik Fløttum	
Project	Slarkefri Ledeskovel	
Project number	MSc Jørgen Haugum	
Tolerance standard		
Date of issue	19.04.2023	
Rev	1/1	






Created by	Fredrik Fløttum	
Project	Slarkefri ledeskovel	
Project number	MSc Jørgen Haugum	
	Lagerplate	
	Tolerance standard	
Date of issue	08.05.2023	
		Rev
		1/1





Created by Fredrik Fløttum	Skiskinne	
Project Slakterfi Ledeskovel	Tolerance standard	
Project number MSc Jørgen Haugum	Date of issue 11.05.2023	Rev 1/1
		

Appendix F

Calculation of conversion ratios

Actuator stroke displacement to governor ring angle

Arm of actuator stroke:

$$\text{arm}_{\text{act.}} = r_{\text{gov. ring. boltholes}} + l_{\text{gov. ring. boltholes-act.}} = 466 \text{ mm} + 840 \text{ mm} = 1306 \text{ mm}$$

For an actuator stroke of 1.0 mm:

$$\Delta\theta_{\text{gov. ring}} = 360^\circ \frac{1.0 \text{ mm}}{2\pi 1306 \text{ mm}} = 0.0439^\circ \quad F.1$$

Governor ring angle to mock-up plate displacement

Arm sliding pin:

$$\text{arm}_{\text{sliding, pin}} = r_{\text{gov. ring. inner. edge}} - x_{\text{pin. position. from. edge}} = 456 \text{ mm} - 23 \text{ mm} = 433 \text{ mm}$$

For an actuator stroke of 1.0 mm:

$$\Delta x_{\text{plate}} = \frac{0.439^\circ}{360^\circ} 2\pi 433 \text{ mm} = 0.3315 \text{ mm} \quad F.2$$

Plate displacement to guide vane shaft angle

Lever arm length = 85 mm

For an actuator stroke of 1.0 mm:

$$\Delta\theta_{\text{guide vane}} = \arctan\left(\frac{0.3315 \text{ mm}}{85 \text{ mm}}\right) = 0.223^\circ \quad F.3$$

Appendix G

Calculation of uncertainties

Instrument resolution

The absolute resolution uncertainty of the dial gauges, e_{res} , is given by the standard method to convert resolution to resolution uncertainty presented by Equation G.1 [31], where R_i is the resolution of 0.01 mm. From this equation it can be seen that the relative resolution uncertainty will become smaller for greater measurements.

$$e_{res} = \pm \frac{R_i}{\sqrt{3}} = \pm 0.0058 \text{ mm} \quad G.1$$

Instrument calibration

The calibration of the gauges was performed by comparing the measurements of the gauges to each other as suggested by [32]. The comparison calibration was done by installing two and two gauges on a lathe via magnetic stands and then setting the measuring sticks on the dial gauges towards the tail stock on the lathe. After setting both dial gauges to zero, the tail stock was turned, and the indicator of both gauges was recorded. For a travel of 4 mm, the test showed the results given in Table G.1, and it was concluded that a relative calibration uncertainty of $f_{cal} = \pm 0.25\%$ was appropriate for all tests.

Table G.1: Dial gauge offset for 4 mm travel.

Test case	Offset from dial gauge 2	Relative offset
Dial gauge 1 vs d.g. 2	+ 0.010 mm	+ 0.250%
Dial gauge 3 vs d.g. 2	+ 0.005 mm	+ 0.125%

Since the instruments were mounted similarly for the calibration test and the experimental tests, and the tail stock was turned back and forth, it was assumed that the calibration uncertainty also included the uncertainty of alignment and hysteresis of the dial gauges.

Variation in measurements

The variations of the readings on the dial gauge in each different case are given as absolute uncertainty, e_{var} , together with its corresponding mean measured value in Table G.2. Here it should be noted that the three first rows presents measurements and uncertainties for the readings on the dial gauge measuring the shaft-rod displacement described in Section 5.1.1, while the last row is presenting the actuator stroke equivalent magnitude of the third row values, converted by the use of Equation 5.1 and F.3. There is no strict confidence interval given for the variations, but it is assumed to be about 95% as all the recorded cases was within the given range. Additionally, the absolute calibration uncertainty, e_{cal} , and the absolute resolution uncertainty, e_{res} , are given in the table. The absolute calibration uncertainty is calculated from multiplying the measured value with the relative calibration uncertainty.

Table G.2: Measured values and absolute uncertainties.

Case	Measured value	e_{var} [mm]	e_{cal} [mm]	e_{res} [mm]
Fixed plate old connection	0.12 mm	± 0.02	± 0.0003	± 0.0058
Fixed plate new connection	0.02 mm	± 0.005	± 0.0001	± 0.0058
GV connection on rig (readings)	0.14 mm	± 0.01	± 0.0004	± 0.0058
Cantilever beam on spiral casing	1.08 mm	± 0.06	± 0.0027	± 0.0058
1 st joint on hydraulic actuator	0.26 mm	± 0.04	± 0.0065	± 0.0058
2 nd joint on hydraulic actuator	0.16 mm	± 0.04	± 0.0004	± 0.0058
Cantilever beam on governor ring	0.71 mm	± 0.04	± 0.0018	± 0.0058
Governor ring, lin. movement	0.03 mm	± 0.01	± 0.0001	± 0.0058
GV connection on rig (converted)	0.36 mm	± 0.03	± 0.0009	± 0.0161

Total uncertainty from mechanical parts

To calculate the sum of the relative uncertainties of the measurements, $f_{\Sigma var}$, a version of the root sum square method is used. This method is derived from the uncertainty analysis theory in chapter 3.9 and annex J in [33], where it is stated that the total relative uncertainty in terms of a measured efficiency can be found from the root sum square of the part-uncertainties, and that a relative uncertainty can be defined as an absolute uncertainty over the measured value. It is assumed that this also will apply for the measurements in this project, and the method is given by Equation G.2, where e_{var_i} is the absolute uncertainty from measurement i , and x_i is the mean value of measurement i .

$$f_{\Sigma var} = \pm \frac{\sqrt{(e_{var_1})^2 + (e_{var_2})^2 + (e_{var_3})^2 + \dots}}{x_1 + x_2 + x_3 + \dots} \quad G.2$$

For the sum of the relative calibration and resolution uncertainties, $f_{\Sigma cal}$ and $f_{\Sigma res}$, the same method was used. The calculations are listed in Table G.3.

Table G.3: Relative uncertainties from measurement variation, calibration, and resolution.

Relative uncertainty	Value
$f_{\Sigma var}$	$\pm 3.55\%$
$f_{\Sigma cal}$	$\pm 0.13\%$
$f_{\Sigma res}$	$\pm 0.80\%$

To give the total relative uncertainty from the mechanical parts, f_{mech} , the root sum square method given in Equation G.3 was used, giving $f_{mech} = \pm 3.64\%$.

$$f_{mech} = \pm \sqrt{(f_{\Sigma var})^2 + (f_{\Sigma cal})^2 + (f_{\Sigma res})^2} \quad G.3$$

The magnitude of the backlash originating from the mechanical parts, is given by the sum of the slack measurements on the rig which are the bottom six cases in Table G.2. These measurements sum up to 2.60 mm, and by multiplying this sum with the relative uncertainty from the mechanical parts, we end up with a total absolute uncertainty, $e_{mech} = \pm 0.09$ mm.

Uncertainty from sensors

The guide vane and actuator stroke positions on the Francis rig in the laboratory, is measured by digital sensors with specifications listed in Table G.4.

Table G.4: Sensor specifications and relative uncertainty.

Sensor	Resolution	Resolution, act. stroke eq.	Hysteresis, act. stroke eq.	$f_{\Sigma sen}$
GV angle: Stegmann AG 612 13-bit	$360^\circ/2^{13}$	0.197 mm	0.179 mm	$\pm 10.3\%$
Actuator stroke: HYDAC HLT 2550-L2	0.05 mm	0.050 mm	0.010 mm	$\pm 1.97\%$

The actuator stroke equivalent for the guide vane position is calculated by the use of the conversion rate from Equation F.3, while the sum of the relative resolution and hysteresis uncertainty for each sensor, $f_{\Sigma sen_i}$, is calculated by the use of Equation G.4, setting the sum of the measurements under the fractional line equal to the sum of the mechanical backlash.

$$f_{\Sigma sen_i} = \pm \frac{\sqrt{(Resolution_i)^2 + (Hysteresis_i)^2}}{2.60 \text{ mm}} \quad G.4$$

The calculation of the relative uncertainty originating from the digital sensors is presented in equation G.5, while the total relative uncertainty is given in Equation G.6. From this, it can be found that the digital and absolute uncertainty, e_{dig} and e_{tot} , is respectively ± 0.27 mm and ± 0.29 mm.

$$f_{dig} = \pm \sqrt{(f_{\Sigma sen_{GV}})^2 + (f_{\Sigma sen_{SS}})^2} = \pm 10.4\% \quad G.5$$

$$f_{tot} = \pm \sqrt{(f_{mech})^2 + (f_{dig})^2} = \pm 11.1\% \quad G.6$$

Uncertainty from new sensors

To find the uncertainty coming from the new guide vane sensor and actuator stroke sensor, the method presented in the previous paragraph was used. The sensor specifications are listed in Table G.5, and the relative uncertainties are calculated by utilizing Equation G.7.

Table G.5: Sensor specifications and relative uncertainty on the new system.

Sensor	Resolution	Resolution, act. stroke eq.	Hysteresis, act. stroke eq.	$f_{\Sigma sen}$
GV angle: Stegmann AG 615 15-bit	$360^\circ/2^{15}$	0.049 mm	0.022 mm	$\pm 9.64\%$
Actuator stroke: HYDAC HLT 2550-L2	0.05 mm	0.050 mm	0.010 mm	$\pm 9.11\%$

$$f_{\Sigma sen_i} = \pm \frac{\sqrt{(Resolution_i)^2 + (Hysteresis_i)^2}}{0.56 \text{ mm}} \quad G.7$$

Equation G.5 is then used to find the relative digital uncertainty of the new system, $f_{dig_{new}} = \pm 13.3\%$, which corresponds to an absolute digital uncertainty, $e_{dig_{new}} = \pm 0.07$ mm.

Appendix H

Calculations of beam deflections

To calculate the deflection of a fixed cantilever beam, Equation H.1 retrieved from Appendix C in [30] is used. Here, δ_a is the deflection of point a , where the force P is acting, while E is the Young's modulus of the material and I the second moment of inertia. An illustration of this is presented in Figure H.1.

$$\delta_a = \frac{Pa^3}{3EI} \quad H.1$$

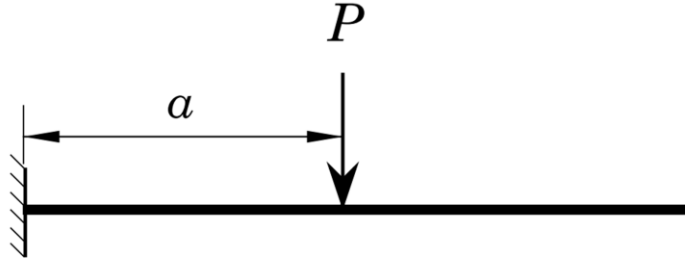


Figure H.1: 2D fixed cantilever beam.

The specifications of the different beams and its corresponding deflections in point a , is presented in Table H.1. Here, the Young's modulus is 200 GPa (steel) and the load is 500 N for all cases. For more extensive elaboration of beam theory please see [30]. The second moments of inertia are calculated by from [34].

Table H.1: Calculations and specifications of beam deflections.

Case	I [mm ⁴]	a [mm]	δ_a [mm]
Existing spiral case cover beam	426667	625	0.48
Spiral case cover beam w/ H-beam	2403274	625	0.08
Existing governor ring beam	192000	700	1.49
Governor ring beam w/ H-beam	1333430	700	0.21

Appendix I

Technical drawings of suggested guide vane system

In this section the technical drawings of the system suggested in Section 6.3 is presented. The drawings are made in SolidWorks and the dimensions are given in mm. For drawings of the parts in “New guide vane Asm” please see Appendix E. Additionally, the technical drawings of “Aktuator stag” and “Aktuator sylinder” remains unchanged from Appendix C.

4

3

2

1

F

F

E

E

D

D

C

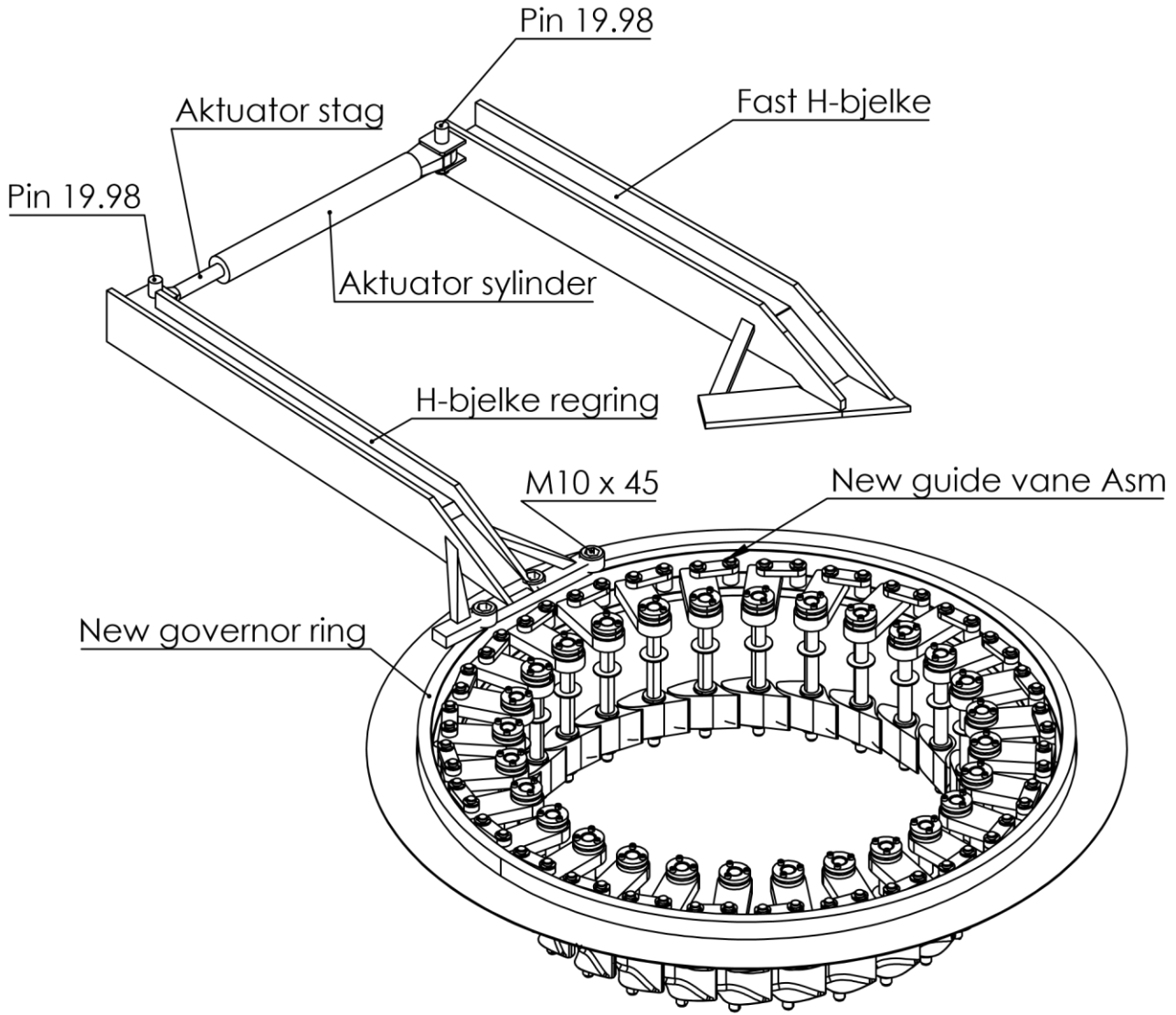
C

B

B

A

A



ISOMETRIC VIEW
SCALE 1:10

Drawn: JH	Date: 25.05.2023
Material:	
SCALE: 1:10	SHEET 1 OF 1



Description: Assembly with new beams and guide vane connections

Part name: Suggested GV-system
Sheet size: A4

4

3

2

1

4

3

2

1

F

F

E

E

D

D

C

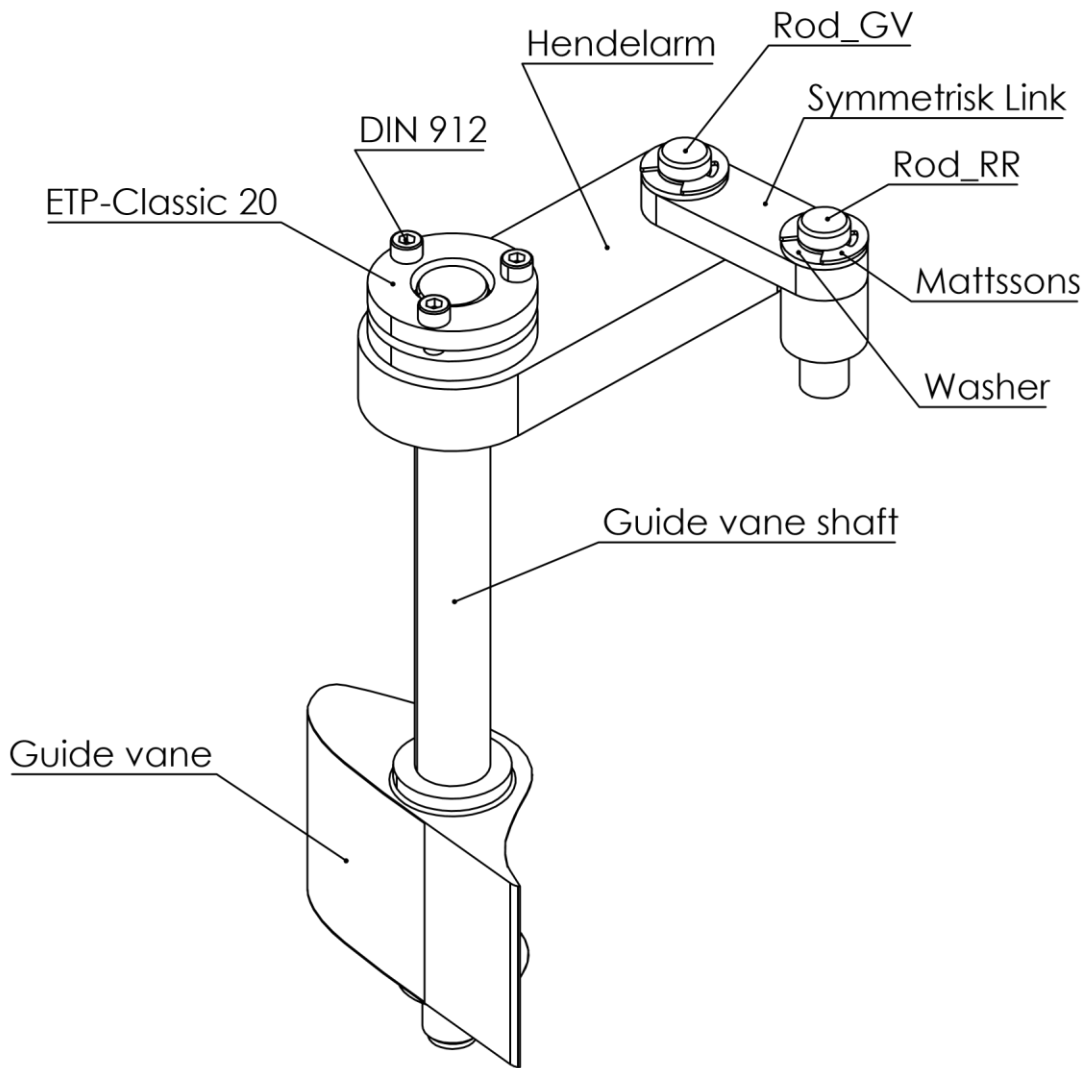
C

B

B

A

A



ISOMETRIC VIEW
SCALE 1:2



Drawn: JH	Date: 25.05.2023
Material:	
SCALE: 1:2	SHEET 1 OF 1

Description: Assembly of suggested guide vane connection	
Part name: New guide vane Asm	Sheet size: A4

4

3

2

1

4

3

2

1

F

F

E

E

D

D

C

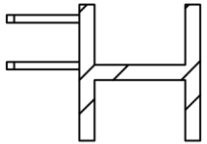
C

B

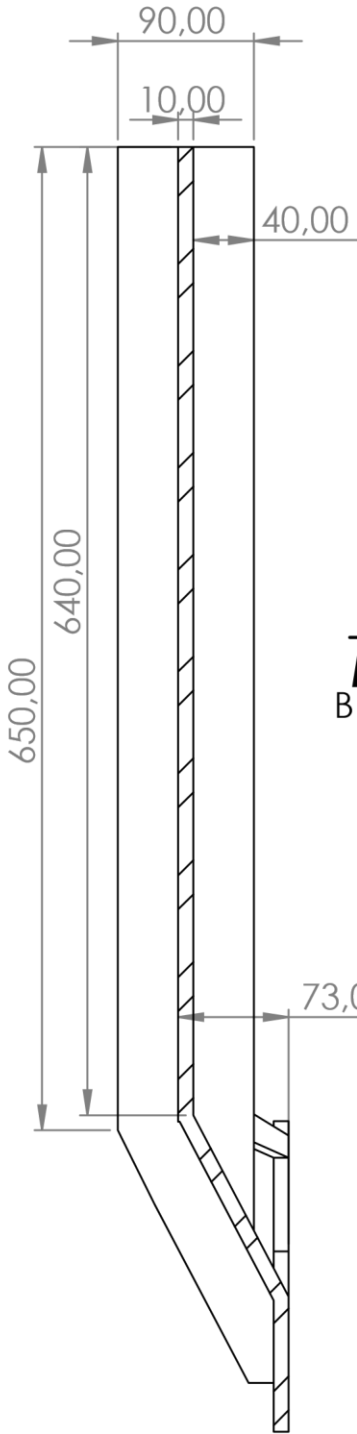
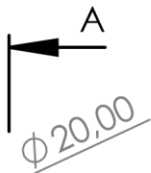
B

A

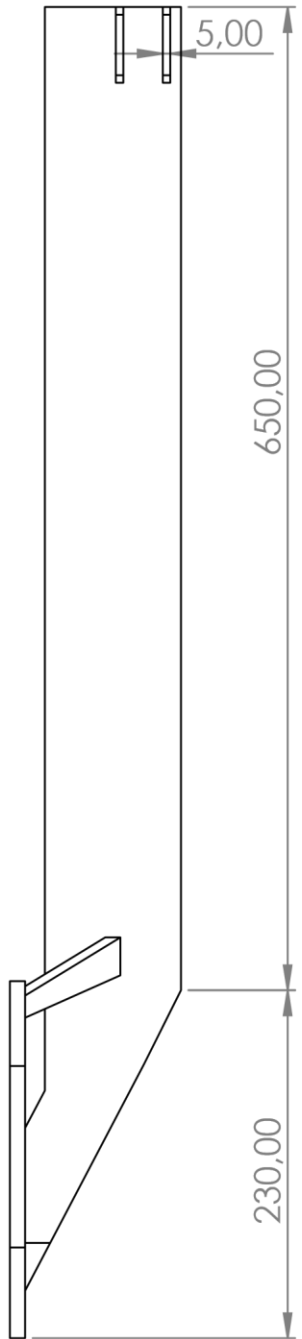
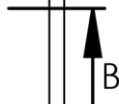
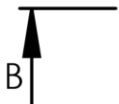
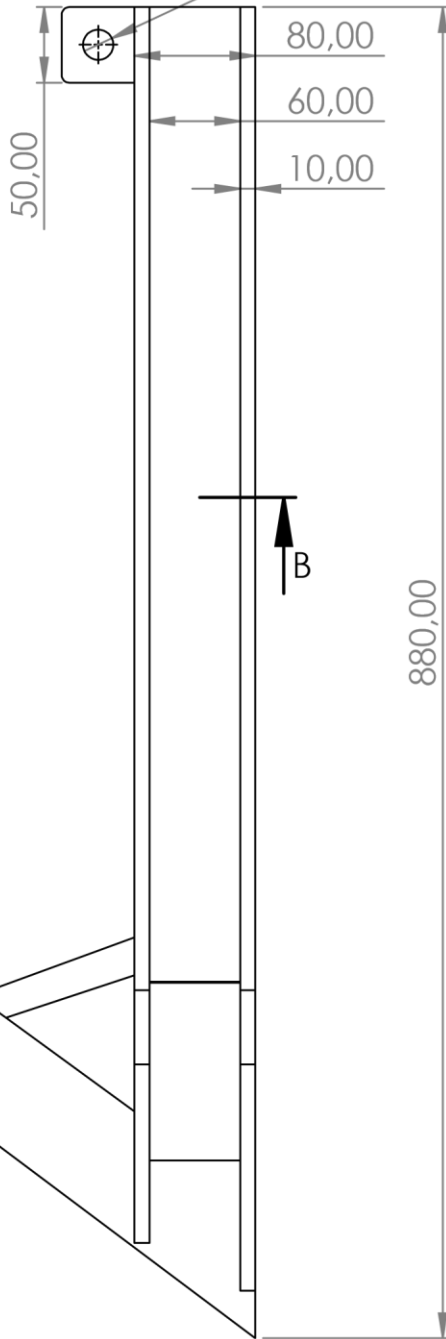
A



SECTION B-B
SCALE 1 : 5



SECTION A-A
SCALE 1 : 5



880,00

650,00

230,00



Drawn: JH	Date: 25.05.2023
Material: Steel	Description: New beam connected to spiral casing
SCALE: 1:5	SHEET 1 OF 1

Part name: Fast H-bjelke	Sheet size: A4
-----------------------------	-------------------

4

3

2

1

4

3

2

1

F

F

E

E

D

D

C

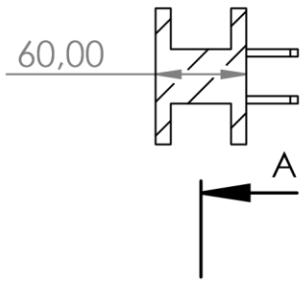
C

B

B

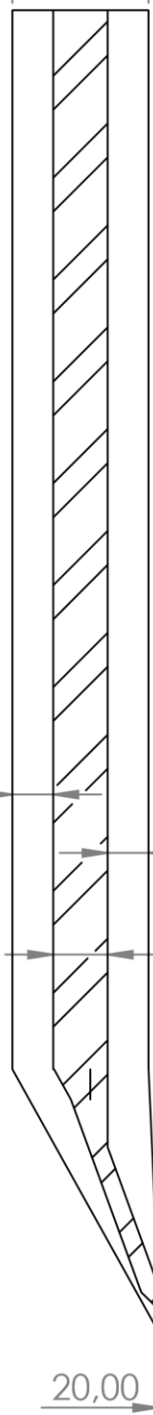
A

A

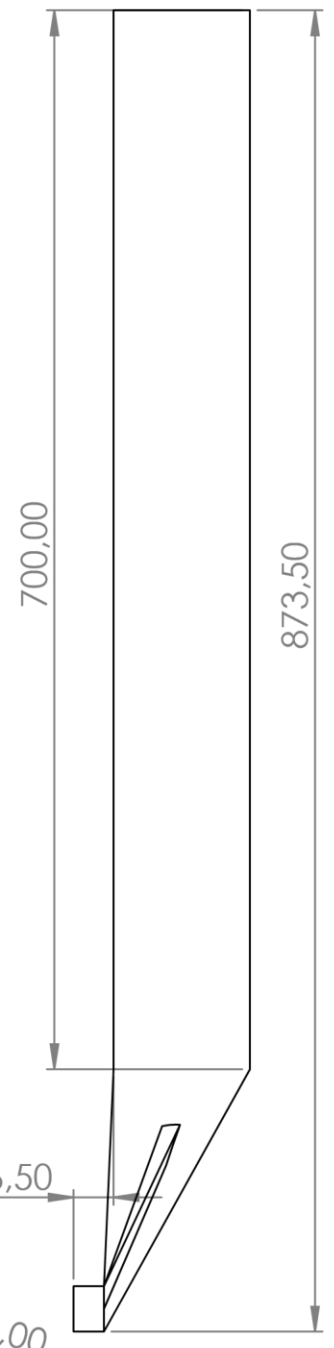
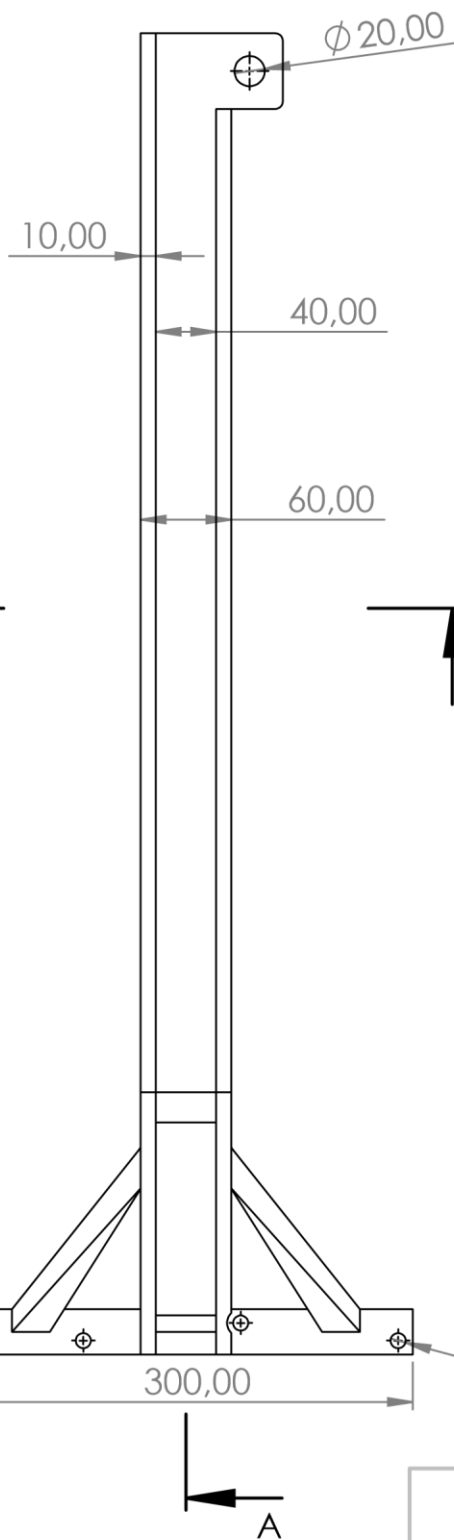


SECTION B-B
SCALE 1 : 5

90,00



SECTION A-A
SCALE 1 : 5



Drawn: JH	Date: 25.05.2023
Material: Steel	Description: New beam connected to gov. ring
SCALE: 1:5	SHEET 1 OF 1



Part name: H-bjelke regring	Sheet size: A4
--------------------------------	-------------------

4

3

2

1

4

3

2

1

F

F

E

E

D

D

C

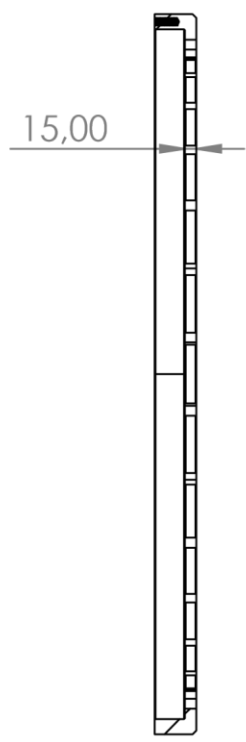
C

B

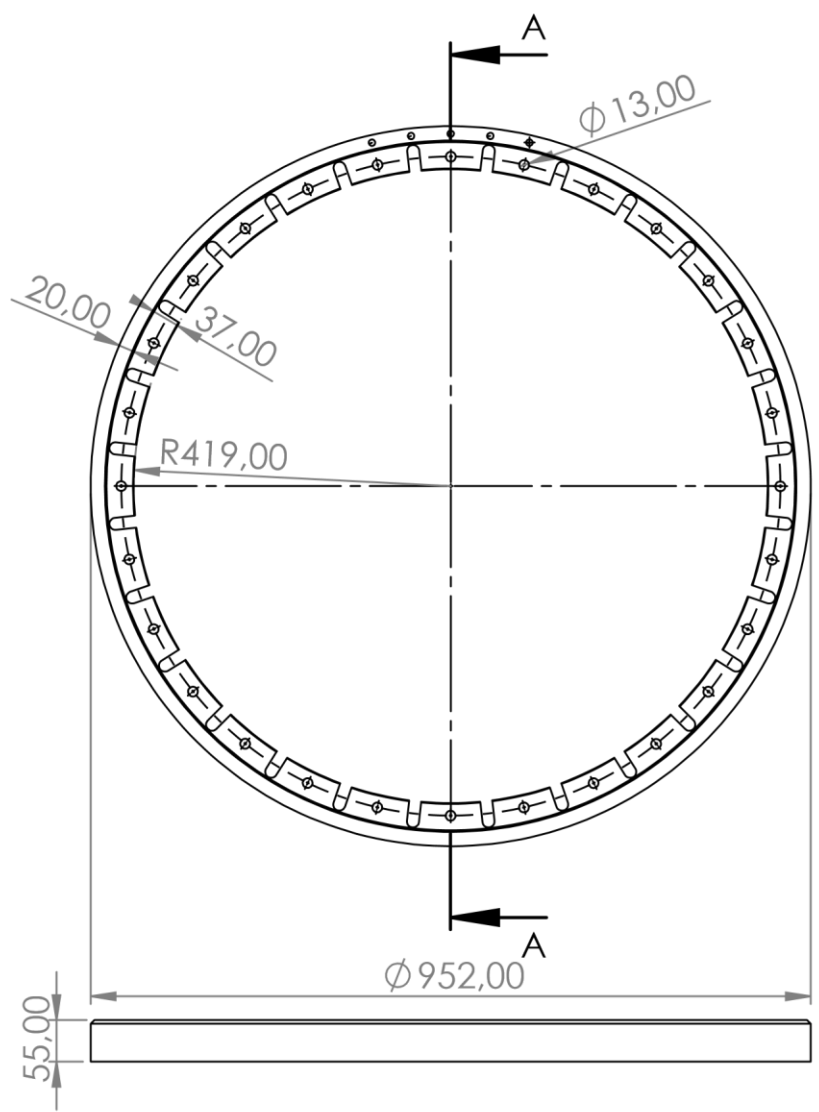
B

A

A



SECTION A-A
SCALE 1 : 10



Drawn: JH	Date: 24.05.2023
Material: Steel	Description: Governor ring with holes and slots
SCALE: 1:10	SHEET 1 OF 1



Part name: New governor ring	Sheet size: A4
---------------------------------	-------------------

4

3

2

1

4

3

2

1

F

F

E

E

D

D

C

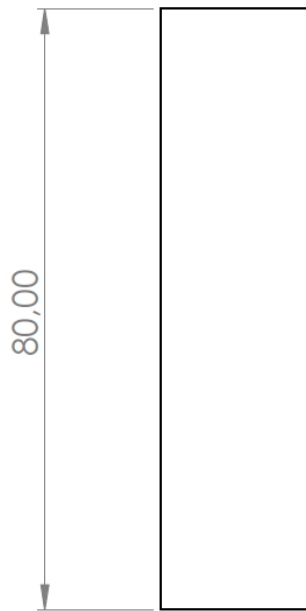
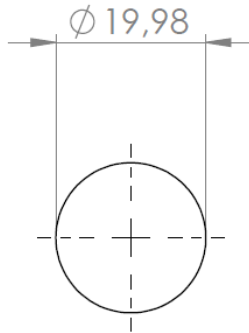
C

B

B

A

A



Drawn: JH	Date: 24.05.2023
Material: Steel	
SCALE: 1:1	SHEET 1 OF 1

 NTNU	
Description:	
Part name:	Pin 19.98
Sheet size:	A4

4

3

2

1



 **NTNU**

Norwegian University of
Science and Technology